Taxonomy, Systematics, and Histopathology of Myxozoan (Cnidaria: Myxozoa) Parasites of Fishes

by

Steven Paul Ksepka

A dissertation submitted to the Graduate Faculty of
Auburn University
in partial fulfillment of the
requirements of the Degree of
Doctor of Philosophy

Auburn, Alabama
December 9, 2023

Keywords: Myxobolidae, *Ellipsomyxa,* phylogenetics

Approved by

Stephen A. Bullard, Chair, Professor of Fisheries, Aquaculture, and Aquatic Science
Nathan V. Whelan, Director of United States Fish and Wildlife Service's Southeast Conservation Genetics Lab
Johnathon W. Armbruster, Professor of Biological Sciences, Director of Auburn University of Natural History
Stephen S. Curran, Research Assistant, School of Fisheries, Aquaculture, and Aquatic Science

Abstract

Myxozoans, a parasitic lineage of cnidarians, comprise over 2500 species infecting primarily freshwater, marine, and estuarine fishes. This includes several demonstrable pathogens to cultured fishes including: *Myxobolus cerebralis,* the causative agent of whirling disease, *Tetracapsuloides bryosalmonae*, the causative agent of proliferative kidney disease, and *Henneguya ictaluri*, the causative agent proliferative gill disease. Muscle infecting species can reduce the value of wild caught fishes by appearance as white cysts in muscle, reducing marketability, or in the case of some *Kudoa* species inducing myoliquefaction, commonly referred to as pudding flesh, rendering fish valueless. Myxozoans have complex life cycles with invertebrate definitive hosts (wherein the parasite matures) and fish intermediate hosts (wherein asexual reproduction occurs). In this dissertation five species of Myxobolidae and one species of *Ellipsomyxa* Køie, 2003 (Bivalvulida) are described, the range for *Myxobolus neurofontinalis* Ksepka and Bullard, 2019 (Bivalvulida: Myxoboidae) is extended, and an alternate definitive host for *Myxobolus cerebralis* Hofer, 1903, the causative agent of salmonid whirling disease, is reported in the southeast US. I use genetic sequencing (PCR; small subunit ribosomal DNA [18S]) to report alternate definitive hosts for *M. cerebralis* in the southeast US, comprising the first report of a definitive host for *M. cerebralis* other than *Tubifex tubifex* (Muller) (Tubificida: Tubificidae). I use morphology, histology, genetic sequencing (PCR; small subunit ribosomal DNA [18S]), and phylogenetic analysis to characterize six new myxozoan species assigned to three genera. *Myxobolus branchiofilum* n. sp. and *Myxobolus branchiopectin* n. sp. from the gill filaments and rakers, respectively, of black redhorse, *Moxostoma duquesnei* (Leseur) (Cypriniformes: Catostomidae) from North Carolina, comprising the first myxozoans reported to infect black redhorse. *Myxobolus intralamina* n. sp. and *Myxobolus infrabractea* n. sp. from the

gill and scales, respectively, of smallmouth bass, *Micropterus dolomieu* (Lacepede) (Centrachiformes: Centrarchidae) from North Carolina, comprising fourth and fifth *Myxobolus* reported to infect smallmouth bass and the first reported from smallmouth bass in the southeast US. *Henneguya albomaculata* n. sp. from the submucosa of the intestine and pyloric ceca of red drum, *Sciaenops ocellatus* (Linnaeus) (Bivalvulida: Myxobolidae) from coastal Alabama, comprising the second species of *Henneguya* reported to infect red drum. *Ellipsomyxa intravesica* n. sp. (Bivalvulida) from the gall bladder of *Pangasisus macronema* (Bleeker) (Siluriformes: Pangasiidae) from Vietnam, comprising the fourth species of *Ellipsomyxa* reported from a catfish and the first from a freshwater fish in southeast Asia. Further, I use morphology, histology, and genetic sequencing to extend the range of *M. neurofontinalis* to anadromous brook trout in Prince Edward Island, Canada, comprising the first report of this speciesoutside of North Carolina and the first report from anadromous brook trout. This work has resulted manuscripts published or accepted at Systematic Parasitology, Journal of Aquatic Animal Health, Journal of Parasitology, Parasitology International, and Diseases of Aquatic Organisms.

Acknowledgements

I thank my mentor Stephen "Ash" Bullard (Aquatic Parasitology Laboratory, School of Fisheries, Aquaculture, and Aquatic Sciences [SFAAS], College of Agriculture [COA], Auburn University, Auburn, AL) for sharing his expertise with me and constantly pushing me to improve as a researcher. I am grateful for his unwavering curiosity and support of wherever my academic curiosity took me. I thank Ash for taking a chance on me when it felt like nobody would.

I am thankful to my committee members Nathan Whelan (United States Fish and Wildlife, SFAAS, COA, AU, Auburn, AL), Johnathon Armbruster (Auburn University), and Stephen Curran (Auburn University) for providing comments on this dissertation; specifically, Nathan for his collaboration and guidance in phylogenetic analysis and Stephen for all the help in the field and working up fish. I also thank Dr. Andrew McElwain (State University of New York Oswego, Oswego, New York) for always being open to calls to troubleshoot microtomy and histological staining techniques.

I thank my laboratory mates Micah "Brett" Warren and Haley Dutton, it is hard to imagine we started working together six years ago, and Triet Truong for their friendship, support, and assistance in the lab and field throughout the program, and John Brule and Jake Shurba for their technical assistance.

I thank Jacob Rash (North Carolina Wildlife Resources Commission) for his collaboration and providing logistical support for fish collections in North Carolina.

I thank my parents Michelle and Steven Ksepka for their love and support; specifically, my father for being one of my closest friends, spending countless hours fishing with me, and teaching me the value of working tirelessly to be the best at your craft and my mother for always

being available in times of need and showing me that regardless of where you start with enough effort there are endless oppurtunities for growth. They were some of the best role models I could have asked for. Thanks to my grandmother Mary Ormsby for always encouraging and supporting my decisions. Finally, I would like to thank the late Kenneth Naylor for being my dearest friend and fishing partner, spending endless hours on the water with me, his “never give up, never surrender” attitude, showing me life is too short to not do what you love, and fostering my love for the water.

Table of contents

List of Tables

Chapter 2

Chapter 3

List of Figures

Chapter 6

CHAPTER 1: DETECTION OF *MYXOBOLUS CERERBALIS* (HOFER, 1903) (BIVALVULIDA: MYXOBOLIDAE) IN TWO NON-*TUBIFEX TUBIFEX* OLIGOCHATES IN THE SOUTHEASTERN UNITED STATES

***Published in Diseases of Aquatic Organsisms (Available 28 January 2021)**

Authors: Steven P. Ksepka, Jacob M. Rash, Wenlong Cai, and Stephen A. Bullard

Abstract

Myxobolus cerebralis, the etiological agent of salmonid whirling disease, reportedly matures in only the oligochaete "*Tubifex tubifex"*. The concept of "*T. tubifex*" is problematic because it is renowned as a species complex (or having "strains") and many sequences ascribed to this taxon in GenBank are misidentified or indicate several cryptic species. These facts cast doubt on the long-held notion that *M. cerebralis* is strictly host specific to the single definitive host, *T. tubifex*. Herein, as part of an ongoing regional whirling disease monitoring project, oligochaetes (452 specimens) were collected from 31 riverine sites in western North Carolina (August through September 2015) and screened for infection by *M. cerebralis*. The species-specific nested PCR for *M. cerebralis* was positive for 8 oligochaete specimens from the French Broad River Basin (Mill Creek and Watauga River) and New River Basin (Big Horse Creek). We individually barcoded these *M. cerebralis*-positive oligochaete specimens using cytochrome oxidase 1 (CO1) primers and then conducted a Bayesian inference phylogenetic analysis. We identified two oligochaete genotypes: one sister to a clade comprising *Limnodrilis udekemianus* (Tubificinae: Naididae) and another sister to *Limnodrilus hoffmeisteri*. This is the first detection of *M. cerebralis* from an oligochaete in the SE United Sates and the first detection of *M. cerebralis* from an oligochaete other than *T. tubifex*. These results suggest that other non-*T. tubifex* definitive hosts can harbor the pathogen and should be considered in the context of fish hatchery

biosecurity and monitoring wild trout streams for *M. cerebralis* and whirling disease in the southeastern United States.

1. INTRODUCTION

The cartilage/bone-infecting myxozoan species, *Myxobolus cerebralis* (Hofer, 1903) (Bivalvulida: Myxobolidae), the causative agent of whirling disease, is a demonstrable pathogen of salmonids and is one of the most extensively studied species of *Myxobolus*. *Myxobolus cerebralis* has a complex life cycle using trouts (Salmoniformes: Salmonidae) as the intermediate host and the oligochaete *Tubifex tubifex* (Müller, 1774) (Tubificinae: Naididae) as the definitive host (Marki & Wolf 1983, El-Matbouli et al. 1992, Hedrick & El-Matbouli 2002). In the salmonid host, myxospores are produced asexually within the cranial cartilage until myxospores are cleared by the host or host death when they are shed by either decomposition or passing through the digestive tract of a predator (Taylor & Lott 1984, El-Matbouli & Hoffman 1991, Ksepka et al. 2020). Once shed into the environment, myxospores are consumed by *T. tubifex*. In the coelomic cavity of *T. tubifex*, actinospores are produced via sexual reproduction in pansporocysts and shed before encountering a susceptible salmonid host and thereby completing the life cycle (El-Matbouli et al. 1992, Hedrick & El-Matbouli 2002). *Myxobolus cerebralis* can infect several salmonid species; however, *T. tubifex* is the only reported oligochaete host (Bartholomew et al. 2002, Hedrick & El-Matbouli 2002, Kerans et al. 2004).

As part of an ongoing regional whirling disease monitoring project, oligochaetes (452 specimens) were collected from 31 riverine sites in western North Carolina (August through September 2015) and screened for infection by *M. cerebralis*. Eight of those oligochaetes (comprising 2 species) were positive for *M. cerebralis*, and we herein report those results and their significance.

2. MATERIALS & METHODS

During September 2015, sediment samples were collected from 31 sites in North Carolina using a shovel, placed in bags and shipped overnight to Auburn University. Upon arrival, sediment samples were emptied into sorting trays and oligochaetes were isolated, rinsed in water to remove any myxospores or actinospores from the surface of the oligochaetes, and placed into sterile vials of 95% ethanol, yielding 452 vials each containing 1 oligochaete each. Prior to DNA extraction oligochaetes were transferred from vials of 95% ethanol to presterilized 1.7 ml microcentrifuge tubes, rinsed thoroughly twice with sterile water, and transferred to presterilized 1.7 ml microcentrifuge tubes containing the ATL lysis buffer (Qiagen, Hilden, Germany). DNA was extracted from oligochaetes using the DNeasy Blood & Tissue Kit (Qiagen, Hilden, Germany) according to manufacturer protocol. Following extraction, DNA was quantified using a NanoDrop–1000 spectrophotometer (Thermo Scientific, Nanodrop Technologies), diluted to 20 ng/µl, and stored at –20 ºC. To determine the abundance of *T. tubifex* from collected oligochaetes, all samples were subjected to a *T. tubifex* specific PCR, which amplifies a region of the internal transcribed spacer 1 using primers Ttlr (5'–AGTGGGCACACGTTC–3') and ITS1A (5'–CACACCGCCCGTCGCTACTACCG–3') using thermocycling parameters that follow Hallett et al. (2005). Samples were presumed to be positive for *T. tubifex* if the expected 192 base pair fragment was detected. All samples were subsequently subjected to the *M. cerebralis* specific nested PCR.

The specificity of the species-specific nested PCR primers was checked using a Nucleotide BLAST search for each primer (listed below) with the Myxozoa as the search set. Sequences representing the most likely species to be cross reactive for each primer was downloaded,

aligned with the primer sequence, and checked by eye to determine the number and positions of base pair differences in Geneious version 11.1.5 (http://www.geneious.com).

Myxobolus cerebralis was detected in samples using species-specific nested PCR, which amplifies a region of the 18S rDNA specific to *M. cerebralis.* The target region was amplified using primers Tr3–16 (5'–GAATCGCCGAAACAATCATCGAGCTA–3') and Tr5–16 (5'–GCATTGGTTTACGCTGATGTAGCGA–3') for the first PCR cycle and Tr3–17 (5'–GGCACACTACTCCAACACTGAATTTG–3') and Tr5–17 (5'–GCCCTATTAACTAGTTGGTAGTATAGAAGC–3') for the second PCR cycle, with thermocycling conditions that followed Andree et al. (1998). Negative controls containing the PCR master mix with no template were included in each PCR reaction. Samples were presumed to be positive for *M. cerebralis* if the expected 415 base pair fragment was detected and no bands were present on the negative controls.

Samples positive for *M. cerebralis* by the species-specific nested PCR were isolated, and a region of the oligochaete cytochrome oxidase 1 (CO1) was amplified using primers LCO1490 (5'–GGTCAACAAATCATAAAGATTTGG–3') and HCO2198 (5'–TAAACTTCAGGGTGACCAAAAAATCA–3') using the following thermocycling conditions: initial denaturation step of 95 C for 5 min, followed by 35 cycles of 95 ºC for 40 sec, 44 ºC for 45 sec, and 72 ºC for 1 min, with a final extension step of 72 ºC for 8 min (Folmer et al. 1994). PCR products were purified using the QIAquick PCR Purification Kit (Qiagen, Hilden, Germany). DNA sequencing was performed by GENEWIZ (New Jersey, USA). All oligochaete sequences were deposited in GenBank.

Taxon selection for the phylogenetic analysis was based on a recent CO1 phylogeny for Tubificinae (see Vivien et al. 2017), which sequenced the posterior end of oligochaetes that first

were identified using Timm's (2009) taxonomic key and then deposited as vouchers/hologenophores (the anterior end of each sequenced specimen) in the Natural History Museum Geneva (Geneva, Switzerland). The phylogenetic analysis included 51 sequences representing 17 nominal species and 8 cryptic species of Tubificinae and included 1 species of Haplotaxidae, 1 species of Enchytraeidae, 1 species of Lumbricidae, 1 species of Lumbruculiadae, and 1 species of Naidinae as an outgroup (Vivien et al. 2017). Herein, polyphyletic, paraphyletic, and variously problematic taxa are written within quotes to highlight gaps in knowledge and/or uncertain taxonomic status. Sequences were aligned using MAFFT and trimmed to the length of the shortest sequence (611 bps) in the analysis (Katoh & Standley 2013). JModelTest2 version 2.1.10 was used to select the best–fit nucleotide substitution model using Bayesian information criteria (Darriba et al. 2012). Bayesian phylogenetic inference (BI) was performed in MrBayes version 3.2.5 (Ronquist & Huelsenbech 2003) using substitution model averaging (nst = mixed) and a gamma distribution to model rate–heterogeneity, as indicated by JModelTest. Three runs with 4 Metropolis–coupled chains were run for 5,000,000 generations. Stationarity was checked in Tracer 1.7 (Rambaut et al. 2018) and an appropriate burn–in of 25% of generations was determined. Evidence of convergence was further checked with the "sump" command in MrBayes. All parameters had a potential scale reduction factor of 1.00. A majority rule consensus tree of the post burn–in posterior distribution was generated with the "sumt" command in MrBayes. The phylogenetic tree was visualized in FigTree v1.4.3 (Rambaut et al. 2014) and edited with Adobe Illustrator (Adobe Systems).

3. RESULTS

Barcoding oligochaetes: In total, 11 of 452 (2%) oligochaetes from 5 localities across 3 river basins were identified as "*T. tubifex*" using species-specific PCR primers: 1 of 5 (20%)

oligochaetes from Stone Mountain Creek (New River Basin), 4 of 12 (33%) from Big Horse Creek (New River Basin), 2 of 33 (6%) from the Watauga River (French Broad River Basin), 2 of 21 (9%) from the Tuckasegee River (Little Tennessee River Basin), and 2 of 33 (6%) from Spring Creek (French Broad River Basin). Of these 11 oligochaete specimens, 6 (all from Big Horse Creek and Watauga River) were positive for *M. cerebralis* by nested PCR. CO1 sequences from these 6 oligochaete specimens were most similar and recovered sister to isolates of "*Limnodrilus hoffmeisteri*" Claparède, 1862 (Tubificina: Naididae) (see below), suggesting that the primers Ttlr and ITS1A are not specific to "*T. tubifex*" as reported by Hallett et al. (2005), i.e., they amplify DNA from related naidids.

Primer specificity: The nucleotide BLAST search of the *M. cerebralis* nested PCR primers Tr3–16, Tr5–16, Tr3–17, and Tr5–17 suggested that the primers are most likely to be cross reactive with *Myxidium kudoi* Meglitsch, 1937 (Bivalvulida: Myxidae), *Myxobolus toyamai* Kudo, 1917, *Kudoa igami* Shirakashi, Yamane, Ishitani, Yanagida, &Yokoyama, 2014 (Multivalvulida: Kudoidae), and *Myxobolus squamalis* Iversen, 1954 respectively. Reverse outer primer Tr3–16 differed by 10 out of 26 bps from a partial 18S rDNA sequence ascribed to *M. kudoi* (MN963994). Forward outer primer Tr5–16 differed by 8 of 26 bps from a partial 18S rDNA sequence ascribed to *M. toyamai* (HQ338729). Reverse inner primer Tr3–17 differed by 13 of 26 bps from an internal transcribed spacer 1 sequence ascribed to *K. igami* (LC382002). Forward inner primer Tr5–17 differed by 3 of 30 bps from a partial 18S rDNA sequence ascribed to *M. squamalis* (MK480606). All nested PCR primers were identical to 18S rDNA sequences ascribed to *M. cerebralis*. The *M. cerebralis* nested PCR primers are not cross reactive with any other myxozoan species with available sequence data.

Prevalance of M. cerebralis in oligochaete specimens: *Myxobolus cerebralis* was detected in 8 of 452 (2%) oligochaetes specimens: 4 of 12 (33%) from Big Horse Creek (New River Basin), 1 of 11 (9%) from Mill Creek (French Broad River Basin), and 3 of 33 (9%) from the Watauga River (French Broad River Basin). All positive oligochaetes were genotyped and included in the phylogenetic analysis. The remaining 444 oligochaetes from 28 localities were negative for *M. cerebralis* by nested PCR

Phylogenetic results: The CO1 fragments generated for nested PCR positive oligochaetes comprised 653 nucleotides (trimmed to 611 nucleotides after alignment). The recovered phylogeny was largely consistent with Vivien et al. (2017). The CO1 sequences of 7 of 8 infected oligochaetes (Tubificinae sp. 1–7) were identical and recovered within a polytomy with two "*L. hoffmeisteri"* isolates (LT905378, LN810411); differing by 6 (0.9%) and 7 (1.1%) nucleotides, respectively (Figure 1). The CO1 fragment sequence of 1 of 8 nested PCR positive oligochaetes (Tubificinae sp. 8) was recovered sister to 3 isolates of *Limnodrilus udekemianus* Claparède, 1862 (LT906433, LN810320, LT903785); differing by 90 (14.7%), 94 (15.4%), and 94 (15.4%) nucleotides, respectively (Figure 1). The *M. cerebralis*-positive oligochaetes were polyphyletic, therefore, likely not conspecific.

4. DISCUSSION

The basic comparisons we made with GenBank accessioned myxozoan sequences indicated that the *M. cerebralis* nested PCR primers do not cross react. It has been anecdotally asserted that these primers cross react with other myxozoans; however, published empirical evidence of this is wholly lacking. This is not surprising given our understanding of the diagnostic sensitivity of these primers to *M. cerebralis* and the fact that morphologically similar myxobolids do not amplify using these nested PCR primers (Andree et al. 1998, Ksepka et al. 2019) Primers Tr3–

16, Tr5–16, and Tr3–17 differed from sequences of the myxozoan species most likely to be cross reactive by 31–50% of the primer length, which is not stringent enough for these primers to amplify DNA from these species without lowering the annealing temperature to the point of PCR failure (Sommer & Tautz 1989, Lindeman et al. 1991,). The reverse inner primer Tr3–17 is the most likely primer to cross react because it only differs by 3 bps from an 18S rDNA sequence ascribed to *M. squamalis*; however, these primers were tested for cross reactivity with *M. squamalis* and did not amplify *M. squamalis* DNA (Andree et al. 1998).

Oligochaetes are currently identified using taxonomic keys with ambiguous characters, insufficient to accurately identify specimens to the species level (Holmquist 1983, Liu et al. 2017). Liu et al. (2017) found that variability in the penis and chaetae shapes of "*L. hoffmeisteri"* isolates indicated that they represent at least 10 innominate species. Holmquist (1983) noted variability in the genitalia of "*T. tubifex"* and asserted that numerous museum specimens of "*T. tubifex*" have been misidentified. This author also suggested that "*T. tubifex*" is a polytypic taxon and that the type series includes specimens of more than one species. This has led to some oligochaetes, particularly the cosmopolitan "*L. hoffmeisteri*" and "*T. tubifex*", to be represented by numerous sequences that represent misidentifications or cryptic species. Isolates of "*T. tubifex*" and "*L. hoffmeisteri*" have been recovered as polyphyletic in phylogenetic analyses, further suggesting that these sequences represent a number of cryptic species (Crottini et al. 2008, Liu et al. 2017, Vivien et al. 2017). Consistent with this, we recovered "*L. hoffmeisteri*" isolates as polyphyletic, indicating some of these isolates constitute misidentifications.

The *M. cerebralis*-positive infected oligochaetes genotyped herein comprise the first detection of *M. cerebralis* from an oligochaete other than *T. tubifex* and the first detection of *M. cerebralis* from an oligochaete in the southeast US; however, we cannot be sure that *M.*

cerebralis individuals were having sex or producing triactinomyxons in the *M. cerebralis*-positive oligochaetes. However, we also have no justification for rejecting that notion. Several factors make these findings highly significant and worthy of future experimental study. First, it has been demonstrated that two species of *Myxobolu*s can infect more than one oligochaete definitive host (Mansy & Molnár 1997, Székely et al. 1999). Mansy & Molnár (1997) exposed oligochaetes to myxospores of *Myxobolus hungaricus* Jaczó, 1940, described from the gills of *Abramis brama* (Linnaeus, 1758) (Cypriniformes: Cyprinidae), and found that actinospores developed in both *T. tubifex* and *L. hoffmeisteri*. Székely et al. (1999) exposed *T. tubifex* and *L. hoffmeisteri* to myxospores of *Myxobolus pseudodispar* Gorbunova, 1936, described from the muscle of *Rutilus rutilus* (Linnaeus, 1758) (Cypriniformes: Cyprinidae), and observed actinospore development in both species. Second, oligochaetes were kept alive for >24 hrs prior to processing, and published work indicates that myxospores can be cleared from the gut of non-susceptible oligochaetes within 4 hrs (Rodriguez et al. 2001). Third, *M. cerebralis*-infected salmonids are sympatric with *M. cerebralis*-positive oligochaetes within our sample sites in North Carolina (Ruiz et al. 2017, Ksepka et al. 2020). Finally, we have documented whirling disease in these rivers (Ksepka et al. 2020). These results are valuable in the context of biosecurity and monitoring trout streams for infections by *M. cerebralis*, as it indicates the life cycle of *M. cerebralis* can potentially be completed in the absence of *T. tubifex*.

ACKNOWLEDGEMENTS

We thank Doug Besler, Amanda Bushon, Joe Coleman, David Deaton, David Goodfred, Ken Hodges, Thomas Johnson, Kenneth Lingerfelt, Powell Wheeler, and Chris Wood (North Carolina Wildlife Resources Commission) for assisting J.M.R. with sediment collection in North Carolina and Cova Arias, Matthew Womble, Jackson Roberts, Raphael Orélis-Ribeiro, and

Carlos Ruiz (Auburn University) for initially processing the oligochaetes. This project was supported by research grants from the Alabama Department of Conservation and Natural Resources, Alabama Agricultural Research Station, and North Carolina Wildlife Resources Commission.

LITERATURE CITED

Andree K B, MacConnell E, Hedrick R P (1998). A nested polymerase chain reaction for the detection of genomic DNA of *Myxobolus cerebralis* in rainbow trout *Oncorhynchus mykiss*. Dis Aquat Org 34: 145−154

Bartholomew J L, Reno P W (2002) The history and dissemination of whirling disease. Am Fish Soc Symp 26, 1−22

Beauchamp K A, Kathman R D, McDowell T S, Hedrick R P (2001) Molecular phylogeny of tubificid oligochaetes with special emphasis on *Tubifex tubifex* (Tubificidae). Mol Phyl Evol 19: 216–224

Crottini A, Marotta R, Barbuto M, Casiraghi M, Ferraguti M (2008) The world in a river? A preliminary analysis of the 16S r DNA variability of *Tubifex* species (Clitellata: Tubificidae) from the Lambro River. Mol Phyl Evol 48: 1189–1203

Darriba, D., G. L. Taboada, R. Doallo, and D. Posada. 2012. jModelTest 2: More models, new heuristics, and parallel computing. Nat Methods 9: 772

El-Mansy A, and Molnár K (1997) Development of *Myxobolus hungaricus* (Myxosporea: Myxobolidae) in oligochaete alternate hosts. Dis Aquat Org 31: 227–232

El-Matbouli M, Hoffmann R W (1991). Effects of freezing, aging, and passage through the alimentary canal of predatory animals on the viability of *Myxobolus cerebralis* spores. J Aquat Anim Health 3: 260–262.

El-Matbouli, M, Fischer-Scherl, T, Hoffmann R W (1992) Present knowledge on the life cycle, taxonomy, pathology and therapy of some Myxosporea spp. important for freshwater fish. Annu Rev Fish Dis 3: 367–402.

El-Matbouli M, Hoffmann R W (1998) Light and electron microscopic studies on the chronological development of *Myxobolus cerebralis* to the actinosporean stage in *Tubifex tubifex*. Int J Parasitol 28: 195–217.

Folmer O, Black M, Woeh W, Lutz R, Vrijenhoek R (1994) DNA primers for amplification of mitochondrial cytochrome c oxidase subunit 1 from diverse metazoan invertebrates. Mol Mar Bio Biotech 3: 294–299

Hallett S L, Atkinson S D, Bartholomew J L (2005) Countering morphological ambiguities: development of a PCR assay to assist the identification of *Tubifex tubifex* oligochates. Hydrobiologia 543: 305–309

Hedrick R P, El-Matbouli M (2002) Recent advances with taxonomy, life cycle, and development of *Myxobolus cerebralis* in the fish and oligochaete hosts. Am Fish Soci Symp 29: 45–53

Holmquist C (1983) What is *Tubifex tubifex* (O. F. Müller) (Oligochaeta, Tubificidae)?. Zoologica Scripta 12: 187–201

Katoh K, D M Standley (2013) MAFFT multiple sequence alignment software version 7: Improvements in performance and usability. Mol Biol Evol 30: 772–780

Kerans B L, Rasmussen C, Stevens R, Colwell A E L, Winton J R (2004) Differential propagation of the metazoan parasite *Myxobolus cerebralis* by *Limnodrilus hoffmeisteri*, *Ilyodrilus templetoni*, and genetically distinct strains of *Tubifex tubifex*. J Parasitol 90: 1366–1373

Ksepka S P, Rash J M, Whelan N, Bullard S A (2019) A new species of *Myxobolus* (Myxozoa: Bivalvulida) infecting the medulla oblongata and nerve cord of brook trout *Salvelinus fontinalis* in southern Appalachia (New River, NC, USA). Parasitol Res 118: 3241–3252

Ksepka S P, Rash J M, Simcox B L, Besler D A, Dutton H R, Warren M B, Bullard S A (2020) An updated geographic distribution of *Myxobolus cerebralis* (Hofer, 1903) (Bivalvulida: Myxobolidae) and the first diagnosed case of whirling disease in wild-caught trout in the south-eastern United States. J Fish Dis 43: 813–820

Lindeman R, Hu S P, Volpato F, Trenth R J (1991) Polymerase chain reaction (PCR) mutagenesis enabling rapid non-radioactive detection of common ß-thalassaemia mutation in Mediterraneans. Br J Haematol 78: 100–104

Liu Y, Fend S V, Martinsson S, Erséus C (2017) Extensive cryptic diversity in the cosmopolitan sludge worm *Limnodrilus hoffmeisteri* (Clitellata, Naididae). Org Divers Evol 17: 477–495

Markiw M E, Wolf K (1983) *Myxosoma cerebralis* (Myxozoa: Myxosporea) etiologic agent of salmonid whirling disease requires tubificid worm (Annelida: Oligochaeta) in its life cycle. J Protozool 30: 561–564

Rambaut A, Drummond A J, Xie D, Baele G, Suchard M A (2018) Posterior summarization in bayesian phylogenetics using Tracer 1.7. *Syst Biol* 67: 901–904

Rambaut A, Suchard M A, Xie D, Drummond A J (2014) FigTree v1.4.3. Available from http://tree.bio.ed.ac.uk/software/figtree

Rodriguez P, Martinez-Madrid M, Arrate J A, Navarro E (2001) Selective feeding by the aquatic oligochaete *Tubifex tubifex* (Tubificidae, Clitellata). Hydrobiol 663: 133–140

Ronquist F, Huelsenbeck J P (2003) MrBayes 3: Bayesian phylogenetic inference under mixed models. Bioinformatics 19:1572–1574.

Ruiz C F, Rash J M, Arias C R, Besler D A, Orélis-Ribeiro R, Womble M R, Roberts J R, Warren M B, Ray C L, Lafrentz S, Bullard S A (2017) Morphological and molecular confirmation of *Myxobolus cerebralis* myxospores infecting wild-caught and cultured trout in North Carolina (SE USA). Dis Aquat Org 126: 185–198

Sommer R, Tautz D (1989) Minimal homology requiremnents for PCR primers. Nucleic Acids Res 17: 6749

Székely, C S, Molnár K, Eszterbauer E, Baska F (1999) Experimental detection of the actinospores of *Myxobolus pseudodispar* (Myxosporea: Myxobolidae) in oligochaete alternate hosts. Dis Aquatic Org 38: 219–224

Taylor R L, Lott M (1984). Transmission of salmonids whirling disease by birds fed trout infected with *Myxosoma cerebralis.* J Protozool 25, 105–106.

Timm, T. 2009. A guide to the freshwater Oligochaeta and Polychaeta of northern and central Europe. Lauterbornia 66: 1–235

Vivien R, Holzmann M, Werner I, Pawlowski J, Lafont M, Ferrari B J D (2017) Cytochrome c oxidase barcodes for aquatic oligochaete identification: development of a swiss reference database. PeerJ 5:e4122

Figure legends

Figure 1. Phylogenetic relationships of species of Tubificinae and oligochaetes infected with *Myxobolus cerebralis* (Hofer, 1903) (Bivalvulida: Myxobolidae) collected in this study reconstructed with the cytochrome oxidase 1 using Bayesian inference. Quotes indicate polyphyletic or paraphyletic taxa. Scale bar is in substitutions per site. Bold text indicates infected oligochaetes collected in this study.

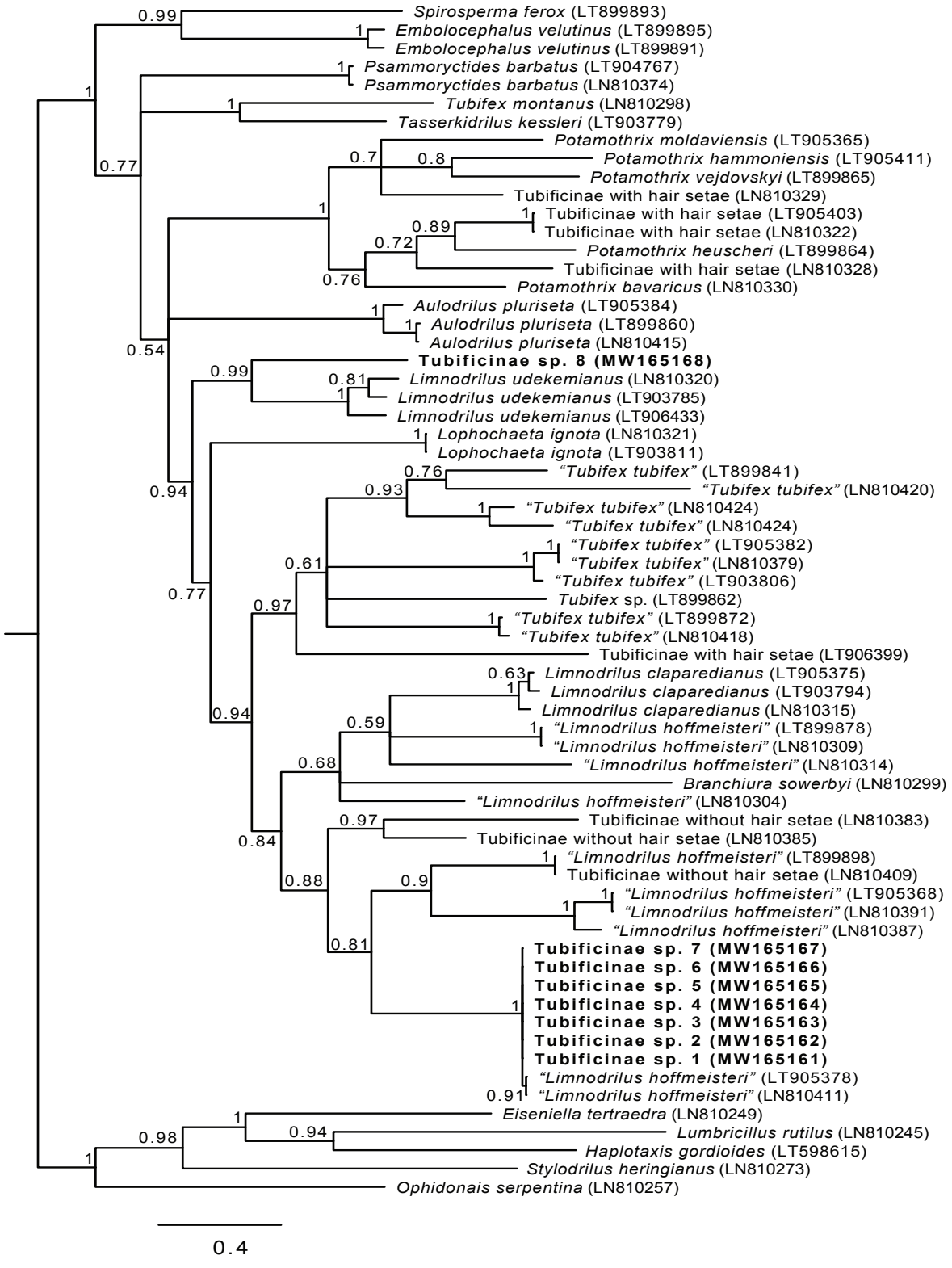
Spirosperma ferox (LT899893)
Embolocephalus velutinus (LT899895)
Embolocephalus velutinus (LT899891)
Psammoryctides barbatus (LT904767)
Psammoryctides barbatus (LN810374)
Tubifex montanus (LN810298)
Tasserkidrilus kessleri (LT903779)
Potamothrix moldaviensis (LT905365)
Potamothrix hammoniensis (LT905411)
Potamothrix vejdovskyi (LT899865)
Tubificinae with hair setae (LN810329)
Tubificinae with hair setae (LT905403)
Tubificinae with hair setae (LN810322)
Potamothrix heuscheri (LT899864)
Tubificinae with hair setae (LN810328)
Potamothrix bavaricus (LN810330)
Aulodrilus pluriseta (LT905384)
Aulodrilus pluriseta (LT899860)
Aulodrilus pluriseta (LN810415)
Tubificinae sp. 8 (MW165168)
Limnodrilus udekemianus (LN810320)
Limnodrilus udekemianus (LT903785)
Limnodrilus udekemianus (LT906433)
Lophochaeta ignota (LN810321)
Lophochaeta ignota (LT903811)
"Tubifex tubifex" (LT899841)
"Tubifex tubifex" (LN810420)
"Tubifex tubifex" (LN810424)
"Tubifex tubifex" (LN810424)
"Tubifex tubifex" (LT905382)
"Tubifex tubifex" (LN810379)
"Tubifex tubifex" (LT903806)
Tubifex sp. (LT899862)
"Tubifex tubifex" (LT899872)
"Tubifex tubifex" (LN810418)
Tubificinae with hair setae (LT906399)
Limnodrilus claparedianus (LT905375)
Limnodrilus claparedianus (LT903794)
Limnodrilus claparedianus (LN810315)
"Limnodrilus hoffmeisteri" (LT899878)
"Limnodrilus hoffmeisteri" (LN810309)
"Limnodrilus hoffmeisteri" (LN810314)
Branchiura sowerbyi (LN810299)
"Limnodrilus hoffmeisteri" (LN810304)
Tubificinae without hair setae (LN810383)
Tubificinae without hair setae (LN810385)
"Limnodrilus hoffmeisteri" (LT899898)
Tubificinae without hair setae (LN810409)
"Limnodrilus hoffmeisteri" (LT905368)
"Limnodrilus hoffmeisteri" (LN810391)
"Limnodrilus hoffmeisteri" (LN810387)
Tubificinae sp. 7 (MW165167)
Tubificinae sp. 6 (MW165166)
Tubificinae sp. 5 (MW165165)
Tubificinae sp. 4 (MW165164)
Tubificinae sp. 3 (MW165163)
Tubificinae sp. 2 (MW165162)
Tubificinae sp. 1 (MW165161)
"Limnodrilus hoffmeisteri" (LT905378)
"Limnodrilus hoffmeisteri" (LN810411)
Eiseniella tertraedra (LN810249)
Lumbricillus rutilus (LN810245)
Haplotaxis gordioides (LT598615)
Stylodrilus heringianus (LN810273)
Ophidonais serpentina (LN810257)
0.4

CHAPTER 2: TWO NEW SPECIES OF *MYXOBOLUS* BÜTSCHLI, 1882 (CNIDARIA: BIVALVULIDA: MYXOBOLIDAE) INFECTING THE GILL OF THE BLACK REDHORSE, *MOXOSTOMA DUQUESNEI* (LESEUR) (CYPRINIFORMES: CATOSDTOMIDAE) IN THE LITTLE TENNESSEE RIVER BASIN, NORTH CAROLINA

***Published in Systematic Parasitology (Available 22 October 2021)**

Authors: Steven P. Ksepka and Stephen A. Bullard

Abstract Two new species of *Myxobolus* Bütschli, 1882 (Bivalvulida: Myxobolidae) are described from the gill of the black redhorse (*Moxostoma duquesnei* [Leueur][Cypriniformes: Catostomidae]) from the Little Tennessee River Basin, North Carolina, United States. *Myxobolus branchiofilum* n. sp. infects lumen of the lamellar arterioles and *Myxobolus branchiopecten* n. sp. infects the bone and cartilage at the tip of the gill rakers. They differ from all congeners by a combination of myxospore dimensions and the presence or absence of an iodinophilic vacuole in the sporoplasm, mucous envelope, intercapsular process and sutural markings. A phylogenetic analysis of the small subunit ribosomal DNA recovered *M. branchiopectin* sister to *Myxobolus* sp. (AF378343) in a clade composed of 6 species of *Myxobolus,* which infect predominately cypriniform intermediate hosts. *Myxobolus branchiofilum* was recovered sister to *Myxobolus ictiobus* Rosser, Griffin, Quiniou, Alberson, Woodyard, Mischker, Greenway, Wise & Pote, 2016 in a clade composed of 8 species of *Myxobolus*, which predominately infect catostomid intermediate hosts. Histological sections of infected gill revealed intra-lamellar plasmodia of *M. branchiofilum* in the lumen of the lamellar arterioles and foci of *M. branchiopecten* developing in the bone and cartilage of the gill raker tip. These are the first myxozoans reported from the

black redhorse. Given that these two new species are morphologically congeneric but recovered in distantly related clades, we discuss the persistent issue of myxobolid genera paraphyly/polyphyly.

Introduction

Myxobolus Bütschli, 1882 (Bivalvulida: Myxobolidae), the most species-rich myxozoan genus, comprises >900 species infecting predominately freshwater fishes as intermediate hosts (Eiras et al., 2021). There is a lack of taxonomic information regarding species of *Myxobolus* infecting catostomids in the southeast US, with only 3 of 34 species of *Myxobolus* reported to infect catostomid fishes reported to range in the southeast US: *Myxobolus diminutus* (Rosser, Griffin, Quiniou, Alberson, Woodyard, Mischker, Greenway, Wise & Pote, 2016) Ksepka & Bullard, 2020, *Myxobolus ictiobus* Rosser, Griffin, Quiniou, Alberson, Woodyard, Mischker, Greenway, Wise & Pote, 2016 and *Myxobolus naylori* Ksepka & Bullard, 2020 (Table 1) (Eiras et al., 2005; Vidal et al., 2017; Liu et al., 2019). *Myxobolus dimintus* and *M. ictiobus* infect the gill filaments of smallmouth buffalo (*Ictiobus bubalis* [Rafinesque][Cypriniformes: Catostomidae]) and *Myxobolus naylori* was described from the stratum spongiosum of the imperiled sicklefin redhorse (*Moxostoma* sp.)(Cypriniformes: Catostomidae) (Rosser et al., 2016; Ksepka & Bullard, 2020a). No myxozoan has been reported from the black redhorse (*Moxostoma duquesnei* [Lesueur]).

Thirty-one of the 85 species of Catostomidae are endemic to the southeast US, with *Moxostoma* Rafinesque being the most species-rich catostomid genus in the region (Etnier & Starnes, 1993; Boschung & Mayden, 2004; Fricke et al., 2019). *Moxostoma* is composed of 22 species, of which 14 species are endemic to the southeast US; comprising nearly half of the

catostomid diversity in the region (Etnier & Starnes, 1993; Boschung & Mayden, 2004; Fricke et al., 2019). With the exception of the imperiled sicklefin redhorse and robust redhorse (*Moxostoma robustum* [Cope]), these species are relatively common and abundant in their range (Etnier & Starnes, 1993; Boschung & Mayden, 2004). The black redhorse is endemic to the Lower Great Lakes, Mississippi River and Mobile Bay basins, is commonly found in deep pools of small rivers, and is common throughout its range in the US, however, listed as threatened in Canada (Boschung & Mayden, 2004; Reid et al., 2008).

During a 2019 United States Fish and Wildlife survey of sicklefin redhorse to collect gametes for stock enhancement efforts in the Little Tennessee River Basin, 3 black redhorses were collected from the Oconaluftee River (35°26'46.7844"N, 83°22'58.5732"W) and examined for myxozoan infection. Myxospores consistent with *Myxobolus* were collected from the gill rakers and lumen of the lamellar arterioles (Figs. 1–4). Herein, based upon myxospore morphology, histological sections and a phylogenetic analysis, we describe two new species of *Myxobolus* infecting the gill of the black redhorse from the Oconaluftee River. The new species are the first myxozoans reported from the black redhorse.

Materials and methods

On May 7 2019, 3 black redhorses were collected from the Oconaluftee River (35°26'46.7844"N, 83°22'58.5732"W) using a boat electroshocker, placed on ice and transported to Auburn University. Upon arrival, fish were measured (mm), weighed (g), photographed and examined for myxozoan infections. Plasmodia were excised and fixed in 10% neutral buffered formalin (n.b.f) for morphology and 95% ethanol for DNA extraction. Two gill arches with infected gill

rakers and filaments, one from each black redhorse infected with both new species, were fixed in 10% n.b.f for histology. Molnar (2002) was referenced when assigning site of infection.

Myxospores were measured from n.b.f.-fixed myxospores at ×1000 magnification. Lugol's iodine and India ink were used to stain the iodiniphilic vacuole and mucous envelope respectively, per Lom & Arthur (1989). All measurements are reported in micrometers unless otherwise specified. To illustrate myxospores, plasmodia were ruptured and vortexed to suspend myxospores before a drop of the suspension was cover-slipped, inverted and placed onto a thin layer of 1% agar (Lom 1969). Illustrations were generated using 100× oil immersion objective on an Olympus BX51 compound scope equipped with 1.5× magnifier, differential interference contrast (DIC) components, and drawing tube.

After fixation, 4 infected gill rakers and filaments were excised from the n.b.f-fixed gill arches for sectioning. This yielded a total of 8 portions of tissue that were processed routinely for histology, sectioned at 4 µm, and stained with Gill's #2 hematoxylin and eosin (Luna, 1968). Ten slides were cut from each portion of tissue yielding > 400 sections on 80 slides.

DNA was extracted from one microscopically/morphologically confirmed isolate of myxospores from each site of infection from the same host, each isolate contained myxospores from a single plasmodium, using the DNeasy Blood & Tissue kit (Qiagen) following the manufacturers protocol, with the exceptions that the proteinase K incubation step was extended overnight and 100 µl of AE buffer were used for the elution step to increase DNA concentration. DNA concentration was measured using a NanoDrop-1000 spectrophotometer (Thermo Scientific, Nanodrop Technologies), diluted to 20 ng/µl and stored at -20ºC. A 1692 base pair fragment of the small subunit ribosomal DNA (SSU rDNA) was amplified using primers M153–F (5'–CATTGGATAACCGTGGGAAATCT–3') and M2192–R (5'–

TAGTAGCGACGGGCGGTGT–3') (Ksepka et al., 2019, 2020b). PCR amplification used the following thermocycler parameters: initial denaturation step of 95ºC, for 4 min, followed by 35 cycles of 95ºC for 30 s, 60ºC for 30s and 72ºC for one min, with a final extension step of 72ºC for 5 min. Sequencing primers M473–F (5'–GCTTGAGAAWCGGCTACCAC–3') and M1480–R (5'–GTGGTGCCCTTCCGTCAATTCC–3') were used to improve sequencing coverage (Ksepka et al., 2019, 2020b). PCR products were visualized on a 1% agarose gel, purified using the QIAquick PCR Purification Kit (Qiagen), and sequenced by Genewiz (South Plainfield, New Jersey). Chromatograms were assembled based on sequence overlap and proofread by eye in Geneious version 2019.2.3 (http://www.geneious.com).

Additional taxon selection for phylogenetic analysis was based on recent phylogenetic analysis of Myxobolidae in Liu et al. (2019) and Ksepka et al. (2020a) and included 51 species of Myxobolidae from "clade B" of Ksepka et al. 2020a, 16 species of Myxobolidae from "subclades III, IV, and V" of Liu et al. 2019, which were represented by sequences > 1,300 base pairs tethered to a morphological diagnosis, all available sequences of *Myxobolus* spp. infecting catostomids and 3 species of Myxidiidae as an outgroup (Liu et al., 2019; Ksepka et al., 2020a). Sequences were aligned using MAFFT with an E–INS–i alignment strategy with a maxiterate value of 1,000 in Geneious version 2021.1.1 (Katoh & Standley 2013). The alignment was trimmed to the length of the sequences presented herein (1,920 base pairs) to minimize missing data at the 5' and 3' end of the alignment. JModelTest2 version 2.1.10 was used to select best-fit models of nucleotide substitution based on Bayesian information criteria (Darriba et al., 2012). Bayesian inference was performed in MrBayes version 3.2.5 using substitution model averaging (nst=mixed) and a gamma distribution to model rate heterogeneity. Defaults were used for all other parameters. Three runs with four Metropolis-coupled chains were run for 5,000,000

generations. Stationarity was checked using Tracer 1.7 (Rambaut et al., 2018) and a burn-in of 25% of generations was determined. Evidence of convergence was further checked with the "sump" command in MrBayes. All parameters had a potential scale reduction factor of 1.00. A majority rule consensus tree of the post burn-in posterior distribution was generated with the "sumt" command in MrBayes. The phylogenetic tree was visualised in FigTree v1.4.3 (Rambaut et al., 2014) and rendered for publication with Adobe Illustrator (Adobe Systems).

Myxobolidae Thélohan, 1892

***Myxobolus* Bütschli, 1882**

Type species: *Myxobolus muelleri* Bütschli, 1882, by monotypy

***Myxobolus branchiofilum* Ksepka & Bullard n. sp. (Figs. 1, 3, 5–8, 13)**

Type host: Moxostoma duquesnei (Lesueur) (Cypriniformes: Catostomidae), black redhorse.

Type locality: Oconaluftee River (35°26'46.7844"N, 83°22'58.5732"W), Little Tennessee River Basin, North Carolina

Type material: Myxospores of *M. branchiofilum* fixed in 10% NBF (1 vial; syntype; USNM 1660504), and within paraffin sections (2 slides; syntypes; USNM 1660505– 1660506); GenBank No. (SSU rDNA: OK274149).

Site in host: Intra-lamellar plasmodia infecting the lumen of the lamellar arterioles. Intra-lamellar small-cysts, central type (LV_2) per Molnar (2002).

Prevalence: Myxospores were detected in 3 of 3 (prevalence=100%) black redhorses collected from the Oconaluftee River (35°26'46.7844"N, 83°22'58.5732"W), Little Tennessee River Basin, North Carolina

Zoobank registration: To comply with the regulations set out in Article 8.5 of the emended 2012 version of the International Code for Zoological Nomenclature (ICZN 2012), details of the new species have been submitted to ZooBank. The Life Science Identifier (LSID) for *Myxobolus branchiofilum* n. sp. is urn:lsid:zoobank.org:act:6764361E-469E-442E-A807-1731B85BCA45.

Etymology: The latin specific name "*branchiofilum*" is from "branchio" (gill) and "filum" (filament), referring to the apparent specificity to the gill lamellae.

Description

Diagnosis of myxospores (based on 55 n.b.f-fixed myxospores using differential interference contrast microscopy [10 stained with Lugol's iodine; 10 stained with India ink]; USNM coll. Nos. 1660504–1660506): Myxospore comprising 2 smooth symmetrical valves juxtaposed at sutural rim, 2 polar capsules, and sporoplasm; myxospore subspherical, 10.0–12.0 (mean ± SD = 11.4 ± 0.5; N = 51) long (Figs. 5–7), 9.0–11.0 (10.2 ± 0.6; 41) wide (Figs. 5–7), 7.0–9.0 (7.9 ± 0.6; 10) thick (Fig. 8); sutural rim with prominent seam (Fig. 5–7), 1.0 (40) thick (lateral margin in frontal view) (Figs. 5–7), 1.0 (40) thick (posterior margin in frontal view) (Figs. 5–7), without flanking lateral ridges (sutural), lacking sutural markings; polar capsules equal (Figs. 5–7), clavate (Figs. 5–7), 4.0–6.0 (5.1 ± 0.5; 80) long (Figs. 5–7), 2.0–4.0 (3.1 ± 0.4; 80) wide (Figs. 5–7), with 5–7 polar tubule coils (Figs. 5–7); sporoplasm lacking iodinophilic vacuole (Figs. 5–7), having 2 nuclei (Figs. 5–7); 4–7 (5.9 ± 1.1; 10) thick mucous envelope prominent on the rounded posterior margin (Figs. 5–7).

Taxonomic remarks

The myxospores of *M. branchiofilum* n. sp. differ from those of its 34 congeners infecting catostomids by dimensions and polar tubule coil count as well as by the absence of an intercapsular process, iodinophilic vacuole in the sporoplasm and sutural markings and the presence of a mucous envelope (Table 1). Of those 34 species, the myxospore of the new species differs from all but 5 (*Myxobolus catostomi* [Kudo, 1923], *Myxobolus discrepans* Kudo, 1919, *Myxobolus gravidus* Kudo, 1934, *Myxobolus lamellus* Grinham & Cone 1990, and *Myxobolus subcircularis* Fantham, Porter & Richardson, 1939) by myxospore dimensions and polar tubule coil number (Table 1). Of those, the myxospore of the new species differs from that of *M. catostomi* by the absence of an intercapsular process, and iodinophilic vacuole in the sporoplasm; differs from those of *M. discrepans* and *M. gravidus* by the absence of sutural markings and an iodinophilic vacuole in the sporoplasm; differs from that of *M. lamellus* by the absence of an intercapsular process and iodinophilic vacuole in the sporoplasm; and differs from that of *M. subcircularis* by the absence of an iodinophilic vacuole in the sporoplasm (Table 1).

Myxospores of 10 species of *Myxobolus* that infect non-catostomid intermediate hosts have overlapping dimensions and lack an intercapsular process, sutural markings, and an iodinophilic vacuole in the sporoplasm (Table 2). Myxospores of the new species differ from those of *M. anilii*, *M. medius* and *M. paludinosus* by being subcircular, opposed to ellipsoid or pyriform myxospores; differs from those of *M. latesi* and *M. rigida* by being longer and wider; differs from those of *M. bouixi* and *M. goreensis* by having longer polar capsules; and differs from those of *M. edellae* and *M. impressus* by having shorter polar capsules. The myxospore of the new species is most similar to that of *M. varius*, described from the kidney of silver carp (*Hypophthalmichthys molitrix* [Valenciennes][Cypriniformes: Cyprinidae]) in Russia, but differs by lacking sutural markings (Table 2).

***Myxobolus branchiopecten* Ksepka & Bullard n. sp. (Figs. 2, 4, 9–12, 14–16)**

Type host: Moxostoma duquesnei (Lesueur) (Cypriniformes: Catostomidae), black redhorse.

Type locality: Oconaluftee River (35°26'46.7844"N, 83°22'58.5732"W), Little Tennessee River Basin, North Carolina

Specimens deposited: Myxospores of *M. branchiopecten* fixed in 10% NBF (1 vial; syntype; USNM 1660507), and within paraffin sections (2 slides; syntypes; USNM 1660508– 1660509); GenBank No. (SSU rDNA: OK274150).

Site in host: Intercellular, infecting bone and cartilage of the tip of gill rakers.

Prevalence: Myxospores were detected in 2 of 3 (prevalence=66%) black redhorses collected from the Oconaluftee River (35°26'46.7844"N, 83°22'58.5732"W), Little Tennessee River Basin, North Carolina

Zoobank registration: To comply with the regulations set out in Article 8.5 of the emended 2012 version of the International Code for Zoological Nomenclature (ICZN 2012), details of the new species have been submitted to ZooBank. The Life Science Identifier (LSID) for *Myxobolus branchiopecten* n. sp. is urn:lsid:zoobank.org:act:EE12F377-33E0-4DAA-999B-53F96EA289FD.

Etymology: The latin specific name "*branchiopecten*" is from "branchio" (gill) and "pecten" (comb), referring to the apparent specificity to the gill rakers.

Description

Diagnosis of myxospores (based on 51 n.b.f.-fixed myxospores using differential interference contrast microscopy [10 stained with Lugol's iodine; 10 stained with India ink]; USNM coll.

Nos. 1660507–1660509): Myxospore comprising 2 smooth symmetrical valves juxtaposed at sutural rim, 2 polar capsules, and sporoplasm; myxospore subspherical, 8.0–11.0 (mean ± SD = 9.1 ± 0.7; N = 51) long (Figs. 9–11), 6.0–9.0 (7.6 ± 0.7; 41) wide (Figs. 9–11), 5.0–6.0 (5.8 ± 0.4; 11) thick (Fig. 12); sutural rim with prominent seam (Fig. 9–11), 1.0 (39) thick (lateral margin in frontal view) (Figs. 9–11), 1.0–2.0 (5.8 ± 0.4; 39) thick (posterior margin in frontal view) (Figs. 9–11), without flanking lateral ridges (sutural), 1.0−8.0 (4.0 ± 1.7; 39) sutural markings; polar capsules equal (Figs. 9–11), clavate (Figs. 9–11), 4.0–6.0 (4.4 ± 0.5; 78) long (Figs. 9–11), 2.0–3.0 (2.5 ± 0.5; 78) wide (Figs. 9–11), with 6–8 polar tubule coils (Figs. 9–11); sporoplasm lacking iodinophilic vacuole (Figs. 9–11), having 2 nuclei (Figs. 9–11); 2–3 (2.1 ± 0.3; 10) thick mucous envelope prominent on the rounded posterior margin (Figs. 9–11).

Taxonomic remarks

The myxospore of *M. branchiopecten* n. sp. differs from that of its 34 congeners infecting catostomids by dimensions, polar tubule coil count, and shape as well as the by the presence of sutural markings and an intercapsular process and the lack of an iodinophilic vacuole in the sporoplasm (Table 1). Of those 34 species, the myxospore of the new species differs from all but 6 (*Myxobolus congesticus* Kudo,1934, *Myxobolus microthecus* [Meglitsch, 1937], *Myxobolus naylori* Ksepka & Bullard, 2020, *Myxobolus obliquus* Kudo, 1934, *Myxobolus subcircularis* Fantham, Porter & Richardson, 1939 and *Myxobolus vastus* Kudo, 1934) by myxospore dimensions and polar tubule coil number (Table 1). Of those 6, the myxospore of the new species differs from those of *M. congesticus* and *M. vastus* by the presence of an intercapsular process and absence of an iodinophilic vacuole in the sporoplasm; differs from that of *M. microthecus* by the presence of sutural markings; and differs from that of *M. obliquus* by the absence of an

iodinophilic vacuole in the sporoplasm. The myxospore of the new species is most similar to that of *M. naylori*, which infects the stratum spongiosum of the sicklefin redhorse in North Carolina, but can be differentiated by having fewer polar tubule coils and being shorter (Table 1).

The myxospore of 8 species of *Myxobolus* have overlapping dimensions, an intercapsular process, and sutural markings and lack an iodinophilic vacuole in the sporoplasm (Table 3). Of those 8 species, the myxospore of the new species differs from those of *M. signi* and *M. smithi* by being shorter; differs from those of *M. latesi* and *M. meglitschus* by having longer polar capsules; differs from that of *M. lepturichthyes* by being longer; differs from that of *M. rigida* by being shorter, narrower, and having longer polar capsules; differs from that of *M. corneus* by having a mucous envelope; and differs from that of *M. xiaoi* by lacking the characteristic thickened suture of the myxospore of *M. xiaoi* (Table 3)

Histopathology

Plasmodia of *M. branchiofilum* n. sp. were intra-lamellar in the lumen of the lamellar arterioles of black redhorse. In all infected gill lamellae, plasmodia filled the length of the lumen of the lamellar arteriole and were wide enough to displace the neighboring gill lamellae (Fig 13). Fusion of gill lamellae was observed in regions where infected gill lamellae were in contact with the adjacent lamellae (Fig 13). Only one plasmodium was observed per lamellar arteriole.

Foci of *M. branchiopecten* n. sp. were intercellular in the bone or cartilage at the tip of the gill rakers of black redhorse (Figs. 14–16). No plasmodium was observed enveloping the myxospores. In 3 of 4 infected gill rakers, myxospores were confined to bone of the gill raker with no observable host response (Fig. 14). In 1 of 4 infected gill rakers, myxospores were observed in cartilage and loose in the dermis overlying the gill raker with an associated acute

granulomatous inflammatory response and proliferation of the dermis (Fig. 15–16). The inflammation was characterized by the presence of eosinophilic granulocytes and numerous lymphocytes as well as the proliferation of capillaries in the dermis (Fig. 16).

Phylogenetic analysis

The amplified SSU rDNA fragments of *M. branchiofilum* n. sp. and *M. branchiopecten* n. sp. comprised 1,920 nucleotides after alignment. We recovered 3 well-supported clades (A, B, and C) (Fig. 17). Consistent with Liu et al. (2019) and Ksepka et al. (2020a), catostomid infecting *Myxobolus* spp. were paraphyletic. *Myxobolus branchiofilum* was recovered sister to *M. ictiobus* ("gill filaments" of smallmouth buffalo in Mississippi) in a clade composed of 9 species of *Myxobolus* (infecting Catostomidae, Cyprinidae, Odontobutidae), including 7 of 9 species infecting catostomids in the analysis, which was recovered sister to a clade composed of species of *Myxobolus*, *Thelohanellus* Kudo, 1933 (Bivalvulida: Myxobolidae) and *Dicauda* Hoffman & Walker, 1978 (Bivalvulida: Myxobolidae) infecting cyprinids (Fig. 17). *Myxobolus branchiopecten* n. sp. was recovered within clade B sister to *Myxobolus* sp. (AF378343), collected from the white sucker (*Catostomus commersoni* [Lacepéde]) in California, in a clade composed of 6 species of *Myxobolus*, which infect 4 families of fishes (Catostomidae, Cyprinidae, Eleotridae and Gobiidae), which was recovered sister to a clade composed of 4 *Henneguya* species infecting salmonids (Fig. 17).

Discussion

Host identity and organ infected are not indicative of the phylogenetic relationships of *Myxobolus* (Andree et al., 1999; Liu et al., 2019). Both new species presented herein infect the

same organ, host species (and host individual) and geographic locality; however, they do not share a recent common ancestor. Salim & Desser (2000) described *M. xiaoi* and *Myxobolus pseudokoi* Salim & Desser, 2000 from the gill arches and lamellae, respectively, of the common shiner (*Luxilus cornutus* [Mitchill][Cypriniformes: Cyprinidae]), and have been shown to not share a recent common ancestor in phylogenetic analysis (Salim & Desser, 2000; Holzer et al., 2017; Liu et al., 2019). *Myxobolus koi* and *Myxobolus musseliusae* Liu, Whipps, Gu, Huang, He, Yang & Molnár, 2013 do not share a common ancestor; however, both infect the gill filaments of common carp (*Cyprinus carpio* Linnaeus) (Holzer et al., 2017; Liu et al., 2019). Tissue site of infection may represent a better indicator of the phylogenetic relationships among related species of *Myxobolus* (Andree et al., 1999; Eszterbauer, 2004).

Reporting the organ system or the organ as the site of infections for myxozoans potentially masks patterns in tissue site of infection when viewing phylogenetic analyses. Molnár (2002) and Blaylock et al. (2004) stressed the need for precise sites of infections when describing gill infecting myxozoans and species of *Kudoa* Meglitsch, 1947 (Multivalvulida: Kudoidae), respectively, for this reason. The presented phylogenetic analysis herein supports this, as clade C contains species that infect various organ systems (gill, skin, fins, swim bladder, muscle, kidney, liver and intestine); however, when we consider connective tissue includes blood, bone and cartilage, with exception of 4 species infecting muscle or epithelium and excluding those without adequate data on site of infection, species in this clade infect connective tissue (Fig. 17). This is particularly important when considering myxobolids reported to infect multiple organs, such as *M. erythrophthalmi*, reported to infect the kidney, liver and intestine of rudd (*Scardinius erythrophthalmus* [Linnaeus][Cyrpiniformes: Cyprinidae]). This could signify low tissue site specificity; however, plasmodia of this species develop within the lumen of the blood vessel,

suggesting that *M. erythrophthalmi* is specific to a connective tissue (blood) of the vascular system (Molnár et al., 2009). Thus, we stress the need for detailed descriptions of tissue site of infection when describing myxozoans. At present, there is no better tool for illuminating this detail than good, well-counterstained histological sections.

Herein, we recovered two species that both fit the morphological diagnosis of *Myxobolus* in separate, distantly-related clades (Fig. 17). This exemplifies a long-recognized problem of polyphyly/paraphyly of myxobolid genera, as all myxobolid genera for which we have more than a single nucleotide sequence (i.e., more than a single species is represented by a nucleotide sequence) (*Myxobolus*, *Henneguya*, *Thelohanellus*, *Unicauda* Davis, 1944 [Bivalvulida: Myxobolidae] and *Hennegoides* Lom, Tonguthai & Dykova 1991[Bivalvulida: Myxobolidae]) are routinely recovered as polyphyletic or paraphyletic (Fiala et al., 2015; Holzer et al., 2017; Liu et al., 2019; Zhang et al., 2019). We lack a sequence for the type species of *Thelohanellus*, *Unicauda* and *Hennegoides*; which is a barrier to resolving the taxonomic identities of these genera (the type species of a genus objectively defines the concept of the genus (ICZN articles 42.3 [Application of genus-group names] and 61.6 [Statement of the principal of typification]) and unambiguously identifies the phylogenetic position of the genus) (Ride et al., 2012). The consistent and repeated recovery of myxobolid genera as paryphyletic/polyphyletic from various research groups world-wide forms a strong consensus that *Thelohanellus*, *Henneguya*, *Unicauda* and *Hennegoides* should be considered junior subjective synonyms of *Myxobolus* (see Holzer et al., 2017; Liu et al., 2019; Zhang et al., 2019).

Acknowledgements We thank Dave Matthews (Tennessee Valley Authority, Knoxville, Tennessee), Jason Mays (United States Fish and Wildlife Service [USFWS], Asheville, North

Carolina), Luke Etchison and Dylan Owensby (both North Carolina Wildlife Resources Commission, Asheville, North Carolina) for helping collect black redhorse; Nathan Whelan (USFWS, Auburn, Alabama) and Brian Hickson (USFWS, Fish Health Center, Warm Springs, Georgia) for assistance with sampling logistics.

References

Andree, K. B., Székely, C., Molnár, K., Gresoviac, S. J., & Hedrick, R. P. (1999) Relationships among members of the genus *Myxobolus* (Myxozoa: Bivalvidae) based on small subunit ribosomal DNA sequences. *The Journal of Parasitology*, 85(1), 68–74.

Blaylock, R. B., Bullard, S. A., & Whipps, C. M. (2004). *Kudoa hypoepicardialis* n. sp. (Myxozoa: Kudoidae) and associated lesions from the heart of seven perciform fishes in the northern Gulf of Mexico. *The Journal of Parasitology*, 90(3), 584–593.

Boschung, H. T., & Mayden, R. L. (2004). *Fishes of Alabama*. Smithsonian Books, Washington.

Cone, D. K., Horner, R. W., & Hoffman, G. L. (1990). Description of *Myxobolus corneus* (Myxosporea): a new species from the eye of bluegill from Illinois. *Journal of Aquatic animal Health*, 2, 132–134.

Darriba, D., Taboada, G. L., Doallo, R., & Posada, D. (2012). jModelTest 2: more models, new heuristics, anf parallel computing. *Nature Methods,* 9, 772.

Davis, H. S. (1923). Studies on sporulation and development of the cysts in a new species of myxosporidia, *Lentospora ovalis. Journal of Morphology*, 37, 425–455.

Eiras, J. C., Molnar, K., & Lu, Y. S. (2005). Synopsis of species of *Myxobolus* Butschli, 1882 (Myxozoa: Myxosporea: Myxobolidae) *Systematic parasitology*, 61, 425–455.

Eiras, J. C., Zhang, J., & Molnar, K. (2014). Synopsis of species of *Myxobolus* Butschli, 1882 (Myxozoa: Myxosporea, Myxobolidae) described between 2005 and 2013. *Systematic Parasitology*, 88, 11–36.

Eiras, J. C., Cruz, C. F., Saraiva, A, & Adriano, E. A. (2021) Synopsis of the species of *Myxobolus* (Cnidaria, Myxozoa, Myxosporea) described between 2014 and 2020. *Folia Parasitologica*, 68, 012.

Etnier, D. A., & Starnes W. C. (1993) *The Fishes of Tennessee*. University of Tennessee Press, Knoxville.

Eszterbauer, E. (2004) Genetic relationships among gill-infecting *Myxobolus* species (Myxosporea) of cyprinids: molecular evidence of importance of tissue-specificity. *Diseases of Aquatic Organisms* 58, 35–40.

Fall, M., Kpatcha, K. P., Diebakate, C., Faye, N., & Toguebaye, B. S. (1997). Obervations sur des Myxosporidies (Myxozoa) du genre *Myxobolus* parasites de *Mugil cephalus* (Poisson, Teleosteen) du Senegal. *Parasite*, 2, 173–180.

Fantham, H. B., Porter, A., & Richardson, L. R. (1939). Some myxosporidia found in certain freshwater fishes in Quebec province, Canada. *Parasitology*, 31, 1–77.

Fiala, I., Bartošová-Sojková, P., & Whipps, C. M. (2015). Classification and phylogenetics of Myxozoa. In B. Okamura, A. Gruhl, & J. L. Bartholomew (Eds.), *Myxozoan Evolution, Ecology and Development* (pp. 85–110). Springer.

Fomena, A., Folefack, G. B. L., & Tang, C. I. I. (2007). New species of *Myxobolus* (Myxosporea: Myxobolidae) parasites of fresh water fishes in Cameroon (Central Africa). *Journal of Biological Sciences*, 7, 1171–1178.

Fricke, R., Eschmeyer, W. N., Van Der Laan, R. (eds) (2021). Eschmeryer's catalog of fishes: Genera, species, references. Accessed on March 5, 2021, from http://researcharchive.calacademy.org/research/ichthyology/catalog/fishcatmain.asp.

Grinham, T., & Cone, D. K. (1990). A review of *Myxobolus* (Myxosporea) parasitizing catostomid fishes, with a redescription of *Myxobolus bibullatus* (Kudo, 1934) n. comb. And description of *Myxobolus lamellus* n. sp. from *Catostomus commersoni* in Nova Scotia. *Canadian Journal of Zoology*, 68, 2290–2298.

Gurley, M. D. (1893). On the classification of the Myxosporidia, a group of protozoan parasites infecting fishes. *Bulletin of the United States Fisheries Commission*, 11, 407–420.

Ha, K. Y. (1971). Some myxosporidians of freshwater fishes of the North Vietnam. *Acta Protozooligica*, 8, 283–298.

Holzer, A. S., Bartošová-Sojková, P, Born-Torrijos, A., Lövy, Hartigan, A., & Fiala, I. (2017). The joint evolution of the Myxozoa and their alternate hosts: A cnidarian recipe for success and vast biodiversity. *Molecular Ecology*, 27, 1651–1666.

Katoh, K., & Standley, D. M. (2013). MAFFT multiple sequence alignment software version 7: improvements in performance and usability. *Molecular Biology and Evolution*, 30, 772–780.

Ksepka, S. P., Rash, J. M., Whelan, N., & Bullard, S. A. (2019). A new species of *Myxobolus* (Myxozoa: Bivalvulida) infecting the medulla oblongata and nerve cord of brook trout *Salvelinus fontinalis* in southern Appalachia (New River, NC, USA). *Parasitiology Research*, 118, 3241–3252.

Ksepka, S. P., Hickson, B. H., Whelan, N. V., & Bullard, S. A. (2020a). A new species of *Myxobolus* Butschli, 1882 (Bivalvulida: Myxobolidae) infecting stratum spongiosum of the imperiled sicklefin redhorse, *Moxostoma* sp. (Cypriniformes: Catostomidae) from the Little Tennessee River, North Carolina. *Folia Parasitologica*, 67, 2020.000.

Ksepka, S. P., Whelan, N., Whipps, C. M., & Bullard, S. A. (2020b). A new species of *Thelohanellus* Kudo, 1933 (Myxozoa: Bivalvulida) infecting the skeletal muscle of blacktail shiner, *Cyprinella venusta* Girard, 1856 (Cypriniformes: Cyprinidae) in the Chattahoochee River Basin, Georgia. *Journal of Parasitology*, 106, 350–359.

Kudo, R. (1919). Studies on Myxosporidia. A synopsis of genera and species of Myxosporidia. *Illinois Biological Monographs*, 5, 1–265.

Kudo, R. (1929). Histozoic myxosporidia found in fresh-water fishes of Illinois. *Archiv für Protistenkunde*, 65, 364–378.

Kudo, R. (1939) .Studies on some protozoan parasites of fishes of Illinois. *Illinois Biological Monographs*, 13, 7–44.

Liu, Y., Lovy, A., Gu, Z., & Fiala, I. (2019). Phylogeny of Myxoboloidae (Myxozoa) and the evolution of myxospore appendages in the *Myxobolus* clade. *International Journal of Parsitology*, 49, 523–530.

Lom, J. (1969). On a new taxonomic character of Myxosporidia, as demonstrated in descritions of two new species of *Myxobolus*. *Folia parasitologica*, 16, 97–103.

Lom, J., & Arthur, J. R. (1989). A guideline for the preparation of species descriptions in Myxosporea. *Journal of Fish Diseases*, 12, 151–156.

Lom, J., & Cone, D. K. (1996). Myxosporeans infecting the gills of the bigmouth buffalo (*Ictiobus bubalis*) in Illinois, USA. *Folia parasitologica*, 43, 37–42.

Luna, L. G. (1968). *Manual of histologic staining methods of the armed forces institute of pathology*. Third edition. McGraw–Hill, New York.

Ma, C. L. (1998). On the myxosporeans from the fishes of Sichuan Province. *Journal of the Chongqing Normal College (Natural Science Edition)*, 7, 341–352 (In Chinese).

Meglitsch, P. A. (1937). On some new and known Myxosporidia of the fishes of Illinois. *Journal of Parasitology*, 23, 467–477.

Meglitsch, P. A. (1942). *Myxosoma microthesum* n. sp. of *Minytrema melanops*. *Transaction of the American Microscopical Society*, 61, 33–35.

Molnar, K. (2002). Site preference of fish myxosporeans in the gills. *Diseases of Aquatic Organisms*, 48, 197–207.

Nigrelli, R. F. (1948). Prickle cell hyperplasia in the snout of the redhorse sucker (*Moxostoma aureolum*) associated with an infection by the myxosporidian *Myxobolus* sp. nov. *Zoologica; Scientific Contributions of the New York Zoological Society*, 33, 43–46.

Otto, G. R., & Jahn, T. L. (1943). Internal myxosporidian infections of some fishes of the Okoboji region. *Proceedings of the Illinois Academy of Science*, 50, 323–335.

Pugachev, O. N. (1980). Parasite fauna of the sucker (*Catostomus catostomus*) from the Kolyma River. *Parazitologiya*, 14, 511–513.

Rambaut, A., Suchard, M. A., Xie, D., & Drummond, A. J. (2014). FigTree v1.4.3. Available from http://tree.bio.ed.ac.uk/software/figtree.

Rambaut, A., Drummond, A. J., Xie, D., Baele, G., & Suchard, M. A. (2018). Posterior summarization in Bayesian phylogenetics using Tracer 1.7. *Systematic Biology*, 67, 901–904.

Reed, C., Basson, L., & Van As, L. L. (2002). *Myxobolus* species (Myxozoa), parasites of fishes in the Okavango River and Delta, Botswana, including descriptions of two new species. *Folia parasitological*, 49, 81–88.

Reid, S. M., Wilson, C. C., Mandrak, N. E., & Carl, L. M. (2008). Population structure and genetic diversity of black redhorse (*Moxostoma duquesnei*) in a highly fragmented watershed. *Conservation genetics*, 9, 531–536.

Rice, V. J., & Jahn, T. L. (1943). Myxosporidian parasites from the gills of some fishes of the Okoboji region. *Proceedings of the Illinois Academy of Science*, 50, 313–321.

Ride, W. D., Cogger, H. G., Dupuis C., Kraus O., Minelli A., Thompson F. C., & Tubbs, P. K. (2012) International Code of Zoological Nomenclature. Fourth edition. International Trust for Zoological Nomenclature, The Natural History Museum, London, United Kingdom.

Rosser, T. G., Griffin, M. J., Quiniou, S. M. A., Alberson, N. R., Woodyard, E. T., Mischke, C. C., Greenway, T. E., Wise, D. J., & Pote, L. M. (2016). *Myxobolus ictiobus* n. sp. (Cnidaria: Myxobolidae) from the gills of the smallmouth buffalo *Ictiobus bubalus* Rafinesque (Cypriniformes: Catostomidae). *Systematic Parasitology*, 93, 565–574.

Salim, K. Y., & Desser, S. S. (2000). Descriptions and phylogenetic systematics of *Myxobolus* spp. from cyprinids in Algonquin Park, Ontario. *Journal of Eukaryotic Microbiology*, 47, 308–318.

Sarkar, N. K. (1989). *Myxobolus anili* sp. nov. (Myxozoa: Myxosporea) from a marine teleost fish *Rhinomugil corsula* Hamiltion. *Proceedings of the Zoological Society of Calcutta*, 42, 71–74.

Shulman, S. S. (1966). *Myxosporidia of the USSR*. Nauka Publishers.

Vidal, L. P., Iannacone, J., Whipps, C. M., & Luque, J. L. (2017). Synopsis of the species of Myxozoa Grassé, 1970 (Cnidaria: Myxosporea) in the americas. *Neotropical Helminthology*, 11(2), 413–511.

Wyatt, E. J. (1979). *Facieplatycauda pratti* gen. n., sp. n. and two new species of *Myxobolus* (Myxosporidia). *International Journal of Parasitology: Parasites and Wildlife*, 8, 56–62.

Figure legends

Figs. 1, 2 Black redhorse, *Moxostoma duquesnei* (Lesueur) (Cypriniformes: Catostomidae) gill infected with plasmodia of *Myxobolus* spp. (Bivalvulida: Myxobolidae) from the Oconaluftee River, Little Tennessee River Basin, North Carolina. 1, Gill lamellae infected with *Myxobolus branchiofilum* Ksepka & Bullard n. sp. 2, Gill rakers infected with *Myxobolus branchiopecten* Ksepka & Bullard n. sp.

Figs. 3, 4 Myxospores of *Myxobolus branchiofilum* Ksepka & Bullard n. sp. (Bivalvulida: Myxobolidae) and *Myxobolus branchiofilum* Ksepka & Bullard n. sp. collected from black redhorse, *Moxostoma duquesnei* (Lesueur) (Cypriniformes: Catostomidae) from the Oconaluftee River, Little Tennessee River Basin, North Carolina; photographed with differential interference contrast optical components. 3, *Myxobolus branchiofilum* n. sp. 4, *Myxobolus branchiopecten* n. sp.

Figs. 5–8 Myxospores of *Myxobolus branchiofilum* Ksepka & Bullard n. sp. (Bivalvulida: Myxobolidae) collected from black redhorse, *Moxostoma duquesnei* (Lesueur) (Cypriniformes: Catostomidae) from Oconaluftee River, Little Tennessee River Basin, North Carolina. 5–7, frontal view. 8, sutural view. Abbreviation: sr – sutural rim; pc – polar capsule; pt– polar tubule; me – mucous envelope; n – nuclei.

Figs. 9–12 Myxospores of *Myxobolus branchiopecten* Ksepka & Bullard n. sp. (Bivalvulida: Myxobolidae) collected from black redhorse, *Moxostoma duquesnei* (Lesueur) (Cypriniformes: Catostomidae) from Oconaluftee River, Little Tennessee River Basin, North Carolina. 9–11, frontal view. 12, sutural view. Abbreviation: sr – sutural rim; ip – intercapsular process; sm – sutural markings; pc – polar capsule; pt – polar tubule; me – mucous envelope; n – nuclei.

Fig. 13–16 Histological sections (hematoxylin and eosin) of black redhorse, *Moxostoma duquesnei* (Lesueur) gill lamellae infected by *Myxobolus branchiofilum* Ksepka & Bullard n. sp. (Bivalvulida: Myxobolidae) and gill rakers infected by *Myxobolus branchiopecten* Ksepka & Bullard n. sp. 13, Infected gill lamellae showing fusion of gill lamellae (*). 14, Infected gill raker showing myxospores developing in bone. 15, Infected gill raker showing myxospores (arrows) in cartilage and proliferation of the dermis (*). 16, Proliferating dermis of gill raker showing myxospores (arrows), lymphocytes (*), eosinophilic granulocytes (arrowheads) and capillaries (C).

Fig. 17 Phylogenetic relationships of species of Myxobolidae infecting catostomids, cyprinids and genetically similar species to *Myxobolus branchiofilum* Ksepka & Bullard n. sp. (Bivalvulida: Myxobolidae) and *Myxobolus branchiopecten* Ksepka & Bullard n. sp. reconstructed with the SSU rDNA using Bayesian inference. Scale bar is in substitutions per site. New species in bold.

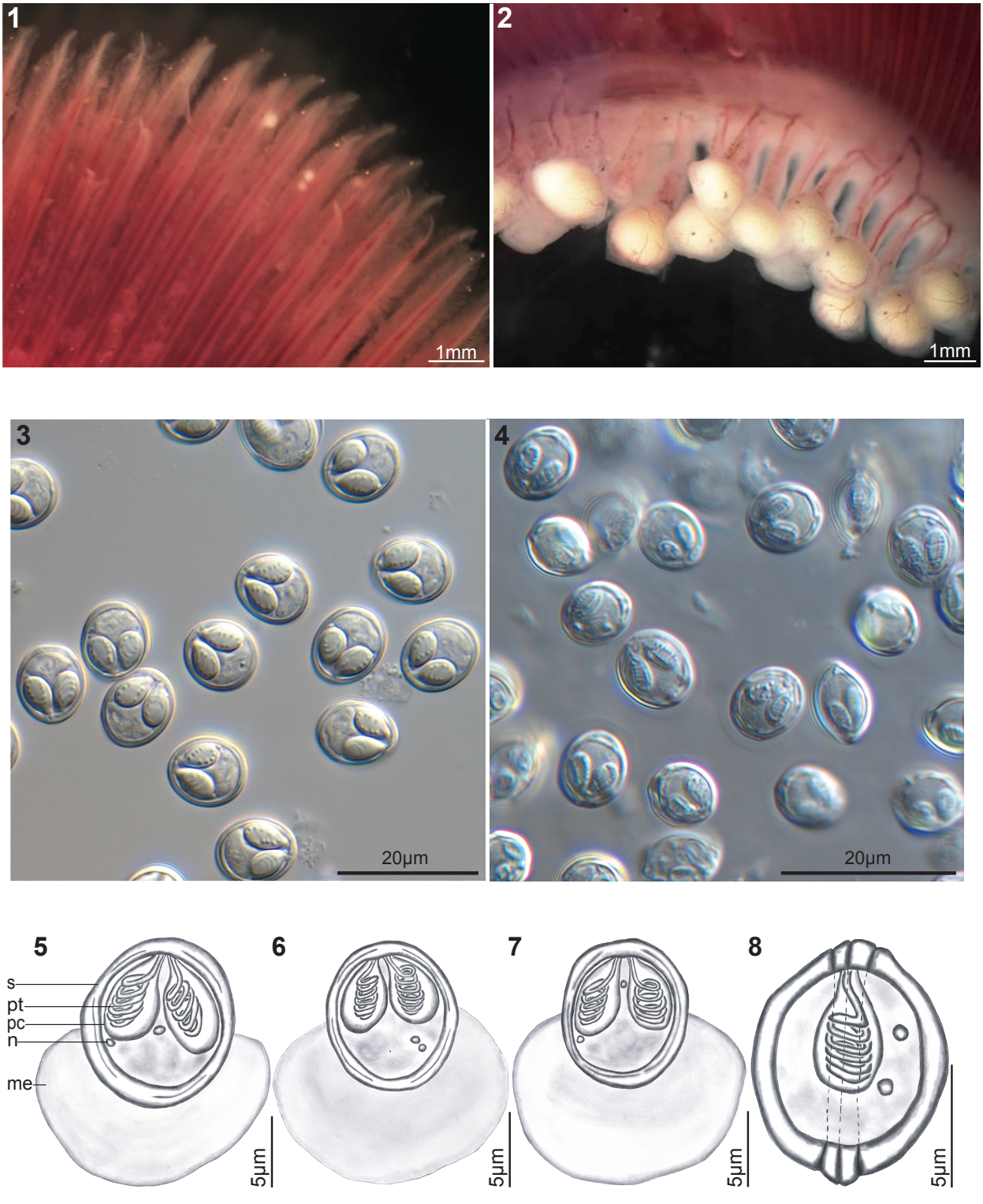
1
1mm
2
1mm
3
20µm
4
20µm
5
s
pt
pc
n
me
5µm
6
5µm
7
5µm
8
5µm

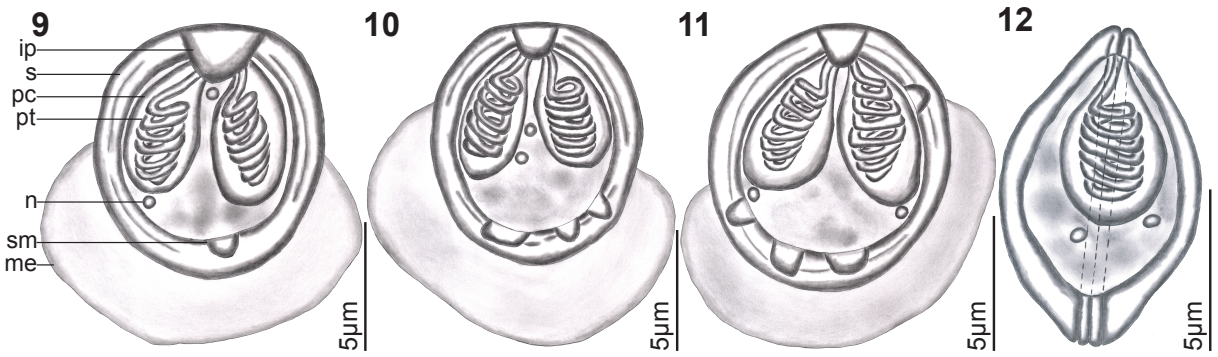
9
ip
s
pc
pt
n
sm
me
5µm
10
5µm
11
5µm
12
5µm

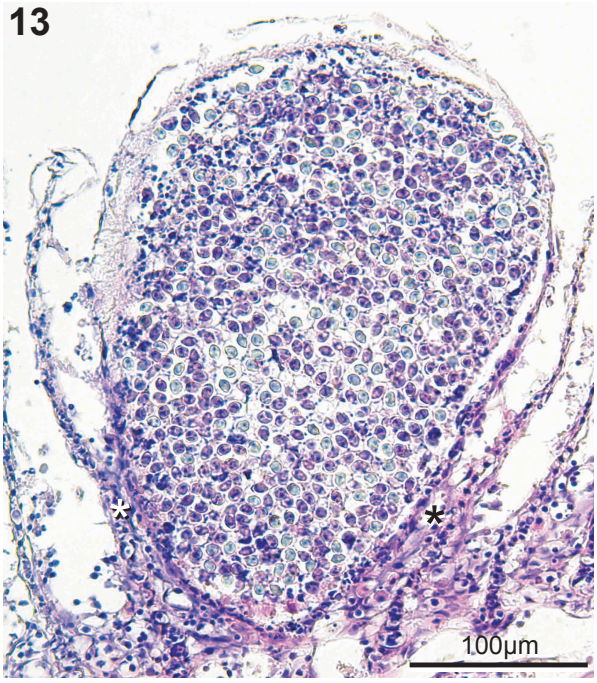
13
100µm


14
500µm

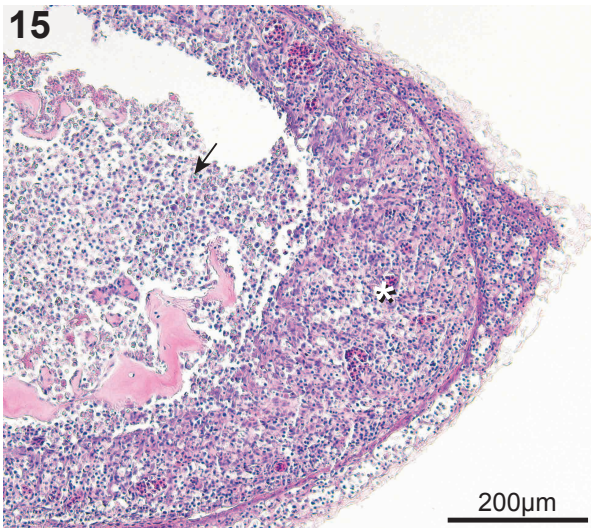
15
200µm

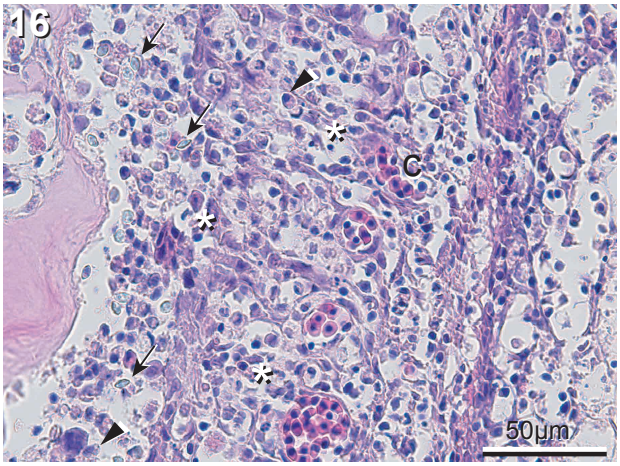
16
C
50µm

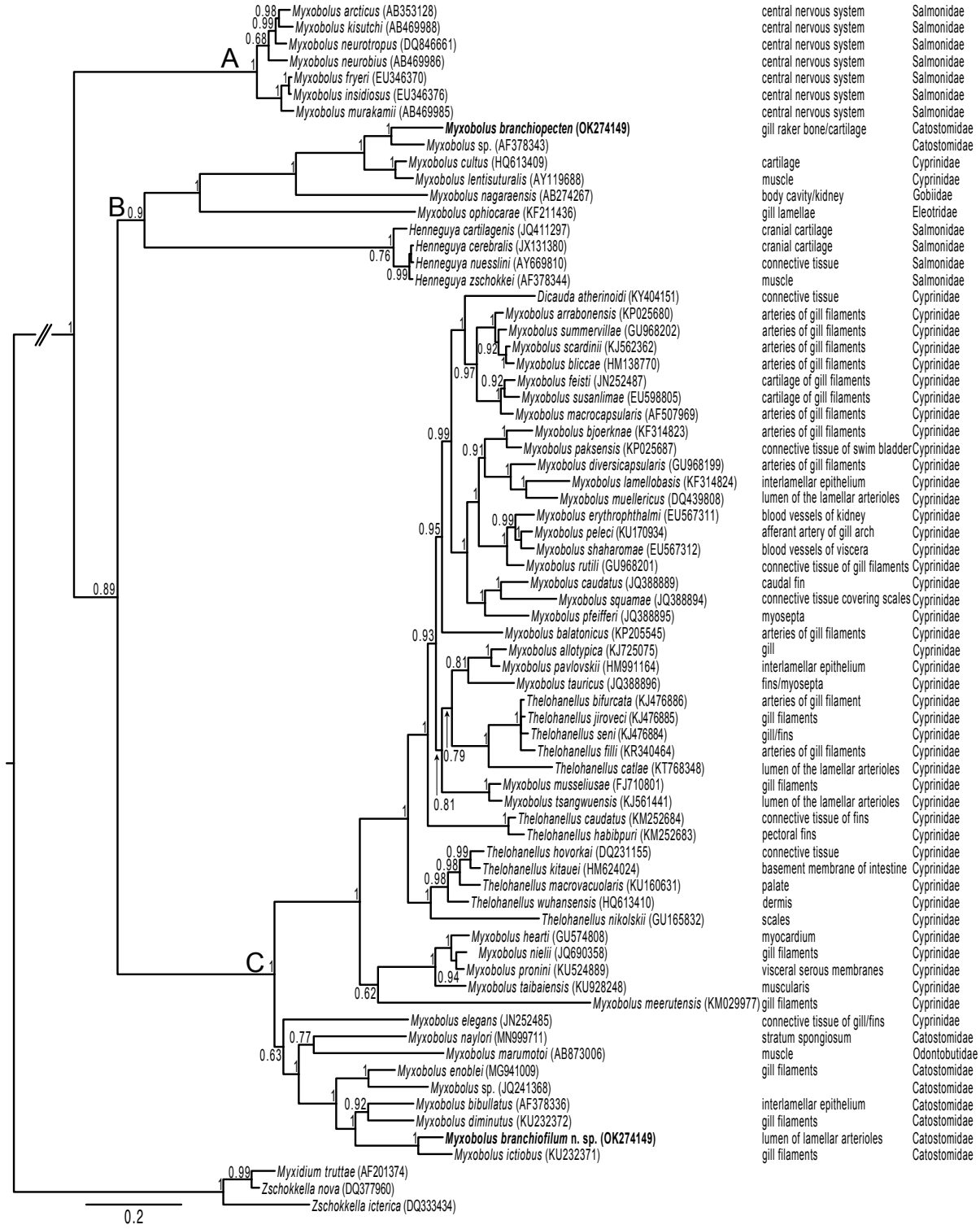
A
B
C
0.2
Myxobolus arcticus (AB353128) central nervous system Salmonidae
Myxobolus kisutchi (AB469988) central nervous system Salmonidae
Myxobolus neurotropus (DQ846661) central nervous system Salmonidae
Myxobolus neurobius (AB469986) central nervous system Salmonidae
Myxobolus fryeri (EU346370) central nervous system Salmonidae
Myxobolus insidiosus (EU346376) central nervous system Salmonidae
Myxobolus murakamii (AB469985) central nervous system Salmonidae
Myxobolus branchiopecten (OK274149) gill raker bone/cartilage Catostomidae
Myxobolus sp. (AF378343) Catostomidae
Myxobolus cultus (HQ613409) cartilage Cyprinidae
Myxobolus lentisuturalis (AY119688) muscle Cyprinidae
Myxobolus nagaraensis (AB274267) body cavity/kidney Gobiidae
Myxobolus ophiocarae (KF211436) gill lamellae Eleotridae
Henneguya cartilagenis (JQ411297) cranial cartilage Salmonidae
Henneguya cerebralis (JX131380) cranial cartilage Salmonidae
Henneguya nuesslini (AY669810) connective tissue Salmonidae
Henneguya zschokkei (AF378344) muscle Salmonidae
Dicauda atherinoidi (KY404151) connective tissue Cyprinidae
Myxobolus arrabonensis (KP025680) arteries of gill filaments Cyprinidae
Myxobolus summervillae (GU968202) arteries of gill filaments Cyprinidae
Myxobolus scardinii (KJ562362) arteries of gill filaments Cyprinidae
Myxobolus bliccae (HM138770) arteries of gill filaments Cyprinidae
Myxobolus feisti (JN252487) cartilage of gill filaments Cyprinidae
Myxobolus susanlimae (EU598805) cartilage of gill filaments Cyprinidae
Myxobolus macrocapsularis (AF507969) arteries of gill filaments Cyprinidae
Myxobolus bjoerknae (KF314823) arteries of gill filaments Cyprinidae
Myxobolus paksensis (KP025687) connective tissue of swim bladder Cyprinidae
Myxobolus diversicapsularis (GU968199) arteries of gill filaments Cyprinidae
Myxobolus lamellobasis (KF314824) interlamellar epithelium Cyprinidae
Myxobolus muellericus (DQ439808) lumen of the lamellar arterioles Cyprinidae
Myxobolus erythrophthalmi (EU567311) blood vessels of kidney Cyprinidae
Myxobolus peleci (KU170934) afferant artery of gill arch Cyprinidae
Myxobolus shaharomae (EU567312) blood vessels of viscera Cyprinidae
Myxobolus rutili (GU968201) connective tissue of gill filaments Cyprinidae
Myxobolus caudatus (JQ388889) caudal fin Cyprinidae
Myxobolus squamae (JQ388894) connective tissue covering scales Cyprinidae
Myxobolus pfeifferi (JQ388895) myosepta Cyprinidae
Myxobolus balatonicus (KP205545) arteries of gill filaments Cyprinidae
Myxobolus allotypica (KJ725075) gill Cyprinidae
Myxobolus pavlovskii (HM991164) interlamellar epithelium Cyprinidae
Myxobolus tauricus (JQ388896) fins/myosepta Cyprinidae
Thelohanellus bifurcata (KJ476886) arteries of gill filament Cyprinidae
Thelohanellus jiroveci (KJ476885) gill filaments Cyprinidae
Thelohanellus seni (KJ476884) gill/fins Cyprinidae
Thelohanellus filli (KR340464) arteries of gill filaments Cyprinidae
Thelohanellus catlae (KT768348) lumen of the lamellar arterioles Cyprinidae
Myxobolus musseliusae (FJ710801) gill filaments Cyprinidae
Myxobolus tsangwuensis (KJ561441) lumen of the lamellar arterioles Cyprinidae
Thelohanellus caudatus (KM252684) connective tissue of fins Cyprinidae
Thelohanellus habibpuri (KM252683) pectoral fins Cyprinidae
Thelohanellus hovorkai (DQ231155) connective tissue Cyprinidae
Thelohanellus kitauei (HM624024) basement membrane of intestine Cyprinidae
Thelohanellus macrovacuolaris (KU160631) palate Cyprinidae
Thelohanellus wuhansensis (HQ613410) dermis Cyprinidae
Thelohanellus nikolskii (GU165832) scales Cyprinidae
Myxobolus hearti (GU574808) myocardium Cyprinidae
Myxobolus nielii (JQ690358) gill filaments Cyprinidae
Myxobolus pronini (KU524889) visceral serous membranes Cyprinidae
Myxobolus taibaiensis (KU928248) muscularis Cyprinidae
Myxobolus meerutensis (KM029977) gill filaments Cyprinidae
Myxobolus elegans (JN252485) connective tissue of gill/fins Cyprinidae
Myxobolus naylori (MN999711) stratum spongiosum Catostomidae
Myxobolus marumotoi (AB873006) muscle Odontobutidae
Myxobolus enoblei (MG941009) gill filaments Catostomidae
Myxobolus sp. (JQ241368) Catostomidae
Myxobolus bibullatus (AF378336) interlamellar epithelium Catostomidae
Myxobolus diminutus (KU232372) gill filaments Catostomidae
Myxobolus branchiofilum n. sp. (OK274149) lumen of lamellar arterioles Catostomidae
Myxobolus ictiobus (KU232371) gill filaments Catostomidae
Myxidium truttae (AF201374)
Zschokkella nova (DQ377960)
Zschokkella icterica (DQ333434)

Table 1. Comparison of *Myxobolus* spp. that infect species of Catostomidae. Mean measurements with range provided in µm. *MXL,* myxospore length; *MXW,* myxospore width; *MXT,* myxospore thickness; *PCL*, polar capsule length; *PCW,* polar capsule width; *PFC,* polar filament coils; *ME,* mucous envelope (present or absent); *IV*, iodinophilic vacuole in sporoplasm (present or absent); *SM*, sutural markings (present or absent); *IP*, intercapsular process (present or absent).

Species	Host	MXL	MXW	MXT	PCL	PCW	PFC	ME	IV	SM	IP	Site*	Locality	Reference
M. bellus Kudo, 1934	*Carpiodes carpio* (Rafinesque)	10.0–11.0	6.5–7.0	4.0–5.0	4.0–5.0	1.5–2.0	9–11	–	P	P	A	1	Illinois, USA	Kudo, 1934
M. bibullatus (Kudo, 1934)	*Catostomus commersonii* (Lacepède)	14.0–15.0	11.5–12.5	6.0–7.5	7	3.5	–	–	A	P	A	1	Illinois, USA	Kudo, 1934
M. branchiofilum n. sp. Ksepka et Bullard	*Moxostoma duquesnei* (Leseueur)	11.4; 10.0–12.0	10.2; 9.0–11.0	7.9; 7.0–9.0	5.1; 4.0–6.0	3.1; 2.0–4.0	5–7	A	A	A	A	2	North Carolina, USA	Present study
M. branchiopectin n. sp. Ksepka & Bullard	*Moxostoma duquesnei* (Lesueur)	9.1; 8.0–11.0	7.6; 6.0–9.0	5.8; 5.0–6.0	4.4; 4.0–6.0	2.5; 2.0–3.0	6–8	P	A	P	P	3	North Carolina, USA	Present study
M. bubalis Otto & Jahn, 1943	*Ictiobus bubalus* (Rafinesque)	13.1–14.7	10.2–11.7	–	5.8–6.3	2.2–2.9	6–7	–	P	P	P	4	Iowa, USA	Otto & Jahn, 1943
M. catostomi (Kudo, 1923)	*Catostomus commersoni* (Lacepède)	11.8–14.5	6.8–9.5	–	4.5–5.8	1.3–3.2	–		P	A	P	5	Canada	Kudo, 1923
M. commersoni (Fantham, Porter & Richardson, 1939)	*Catostomus commersonii*	9.5–16.5	7–11.4	–	7.7	3.2	–	–	A	A	A	1	Québec, Canada	Fantham et al., 1939
M. congesticus Kudo, 1934	*Moxostoma anisurum* (Cope)	9.0–10.0	8.5–9.5	6.0	5.0–6.0	2.5–3.5	–	–	P	P	A	6	Illinois, USA	Kudo, 1934
M. conspicuus Kudo, 1929	*Moxostoma breviceps* (Cope)	9.0–11.5	6.5–8.0	4.5–5.5	5.0–7.0	2.0–2.5	10	–	P	P	A	7	Illinois, USA	Kudo, 1929
M. diminutus nom. nov. (Rosser, Griffin, Quiniou, Alberson, Woodyard, Mischker, Greenway, Wise & Pote, 2016)	*Ictiobus bubalus*	8.6; 7.4–9.6	8.8; 7.5–9.9	6.7; 6.5–7.3	4.3; 3.6–4.9	3.3; 2.8–3.8	5–6	–	A	A	A	1	Mississippi, USA	Rosser et al., 2016
M. discrepans Kudo, 1919	*Carpiodes velifer* (Rafinesque)	11.4–13.5	9.5–11.0	8.5–9.5	5.5–6.0	3.5–4.0	–	–	P	P	A	1	Illinois, USA	Kudo, 1919
M. ellipticoides (Fantham, Porter & Richardson, 1939)	*Catostomus commersonii*	11.4–14.1	6.8–8.2	–	4.5–5.9	1.8–3.2	–	–	A	A	A	7	Québec, Canada	Fantham et al., 1939
M. endovasus (Davis, 1947)	*Ictiobus bubalus*	14.3; 13.1–15.4	13.0; 12.2–13.8	8.5	8.7; 7.7–9.6	5.5; 5.0–6.2	5–7	A	P	A	P	1	Illinois, USA	Lom and Cone, 1996

M. enoblei Lom & Cone, 1996	*Ictiobus bubalus*	14.4; 13.5–15.0	11.1; 10.5–11.5	7.5	8.3; 7.9–8.5	4.8; 4.5–5.5	6–7	A	A	P	P	1	Illinois, USA	Lom and Cone, 1996
M. exsulatus Pugachev, 1980	*Catostomus catostomus* (Forster)	9.7–9.9	9.0–9.1	–	5.4–5.6	3.0	–	–	P	A	P	1	Russia	Pugachev, 1980
M. filamentus (Rice & Jahn, 1943)	*Ictiobus bubalus*	16.3	13.2	–	7.8	6.2	8	–	A	A	P	1	Iowa, USA	Rice and Jahn, 1943
M. globosus Gurley, 1893	*Erimyzon sucetta* (Lacepède)	7.0–8.0	6.0	5.0	–	–	–	–	P	A	A	1	Illinois, USA	Gurley 1893
M. gravidus Kudo, 1934	*Moxostoma anisurum*	12.0–14.0	9.5–10.0	7.0	5.0–5.5	2.5	–	–	P	P	A	1	Illinois, USA	Kudo 1934
M. ictiobus Rosser, Griffin, Quiniou, Alberson, Woodyard, Mischke, Greenway, Wise & Pote, 2016	*Ictiobus bubalus*	13.9; 12.7–14.5	12.5; 10.7–13.6	12.6; 10.3–14.8	6.6; 5.6–7.4	4.5; 3.7–4.9	5–6	–	A	A	A	8	Mississippi, USA	Rosser et al., 2016
M. kozloffi Wyatt, 1979	*Deltistes luxatus* (Cope)	13.5; 13.5–15.5	8.6; 8.0–9.5	7.2; 6.5–7.5	7.7; 7.5–8.5	3.2; 3.0–3.5	–	–	P	P	A	9	Oregon, USA	Wyatt, 1979
M. lamellus Grinham & Cone, 1990	*Catostomus commersonii*	12.0; 9.5–13.5	10.5; 9.0–12.0	7.0; 5.0–8.0	6.0; 5.0–7.0	3.5; 3.0–4.5	5–6	A	P	A	P	8	Nova Scotia, Canada	Grinham and, Cone 1990
M. meglitschi (Meglitsch, 1937)	*Carpiodes cyprinus* (Lesueur)	12.0–14.0	11.0–13.0	7.0–8.5	6.0–7.0	3.0–4.0	6	–	A	A	A	8	Illinois, USA	Meglitsch, 1937
M. microthecus (Meglitsch, 1942)	*Minytrema melanops* (Rafinesque)	11.7; 10.0–12.5	10.2; 8.3–11.4	4.5; 4.3–5.2	5.5; 3.8–6.3	2.4; 1.9–3.2	5–7	–	A	A	P	10	Illinois, USA	Meglitsch, 1942
M. morrisonae Lom & Cone, 1996	*Ictiobus bubalus*	10.0; 9.6–10.5	9.5; 9.1–10.3	5.0	5.5; 5.3–5.8	3.7; 3.4–4.0	6	A	A	P	P	8	Illinois, USA	Lom and Cone, 1996
M. moxostomi Nigrelli, 1948	*Moxostoma macrolepidotum* (Lesueur)	7.6; 6.2–9.4	7.2; 5.5–9.4	3.9; 3.1–4.7	3.6; 2.3–3.9	2.3; 1.6–3.2	3–5	–	P	A	A	1	New York Aquarium	Nigrelli, 1948
M. multiplicatus (Reuss, 1906)	*Ictiobus bubalus*	12.0; 12.0–12.5	9.5; 9.2–9.5	6.0; 6.0–6.5	4.0; 3.5–4.5	2.2; 2.0–2.5	–	–	A	P	A	8	Iowa, USA	Rice and Jahn, 1943
M. musculosus (Kudo, 1923)	*Catostomus commersonii*	13.0–15.0	10.0–11.5	8.0–8.5	5.0–6.0	2.5–3.3	6	–	A	P	A	11	Michigan, USA	Kudo, 1923
M. naylori Ksepka & Bullard 2020	*Moxostoma* sp., sicklefin redhorse	10.8; 10.0–12.0	8.2; 7.0–9.0	5.5; 5.0–6.0	4.8; 4.0–6.0	2.9; 2.0–3.0	7–10	P	A	P	P	12	North Carolina, USA	Ksepka et al., 2020a
M. obliquus Kudo, 1934	*Carpiodes velifer*	8.0–9.0	7.0–8.0	5.0–6.0	4.5	2.0	6–7	–	P	P	P	11	Illinois, USA	Kudo, 1934
M. oblongus Gurley, 1893	*Erimyzon sucetta*	14.0–17.0	8.5	5.5–6.0	–	–	–	–	A	A	A	1	Illinois, USA	Gurley, 1893

M. ovalis (Davis, 1923)	*Ictiobus bubalus*	15.0–17.0	15	11.0	8.0–9.0	6.0	4–6	–	A	A	A	8	Iowa, USA	Davis, 1923
M. ovatus Kudo, 1934	*Ictiobus bubalus*	11.5–13.0	9.0–10.0	7.0	5.5–6.5	2.5–3.0	10	–	P	P	A	1	Illinois, USA	Kudo, 1934
M. pratti (Wyatt, 1979)	*Deltistes luxatus*	18.2; 17.0–20.5	12.6; 11.0–14.0	7.9; 7.5–8.5	6.6; 5.5–7.5	3.2; 2.5–3.5	6–8	–	P	A	A	9	Oregon, USA	Wyatt, 1979
M. subcircularis Fantham, Porter & Richardson, 1939	*Catostomus commersonii*	9.1–11.8	8.2–10.0	–	3.2–5.0	1.8–3.0	–	–	P	A	A	5	Québec, Canada	Fantham et al., 1939
M. transovalis Gurley, 1893	*Clinostomus funduloides* Girard	6.0–7.0	8.0	–	–	–	–	–	P	A	A	11	Virginia, USA	Gurley 1893
M. vastus Kudo, 1934	*Moxostoma macrolepidotum*	9.5–10.5	7.5–8.0	4.0–4.5	4.5–5.5	1.5–2.5	–	–	P	P	A	1	Illinois, USA	Kudo, 1934

*Site: 1, skin; 2, gill filaments; 3, gill rakers; 4, intestine; 5, muscle; 6, fins; 7, dermis; 8, gill; 9, kidney; 10, mesentery; 11, muscle; 12, stratum spongiosum.

Table 2. Comparison of *Myxobolus* spp. that infect non-catostomids and are morphologically similar to *Myxobolus branchiofilum* n. sp. Mean measurements with range provided in µm. *MXL,* myxospore length; *MXW,* myxospore width; *MXT,* myxospore thickness; *PCL*, polar capsule length; *PCW,* polar capsule width; *PFC,* polar filament coils; *ME,* mucous envelope (present or absent); *IV*, iodinophilic vacuole in sporoplasm (present or absent); *SM*, sutural markings (present or absent); *IP*, intercapsular process (present or absent).

Species	Host	MXL	MXW	MXT	PCL	PCW	PFC	ME	IV	SM	IP	Site*	Locality	Reference
M. anili Sarkar, 1989	*Rhinomugil corsula* (Hamilton)	10.7; 9.8–11.6	8.6; 7.9–9.8	–	4.8; 4.7–5.0	3.0; 2.4–3.1	5–6	A	A	A	A	1, 2	India	Sarkar, 1989
M. branchiofilum n. sp. Ksepka & Bullard	*Moxostoma duquesnei* (Leseur)	11.4; 10.0–12.0	10.2; 9.0–11.0	7.9; 7.0–9.0	5.1; 4.0–6.0	3.1; 2.0–4.0	5–7	A	A	A	A	3	North Carolina, USA	Present study
M. bouixi Fomena, Folefack, & Tang, 2007	*Chrysichthys nigrodigitatus* (Lacepede)	11.2; 10.8–12.0	10.1; 9.0–10.5	–	4.4; 4.0–5.0	3.1; 3.0–3.5	5–7	–	A	A	A	4	Cameroon	Fomena et al., 2007
M. edellae Sarkar, 1999	*Ctenopharyngodon idella* (Valenciennes)	10.7; 10.5–11.5	9.4; 9.0–10.0	–	6.1; 5.5–6.5	3.1; 2.5–3.5		–	–	–	A	5	India	Eiras et al., 2014
M. goreensis Fall, Kpatcha, Diebakate, Faye & Toguebaye, 1997	*Mugil cephalus*	10.9; 10.0–13.0	10.9; 10.0–13.0	–	4.1; 4.0–5.0	3.1; 2.0–4.0	6	–	A	A	A	6	Senegal	Fall et al., 1997
M. impressus Miroshnichenko, 1980	*Barbus barbus* (Bleeker)	10.5–13.7	9.2–11.0	6.0–7.5	5.5–6.8	2.8–4.0	–	–	–	–	–	6,7	Ukraine	Eiras et al., 2005
M. latesi Kostoïngué & Toguebaye, 1994	*Lates niloticus* (Linnaeus)	9.8; 9.0–10.5	7.7; 6.0–8.0	–	3.7; 2.7–4.5	2.5; 2.3–2.8	–	–	–	–	–	6, 8	Chad	Eiras et al., 2005

M. medius (Fantham, Porter & Richardson, 1939)	*Luxilus cornutus* (Mitchill)	11.0–16.8	7.0–10.4	–	5.0–8.2	1.8–3.2	–	–	A	A	A	9	Canada	Fantham et al., 1939
M. paludinosus Reed, Basson & Van As, 2002	*Enteromius paludinosus* (Peters)	12.0; 11.2–13.7	8.6; 7.5–10.0	–	5.7; 5.0–6.8	2.4; 2.0–2.5	6–7	–	A	A	A	6	Botswana	Reed et al., 2002
M. rigida Sarkar, 1999	*Amblypharyngodon mola* (Hamilton)	10.8; 10.0–11.0	8.6; 7.5–9.5	–	6.3; 5.5–7.0	3.6; 3.0–4.0	–	–	–	–	–	5	India	Eiras et al., 2014
M. varius Akhmerov, 1960	*Hypophthalmichthys molitrix* (Valenciennes)	9.0–11.0	6.0–11.5	–	4.5–5.0	2.0–3.5	–	–	A	P	A	5	Amur Basin	Shulman, 1966

*Site: 1, intestine; 2, mesentery; 3, gill lamellae; 4, gill arch; 5, kidney; 6, gill; 7, fins; 8, liver; 9, spleen.

Table 3. Comparison of *Myxobolus* spp that infect non-catostomids and are morphologically similar to *Myxobolus branchiopectin* n. sp. Mean measurements with range provided in µm. *MXL,* myxospore length; *MXW,* myxospore width; *MXT,* myxospore thickness; *PCL*, polar capsule length; *PCW,* polar capsule width; *PFC,* polar filament coils; *ME,* mucous envelope (present or absent); *IV*, iodinophilic vacuole in sporoplasm (present or absent); *SM*, sutural markings (present or absent); *IP*, intercapsular process (present or absent).

Species	Host	MXL	MXW	MXT	PCL	PCW	PFC	ME	IV	SM	IP	Site*	Locality	Reference
M. albovae Krassilnikova in Shulman, 1966	*Squalius cephalus* (Linnaeus)	10.5–13.0	8.0–9.8	6.0–6.5	4.8–5.5	2.7–3.3	–	–	P	A	P	1	Russia	Shulman, 1966
M. branchiopectin n. sp. Ksepka & Bullard	*Moxostoma* duquesnei (Leseur)	9.1; 8.0–11.0	7.6; 6.0–9.0	5.8; 5.0–6.0	4.4; 4.0–6.0	2.5; 2.0–3.0	6–8	P	A	P	P	2	North Carolina, USA	Present study
M. clariae Hemananda, Mohilal, Bandyopadhyay & Mitra, 2009	*Clarias batrachus* (Hamilton)	10.5; 10.2–11.5	7.0; 6.8–7.7	–	3.7; 3.4–4.3	2.4; 1.7–2.6	–	A	P	A	P	3	India	Hemananda et al., 2009
M. corneus Cone, Horner & Hoffman, 1990	*Lepomis macrochirus* Rafinesque	9.4; 8.0–10.5	8.0; 6.5–9.0	–	5.3; 4.0–5.5	2.4; 2.5–3.0	7–8	A	A	P	P	4	Illinois, USA	Cone et al., 1990
M. dermitis (Haldar, Mukherjee & Kundu, 1981)	*Labeo rohita* (Hamilton, 1822)	10.3; 9.0–11.0	9.4; 8.0–10.0	–	4.4; 4.0–5.0	2.2; 2.0–3.0	6	A	A	A	P	5	India	Haldar et al., 1981
M. gallaicus Iglesias, Parama, Alvarez, Leiro & Sanmartin, 2001	*Psuedochondrostoma polylepis* (Steindachner)	10.0; 8.5–11.0	8.8; 8.2–9.5	5.7; 5.0–6.0	4.9; 4.5–5.5	2.9;2.7 –3.0	7–8	P	P	P	P	1	Spain	Iglesias et al., 2001
M. garrae Ma, Dong & Wang, 1982	*Ageneiogarra imberba* (Garman)	9.4; 8.8–9.6	8.6; 8.0–9.6	6.1; 5.6–6.4	4.1; 4.0–4.5	2.4; 2.2–2.6	–	P	P	P	P	1	China	Ma et al., 1982

M. gibelio Yukhimenko, 1956	*Carassius gibelio* (Bloch)	10.5–12.6	7.4–10.0	6.0	3.6–5.3	2.6–3.5	–	–	P	P	P	1, 6, 7	China	Yukhimenko, 1956
M. hoshinai (Hoshina, 1953)	*Cyprinus carpio* (linnaeus)	11.4; 9.7–13.4	9.3; 7.9–10.9	6.6; 5.4–7.7	4.5; 3.5–5.1	2.8; 2.3–3.6	6	–	P	P	P	8	Japan	Hoshina, 1953
M. hwangshihensis Nie & Lie, 1992	*Xenocypris macrolepis* (Bleeker)	8.4–9.6	7.0–7.8	5.0	5.0–6.0	2.4–2.8	–	–	P	A	P	7, 9	China	Nie & Lie, 1992
M. irinae Daniyarov, 1975	*Luciobarbus capito* (Güldenstädt)	9.4–10.6	7.0–7.7	–	4.0–5.9	2.4–3.0	–	–	P	A	P	7	Central Asia	Eiras et al., 2005
M. latesi Kostoïngué & Toguebaye, 1994	*Lates niloticus* (Linnaeus)	9.8; 9.0–10.5	7.7; 6.0–8.0	–	3.7; 2.7–4.5	2.5; 2.3–2.8	–	–	–	–	–	1, 10	Chad	Eiras et al., 2005
M. lepturichthys Ma, 1998	*Lepturichthys nicholsi* (Günther)	8.7; 7.0–9.4	7.8; 5.8–8.7	5.7; 5.6–5.8	4.1; 3.9–4.2	2.8	–	–	P	P	P	7	China	Ma, 1998
M. leshanensis Ma & Zhao, 1993	*Onychostoma angustistomatum* (Fang)	10.4; 9.6–12.0	8.5; 8.0–8.8	5.2; 4.8–5.6	4.9; 4.8–5.2	2.0; 1.8–2.4	–	–	P	A	P	7	China	Ma & Zhao, 1992
M. lomi Donec & Kulakovskaya in Shulman, 1962	*Phoxinus phoxinus* (Linnaeus)	9.0–13.0	7.0–9.0	5.8–7.9	4.0–7.0	2.0–2.7	–	P	P	A	P	1	Danube	Shulman, 1966
M. lotae Mitenev, 1971	*Lota lota* (Linnaeus)	8.4–10.4	6.2–6.5	–	3.4–4.4	2.3–3.4	–	–	P	A	P	1	Russia	Mitenev, 1971
M. macrocapsularis Reuss, 1906	*Blicca bjoerkna* (Linnaeus)	9.0–14.5	6.0–9.9	4.5–6.0	5.0–8.6	2.4–3.6	–	A	P	A	P	1	Russia	Eiras et al., 2005
M. megalobromae Wu & Li, 1986	*Megalobrama amblycephala* Yih	8.9; 8.8–9.3	8.6; 8.4–8.9	5.4; 4.8–5.7	4.2; 3.8–4.3	2.8; 2.6–3.1	–	–	P	P	P	10	China	Wu & Li, 1986
M. meglitschus Sarkar, 1996	*Notopterus notopterus* (Pallas)	8.8; 8.0–9.5	6.9; 6.0–7.5	–	4.4; 3.5–5.0	2.0; 1.5–3.0	5–7	–	–	–	P	1	India	Eiras et al, 2014
M. mesopotamiae Molnar, Masoumia & Abasi, 1996	*Arabibarbus grypus* (Heckel)	9.2; 8.9–9.4	8.1; 7.8–8.5	5.8; 5.2–6.0	3.8; 3.6–4.2	2.5; 2.4–2.7	7	A	P	A	P	6	Iran	Molnar et al., 1996
M. microthecus (Meglitsch, 1942)	*Minytrema melanops* (Rafinesque)	11.7; 10.0–12.5	10.2; 8.3–11.4	4.5; 4.3–5.2	5.5; 3.8–6.3	2.4; 1.9–3.2	5–7	–	A	A	P	11	Illinois, USA	Meglitsch, 1942
M. mongolicus Pronin, 1973	*Oreoleuciscus potanini* (Kessler)	11.0–12.0	8.0–11.0	4.0–6.0	3.5–5.0	2.2–3.2	–	–	P	A	P	4, 7, 10, 12	Russia	Eiras et al., 2014
M. muelleri Butschli, 1882	*Squalius cephalus*	6.0–14.5	7.0–12.0	6.0–7.0	3.0–7.5	2.5–3.0	6–7	–	P	P	P	1	Hungary	Molnar et al., 2006
M. muellericus Molnar, Marton, Eszterbauer, & Szekely, 2006	*Squalius cephalus*	9.7; 9.5–10.0	8.1; 8.0–8.2	5.1; 5.0–5.2	4.1; 4.0–4.5	2.2; 2.0–2.5	6	–	P	A	P	1	Hungary	Molnar et al., 2006
M. naffari Abdel–Ghaffar, Ibraheim, Bashtar & Ali, 1998	*Labeo niloticus* (Linnaeus)	11.9; 10.8–13.2	8.8; 7.8–9.8	–	5.1; 4.5–6.2	2.6; 2.5–3.0	7–9	–	P	A	P	1	Egypt	Eiras et al., 2005

M. njoyai Nchoutpouen et Fomena, 2011	*Labeo parvus* Boulenger	9.7; 9.0–10.5	8.7; 7.8–9.0	–	5.2; 4.5–5.8	3.0; 2.8–3.5	6–8	–	P	A	P	1, 6, 7, 13	Cameroon	Nchoutpouen & Fomena 2011
M. obliquus Kudo, 1934	*Carpiodes velifer*	8.0–9.0	7.0–8.0	5.0–6.0	4.5	2.0	6–7	–	P	P	P	14	Illinois, USA	Kudo, 1934
M. rigida Sarkar, 1999	*Amblypharyngodon mola* (Hamilton)	10.8; 10.0–11.0	8.6; 7.5–9.5	–	6.3; 5.5–7.0	3.6; 3.0–4.0	–	–	–	–	–	7	India	Eiras et al., 2014
M. sigini Chen & Ma, 1988	*Hypophthalmichthys molitrix* (Valenciennes)	10.6; 9.8–11.3	7.4; 7.2–7.8	5.3; 4.8–6.0	4.9; 4.8–5.0	2.4; 2.4–2.6	6–7	–	A	A	P		China	Ma, 1998
M. smithi Salim & Desser, 2000	*Chrosomus eos* (Cope)	11.0; 9.8–12.2	8.5; 8.1–9.2	6.0; 5.2–6.9	4.8; 4.2–5.4	2.8; 2.1–3.1	5–7	P	A	P	P	7	Ontario, Canada	Salim & Desser, 2000
M. sommervillae Molnar, Marton, Szekely, & Eszterbauer, 2010	*Rutilus rutilus* (Linnaeus)	11.8; 10.5–13.5	9.7; 8.4–11.2	7.2; 6.6–7.5	6.0; 5.4–6.7	3.3; 3.0–4.2	6	–	P	A	P	1	Hungary	Molnar et al., 2010
M. squamae Keysselitz, 1908	*Cyprinus carpio*	10.0–13.5	7.5–9.0	5.0–6.0	4.5–5.5	3.0	–	A	P	A	P	8	Russia	Eiras et al., 2005
M. strelkovi Kostarev & Kulemina, 1971	*Phoxinus phoxinus*	8.0–12.2	6.0–11.0	4.0–7.0	3.3–5.4	2.0–4.1	–	–	P	A	P	1, 15	Russia	Eiras et al., 2005
M. uyeni Ha, 1971	*Cirrhina molitorella* (Valenciennes)	9.9–10.8	8.0–8.5	–	5.4	2.7	–	–	P	A	P	10	Vietnam	Ha, 1971
M. waleckii Yukhimenko, 1986	Leuciscus waleckii	8.4–9.4	7.3–8.4	5.7–6.3	4.2–4.8	2.2–3.1	–	–	P	A	P	1	Amur Basin	Yukhimenko, 1986
M. xiaoi Salim & Desser, 2000	*Notropus cornutus*	11.0; 9.8–12.2	8.5; 8.1–9.2	6.0; 5.2–6.9	4.8; 4.2–5.4	2.8; 2.1–3.1	5–7	P	A	P	P	16	Canada	Salim & Desser, 2000
M. zilli Sakiti, Blanc, Marques & Bouix, 1991	*Coptodon zillii* (Gervais)	9.8; 8.0–11.0	7.5; 6.0–8.0	–	5.1; 4.0–6.0	2.5;2.0 –3.0	–	–	P	A	P	1	Benin	Eiras et al., 2005

*Site: 1, gill; 2, gill rakers; 3, testes; 4, eye; 5, scales; 6, fins; 7, kidney; 8, skin; 9, heart; 10, intestine; 11, mesentery; 12, brain; 13, spleen; 14, muscle; 15, liver; 16, gill arches.

CHAPTER 3: TWO NEW SPECIES OF *MYXOBOLUS* (MYXOZOA: MYXOBOLIDAE) INFECTING THE GILL AND SCALES OF SMALLMOUTH BASS, *MICROPTERUS DOLOMIEU* (CENTRARCHIFORMES: CENTRARCHIDAE) IN THE FRENCH BROAD RIVER BASIN, NORTH CAROLINA

***Published in Parasitology International (Available 7 July 2022)**

Authors: Steven P. Ksepka, Jacob M. Rash, and Stephen A. Bullard

Abstract: Two new species of *Myxobolus* Bütschli, 1882 (Bivalvulida: Myxobolidae) are described from the gill and scales of smallmouth bass (*Micropterus dolomieu* Lacepède, 1802 [Centrarchiformes: Centrarchidae]) from the Watauga River, French Broad River Basin, North Carolina, United States. *Myxobolus intralamina* n. sp. infects the lumen of the lamellar arterioles and *Myxobolus infrabractea* n. sp. infects the inner surface of the scale. They differ from all congeners by a combination of myxospore dimensions, polar tubule coil count, and the presence or absence of an iodinophilic vacuole in the sporoplasm and an intercapsular process. A phylogenetic analysis of the small subunit ribosomal DNA (SSU rDNA) recovered *M. intralamina* n. sp. sister to *Myxobolus lepomis* and *Myxobolus branchiarum* and *M. infrabractea* n. sp. sister to *Myxobolus micropterii* in a clade composed of five *Myxobolus* spp. infecting centrarchids and *Henneguya* spp. (Myxobolidae) infecting percids. Histological sections of infected gill revealed intra-lamellar plasmodia of *M. intralamina* n. sp. within the lumen of the lamellar arterioles and plasmodia of *M. infrabractea* n. sp. developing beneath the scales. These new species comprise the first species of *Myxobolus* reported from a black bass (*Micropterus* Lacepède, 1802) in the Southeast United States.

1. Introduction

Little is known about the taxonomic diversity of species of *Myxobolus* Bütschli, 1882 (Bivalvulida: Myxobolidae) that infect centrarchids in the Southeast United States (SEU). This is noteworthy, as all but five centrarchids are endemic to the SEU (see below). Further surprising about this lack of parasitological information is that black basses comprise the bulk of inland sport fisheries in that region. Twenty-three species of *Myxobolus* reportedly infect centrarchids (Table 1). Only *Myxobolus mississipiensis* Cone and Overstreet, 1998 and *Myxobolus jolimorei* Cone and Overstreet, 1998, which infect the gill lamellae and heart of bluegill (*Lepomis macrochirus* Rafinesque, 1819 [Centrarchiformes: Centrarchidae]), respectively in the Pascagoula River, have been reported from the SEU (Cone & Overstreet [1]). Six species of *Myxobolus* have been reported to infect species of *Micropterus* Lacepède, 1802 (Centrarchiformes: Centrarchidae): *Myxobolus branchiarum* Walsh, Iwanowicz, Glenney, Iwanowicz, and Blazer, 2012, *Myxobolus inornatus* Fish, 1938, *Myxobolus kostiri* Herrick, 1936, *Myxobolus microcystus* Price and Mellen 1980, *Myxobolus micropterii* Walsh, Iwanowics, Glenney, Iwanowicz, and Blazer, 2012, and *Myxobolus osburni* Herrick, 1936 (Table 1). *Myxobolus kostiri* and *M. osburni* infect the dermis of the lower jaw and the mesentery, respectively, of smallmouth bass (*Micropterus dolomieu* Lacepède, 1802) in Lake Erie (Herrick [2]). *Myxobolus inornatus* infects the muscle of smallmouth bass in the Susquehanna River (Fish [3]). *Myxobolus branchiarum* and *M. micropterii* infect the gill lamellae of smallmouth bass and largemouth bass (*Micropterus salmoides* [Lacepède, 1802]), respectively in the Potomac River (Walsh et al. [4]). *Myxobolus microcystus* infects the gill lamellae of largemouth bass in Crab Orchard Lake (Price & Mellen [5]). No species of *Myxobolus* has been reported from a black bass in the SEU to date.

Thirty-three of 38 species of Centrarchidae are endemic to the SEU, with *Micropterus* being the most species rich centrarchid genus (Etnier & Starnes [6]; Boschung & Mayden, [7]; Cooke & Philipp [8]; Fricke et al. [9]). Black basses are composed of 13 species, of which 12 are endemic to the SEU (Etnier & Starnes [6]; Boschung & Mayden, [7]; Cooke & Philipp [8]). While all *Micropterus* spp. are sought after as sportfish, 3 (smallmouth bass, largemouth bass, and spotted bass, *Micropterus punctulatus* [Rafinesque, 1819]), have been widely stocked outside of their native range for sportfishing and are some of the most sought-after freshwater sportfish in North America (Cooke & Phillip [8]). Smallmouth bass are endemic to the Great Lakes, Hudson River, and Mississippi River drainages from southern Quebec to northern Alabama and Texas; however, due to introductions for sportfishing, smallmouth bass can be found in all states except Florida, Louisiana, and Alaska (Cooke & Philipp [8]). Due to their popularity as a sportfish, resource managers are interested in the parasites and potential pathogens of smallmouth bass.

Smallmouth bass were collected from the Watauga River (36°12'45.3"N, 81°46'31.5"W), French Broad River Basin, and examined for parasites. Plasmodia containing myxospores consistent with *Myxobolus* were observed on the gill lamellae and body surface (Figs. 1A,B; 2A,B). Herein, based upon myxospore morphology, histological sections, and phylogenetic analysis, we describe two new species of *Myxobolus* from this collection. The new species are the first species of *Myxobolus* reported from a species of *Micropterus* in the region and the 4th and 5th reported from smallmouth bass.

2. Materials and methods

2.1. Fish collection

From 15 October 2020 through 11 November 2020, 18 smallmouth bass were collected by the North Carolina Wildlife Resources Commission from the Watauga River (36°12'45.3"N, 81°46'31.5"W), French Broad River Basin, using a backpack electroshocker, bagged, placed on ice, and shipped overnight to Auburn University. Upon arrival, fish were measured (mm), weighed (g), photographed, and examined for parasitic infections. Plasmodia were excised and fixed in 10% neutral buffered formalin (n.b.f) for morphology and 95% ethanol for DNA extraction. Two gill arches and one one-centimeter-long trunk section from two smallmouth bass infected by both new species were fixed in 10% n.b.f for histology, yielding 6 portions of tissue for histology.

2.2. Myxospore morphology

Morphological diagnosis based on 10 plasmodia and 50 myxospores (20 stained with Lugol's iodine; 10 stained with India ink). Measurements were taken from n.b.f.-fixed myxospores at ×1000 magnification using differential interference microscopy. Unless otherwise noted N=40. Lugol's iodine and India ink were used to stain the iodiniphilic vacuole and mucous envelope respectively, per Lom & Arthur [10]. All measurements are reported in micrometers unless otherwise specified. To illustrate myxospores, plasmodia were ruptured and vortexed to suspend myxospores before a drop of the suspension was cover-slipped, inverted, placed onto a thin layer of 1% agar (Lom [11]), and illustrated using a 100× oil immersion objective on an Olympus BX51 compound scope equipped with a 1.5× magnifier, differential interference contrast (DIC) components, and drawing tube.

2.3. Histology

After fixation, four infected gill arches and trunk segments were rinsed in distilled water for two hours, decalcified in EDTA for one week, dehydrated in an ethanol series, embedded in paraffin, sectioned at four µm, and stained with Gill's 2 haematoxylin and eosin per Luna [12]. Ten slides were cut from each block yielding >350 sections on 60 slides.

2.4. DNA extraction, amplification, and sequencing

DNA was extracted from one microscopically confirmed isolate of myxospores from each site of infection from the same host, each isolate contained myxospores from a single plasmodium, using the DNeasy Blood & Tissue kit (Qiagen) following the manufacturers protocol, with the exceptions that the proteinase K incubation step was extended overnight and 100 µl of AE buffer were used for the elution step to increase DNA concentration. Before DNA extraction, wet mounts of myxospores were morphologically identified with the use of a compound microscope equipped with DIC (Table 1). Following extraction, concentration was measured using a NanoDrop-1000 spectrophotometer (Thermo Scientific, Nanodrop Technologies), diluted to 20 ng/µl, and stored at -20ºC. A fragment of the small subunit ribosomal DNA (SSU rDNA) was amplified using primers M153–F (5'–CATTGGATAACCGTGGGAAATCT–3') and M2192–R (5'–TAGTAGCGACGGGCGGTGT–3') (Ksepka et al. [13][14]). PCR amplification used the following thermocycler parameters: initial denaturation step of 95ºC, for four min, followed by 35 cycles of 95ºC for 30 s, 60ºC for 30s and 72ºC for 1 min, with a final extension step of 72ºC for five min. PCR products were visualized on a 1% agarose gel, purified using the QIAquick PCR Purification Kit (Qiagen) following manufacturers protocol, and sequenced by Genewiz (South Plainfield, New Jersey).

Sequencing primers M473–F (5'–GCTTGAGAAWCGGCTACCAC–3') and M1480–R (5'–GTGGTGCCCTTCCGTCAATTCC–3') were used to improve sequencing coverage (Ksepka et al. [13][14]). Chromatograms were assembled based on sequence overlap, proofread by eye, and had low-quality read ends trimmed in Geneious version 2021.1.1 (http://www.geneious.com) resulting in sequences of 1694 and 1734 base pairs.

2.5. Phylogenetic analysis

Additional taxon selection for phylogenetic analysis was based on BLAST search of NCBI GenBank and a recent phylogenetic analysis of Myxobolidae in Liu et al. [15] and included 73 species of Myxobolidae from subclade VII, four species of Myxobolidae from subclades V and VI, all available sequences of *Myxobolus* spp. infecting centrarchids and three species of Myxidiidae as an outgroup (Liu et al. [15]). Sequences were aligned using MAFFT with an automatically assigned alignment strategy and a maxiterate value of 1,000 in Geneious version 2021.1.1 (Katoh & Standley [16]). The alignment was trimmed to the length of the sequences presented herein (1969 base pairs) to minimize missing data at the 5' and 3' end of the alignment. JModelTest2 version 2.1.10 was used to select best-fit models of nucleotide substitution based on Bayesian information criteria (Darriba et al. [17]). Bayesian inference was performed in MrBayes version 3.2.5 using substitution model averaging (nst=mixed) and a gamma distribution to model rate heterogeneity. Defaults were used for all other parameters. Three runs with four Metropolis-coupled chains were run for 5,000,000 generations. Stationarity was checked using Tracer 1.7 (Rambaut et al., [18]) and a burn-in of 25% of generations was determined. Evidence of convergence was further checked with the "sump" command in MrBayes. All parameters had a potential scale reduction factor of 1.00. A majority rule

consensus tree of the post burn-in posterior distribution was generated with the “sumt” command in MrBayes. The phylogenetic tree was visualized in FigTree v1.4.3 (Rambaut et al. [19]) and rendered for publication with Adobe Illustrator (Adobe Systems).

3. Results

3.1 Myxobolus intralamina Ksepka & Bullard n. sp. (Figs. 1A, 3A, 4A–D, 6A)

3.1.1 Morphological diagnosis (USNM coll. Nos. 1665682–1667824)

Plasmodia subcircular, 78–306 (mean ± SD = 196.8 ± 62.3; N = 10) long, 66–288 (167.4 ± 60.3; 10) wide, myxospore comprising 2 smooth symmetrical valves juxtaposed at sutural rim, 2 polar capsules, and sporoplasm; myxospore pyriform, 14.0–15.0 (4.4 ± 0.5; 50) long (Fig. 3A–C), 8.0–9.0 (8.4 ± 0.5) wide (Fig. 3A–C), 6.0–7.0 (6.3 ± 0.5; 10) thick (Fig. 3D); sutural rim with prominent seam (Fig. 3A–C), 1.0 thick (lateral margin in frontal view) (Fig. 3A–C), 1.0 thick (posterior margin in frontal view) (Fig. 3A–C), without flanking lateral ridges (sutural), 0–2 sutural markings; polar capsules unequal (Fig. 3A–C), clavate (Fig. 3A–C), with 10–13 polar tubule coils, larger polar capsule 7.0–9.0 (8.3 ± 0.5) long (Fig. 3A–C), 2.0–3.0 (2.9 ± 0.2) wide (Fig. 3A–C), smaller polar capsule 6.0–8.0 (7.5 ± 0.6) long, 2.0–3.0 (2.8 ± 0.4); sporoplasm with iodinophilic vacuole 3–4 (3.5 ± 0.5; 20) in diameter (Fig. 3A–C), having two nuclei (Fig. 3A–C); mucous envelope absent.

3.1.2 Taxonomic summary

Type host: Micropterus dolomieu Lacepède, 1802 (Centrarchiformes: Centrarchidae), smallmouth bass.

Type locality: Watauga River (36°12'45.3"N, 81°46'31.5"W), French Broad River Basin, North Carolina.

Specimens deposited: Myxospores of *M. intralamina* n. sp. fixed in 10% n.b.f (1 vial; syntype; USNM 1665682), and within paraffin sections (2 slides; syntypes; USNM 1665683–1665684); GenBank No. (SSU rDNA: OM420274).

Site in host: Intra-lamellar plasmodia infecting the lumen of the lamellar arterioles. Intra-lamellar large-cysts, central type (LV_3) *sensu* Molnar [20].

Prevalence: Myxospores were detected in 12 of 18 (prevalence=66%) smallmouth bass collected from the Watauga River (36°12'45.3"N, 81°46'31.5"W), French Broad River Basin, North Carolina.

Etymology: The latin specific name "*intralamina*" is from "intra" (within) and "lamina" (thin plate), referring to the apparent specificity to the lumen of the lamellar arterioles.

3.1.3 Taxonomic remarks

The myxospore of *M. intralamina* n. sp. differs from that of its 23 congeners infecting centrarchids by dimensions, polar tubule coil count, and shape as well as by the presence of an iodinophilic vacuole in the sporoplasm and by the lack of an intercapsular process (Table 1). Of those 23 species, the myxospore of the new species differs from all but three (*M. inornatus, M. kostiri,* and *Myxobolus lepomicus* Li and Desser 1985) by having asymmetrical polar capsules (Table 1). Of those 3, the myxospore of the new species differs from that of *M. kostiri* by being longer and wider and having longer polar capsules and from that of *M. lepomicus* by polar tubule coil count (10–13 vs 5–7), being thinner with longer polar capsules, and by lacking an intercapsular process (Table 1). The myxospore of the new species are morphologically most

similar to that of *M. inornatus*, which infects the muscle of smallmouth bass, but differs by having 10–13 polar tubule coil (vs. 6–8) (Table 1).

A total of five species of *Myxobolus* that infect non-centrarchid intermediate hosts have overlapping myxospore dimensions with the new species and asymmetrical polar capsules (Table 2). Of those five species, the lack of an intercapsular process differentiates the myxospore of the new species from those of *Myxobolus orissae* Haldar, Samal, and Mukhopadhyaya, 1996, *Myxobolus prochilodus* (Azevedo, Vieira, Vieira, Silva, and Abdallah, 2014), and *Myxobolus tauricus* Miroshnichenko, 1979. Polar tubule coil count differentiates the myxospore of the new species (10–13) from those of *Myxobolus andhrae* Lalitha Kumari, 1969 (9) and *Myxobolus indiae* Lalitha Kumari, 1969 (8–10) (Table 2).

3.2 Myxobolus infrabractea Ksepka & Bullard n. sp. (Figs. 1B, 2B, 4A–D, 5B)

3.2.1 *Morphological diagnosis (USNM coll. Nos. 1665685–1665687)*

Plasmodia ellipsoid, 372.0–570.0 (506.4 ± 62.3; 10) long, 390–630 (552.0 ± 78.7; 10) wide; myxospore comprising 2 smooth symmetrical valves juxtaposed at sutural rim, 2 polar capsules, and sporoplasm; myxospore capsule shaped, 11.0–13.0 (11.8 ± 0.6; 50) long (Fig. 4A–C), 6.0–7.0 (6.7 ± 0.5) wide (Fig. 4A–C), 4.0–5.0 (4.6 ± 0.5; 10) thick (Fig. 4D); sutural rim with prominent seam (Fig. 4A–C), 1.0 thick (lateral margin in frontal view) (Fig. 4A–C), 1.0 thick (posterior margin in frontal view) (Fig. 4A–C), without flanking lateral ridges (sutural), lacking sutural markings; polar capsules equal (Fig. 4A–C), clavate (Fig. 4A–C), 3.0–5.0 (4.0 ± 0.5; 80) long (Fig. 4A–C), 2.0–3.0 (2.1 ± 0.3; 80) wide (Fig. 4A–C), with 3–4 polar tubule coils; sporoplasm with iodinophilic vacuole 2–3 (2.7 ± 0.4; 20) in diameter (Fig. 4A–C), having 2 nuclei (Fig. 4A–C); mucous envelope absent.

3.2.2 Taxonomic summary

Type host: Micropterus dolomieu Lacepède, 1802 (Centrarchiformes: Centrarchidae), smallmouth bass.

Type locality: Watauga River (36°12'45.3"N, 81°46'31.5"W), French Broad River Basin, North Carolina.

Specimens deposited: Myxospores of *M. infrabractea* n. sp. fixed in 10% n.b.f (1 vial; syntype; USNM 1665685), and within paraffin sections (2 slides; syntypes; USNM 1665686–1665687); GenBank No. (SSU rDNA: OM420273).

Site in host: Intercellular, infecting the internal surface of scales.

Prevalence: Myxospores were detected in 6 of 18 (prevalence=33%) smallmouth bass collected from the Watauga River (36°12'45.3"N, 81°46'31.5"W), French Broad River Basin, North Carolina.

Etymology: The latin specific name "*infrabractea*" is from "infra" beneath and "bractea" "scale" referring to the apparent specificity to the inner surface of the scales.

3.2.3 Taxonomic remarks

The myxospore of *M. infrabractea* n. sp. differs from that of its 23 congeners infecting centrarchids by dimensions and polar tubule coil count (Table 1). Of those 23, the myxospore of the new species differs from all but that of *M. branchiarum* by myxospore dimensions. The myxospore of the new species differs from that of *M. branchiarum* by polar tubule coil count (3–4 vs. 8–9) (Table 1).

A total of eight species of *Myxobolus* that infect non-centrarchid intermediate hosts have overlapping myxospore dimensions with the new species (Table 3). Of those eight species, the presence of an iodinophilic vacuole in the sporoplasm and lack of an intercapsular process differentiates the myxospore of the new species from all but that of *Myxobolus dentium* Fantham, Porter, and Richardson 1939. The myxospore of the new species differs from that of *M. dentium* by having 3–4 polar tubule coils (vs 5–7) and being capsule shaped (vs ellipsoid) (Table 3).

3.3. Histopathology

Plasmodia of *M. intralamina* n. sp. were intra-lamellar within the lumen of the lamellar arterioles of smallmouth bass, intra-lamellar large-cysts central (LV_3) type *sensu* Molnar [20] (Fig. 5A). Myxospore development in the plasmodium was asynchronous, with myxospores in various stages of development filling the plasmodium. Only one plasmodium was observed per lamellar arteriole (Fig. 5A). In infected gill lamellae, plasmodia filled the length of the lumen of the lamellar arteriole and were wide enough to displace neighboring gill lamellae (Fig. 5A). Fusion of gill lamellae was observed where infected lamellae were in contact with the adjacent lamellae (Fig 5A). No demonstrable host cellular response was observed in infected gill lamellae.

Plasmodia of *M infrabractea* n. sp. were intercellular on the interior surface of the scales of smallmouth bass (Fig. 5B). Myxospore development in the plasmodium was asynchronous, with myxospores in various stages of development filling the plasmodium (Fig. 5B). No plasmodium was observed on the exterior surface of the scale. Only one plasmodium was observed per scale. No demonstrable host response was observed in the dermis underlying, nor epidermis overlying, the scale (Fig. 5B). There was no observed thinning of the scale. The tip of infected scales was

raised and, in 6 of 12 (50%) infected scales observed in section, perforated the epidermis (Fig. 5B).

3.4 Phylogenetic analysis

The amplified SSU rDNA fragments of *M. intralamina* n. sp. and *M. infrabractea* n. sp. comprised 1969 nucleotides after alignment and differed from each other by 314 (18.2%) nucleotides. Both sequences were most similar to a sequence from *M. lepomis* (KY203390) in NCBI GenBank, which was included in the phylogenetic analysis, and differed from it by 43 (2.5%) and 149 (11.5%) nucleotides, respectively. We recovered three clades (nodal support >0.8): (A) four species of *Myxobolus* and 13 species of *Henneguya* Thélohan, 1892 (Bivalvulida: Myxobolidae) infecting connective tissues of siluriforms, (B) 14 species of *Myxobolus* and 13 species of *Henneguya*, and (C) nine species of *Myxobolus* and 13 species of *Henneguya* (Fig. 6). Consistent with Liu et al. [15], *Myxobolus* and *Henneguya* were recovered as para/polyphyletic, myxobolids infecting centrarchids were recovered as paraphyletic, and, apart from *Henneguya lesteri* Hallet and Diamant 2001, myxobolids infecting marine intermediate hosts were recovered as monophyletic (Fig. 6). Both new species were recovered within clade B in a clade composed of two species of *Henneguya* infecting percids and five species of *Myxobolus* infecting centrarchids. *Myxobolus infrabractea* n. sp. was recovered sister to *Myxobolus micropterii*, collected from the gill of largemouth bass in the Potomac River Basin. *Myxobolus intralamina* n. sp. was recovered sister to *Myxobolus branchiarum*, collected from the gill of smallmouth bass in the Potomac River Basin, and *Myxobolus lepomis* Rosser, Baumgartner, Barger, and Griffin, 2017, collected from the gill of bluegill in Big Thicket National Preserve, Texas, USA. We recovered myxobolids infecting pimelodids and pangasiids as monophyletic in clade A and

myxobolids infecting mugilids as monophyletic in clade B (Fig. 6). No pattern in site of infection was observed, as species in the analysis predominately infect connective tissues. Low support values (<0.70) are worth noting as increased taxon or character sampling could change tree topology.

4. Discussion

Myxozoans that disrupt the epidermis, such as *M. infrabractea* n. sp. reported herein, may increase host susceptibility to secondary bacterial infections similarly to ectoparasites (Walsh & Blazer [21]). The epidermis is an important component of the immune system, acting as a first line of defense against pathogens which infect through the skin (Barton & Bond [22]). Damage to the epidermis has been reported to increase the susceptibility of the host to secondary bacterial infections (Kotob et al. [23]). Red sore disease, co-infection by *Epistylis* sp. Ehrenberg, 1830 (Sessilida: Epistylidae) and *Aeromonas hydrophila* (Chester, 1901) (Aeromonadales: Aeromonadaceae), is reported to occur when infections by *Epistylis* sp. perforate the epithelium acting as a portal of entry for *A. hydrophila* (Esch et al. [24], Ksepka et al. [25]). Carvalho et al. [26] reported increased lesion severity, time for lesions to resolve, and mortality in Atlantic salmon (*Salmo salar* Linnaeus, 1758 [Salmoniformes: Salmonidae]), co-infected by *Lepeophtheirus salmonis* (Krøyer, 1838) (Siphonostomatoida: Caligidae) and *Moritella vicosa* (Lunder, Sorum, Holstad, Steigerwalt, Mowinckel, and Brenner, 2000) (Alteromonadales: Moritellaceae) compared to those infected by only *M. viscosa* or *L. salmonis*. In Nile tilapia (*Oreochromis niloticus* [Linnaeus, 1758] [Cichliformes: Cichlidae]) culture, high mortality has been reported as a result of co-infection by *A. hydrophila* and either *Gyrodactylus cichlidarum* Paperna, 1968 (Gyrodactylidea: Gyrodactylidae) or *Fusarium oxysporum* (Schlectendahl, 1824)

(Hypocreales: Nectriaceae) (Cutuli et al. [27]; Abdel-Latif & Khafaga [28]). Mahmoud et al. [29] observed pathological changes to gill of striped mullet (*Mugil cephalus* Linnaeus, 1758 [Mugiliformes: Mugilidae]) associated with co-infection by *Ergasilus extensus* El-Rashidy and Boxshall, 2002 (Cyclopoida: Ergasilidae) and *Streptococcus agalactiae* Lehman and Neumann, 1896 (Lactobacillales: Streptococcaceae) or *Enterococcus faecalis* (Andrewes and Horder, 1906) (Lactobacillales: Enterococcaceae). The lesion we report herein associated with infection by *M. infrabractea* n. sp. is minor, and additional study is needed to determine if the perforated epidermis increases hosts susceptibility to secondary infections. Noteworthy is that some bacterial challenge models prescribe epidermal ablation to hasten bacterial entry and infection of the host (Bader et al. [30]; Zhang et al. [31]). While all plasmodia of *M. infrabractea* n. sp. observed in section were complete, it is noteworthy that the infected scales penetrating the epidermis may be adaptive for myxospore dispersal by either plasmodia growing until they rupture or by inducing flashing behavior that could scrape plasmodia from the fish.

Most gill infecting myxobolids represent benign infectors of their hosts; however, several species have been reported as pathogenic. *Myxobolus nanokiensis* Kaur, Katoch, Dar, and Singh, 2015 forms intra-lamellar plasmodia that reportedly cause hemorrhagic gill disease in cultured rohu (*Labeo rohita* [Hamilton, 1922] [Cypriniformes: Cyprinidae]) in India (Kaur et al. [32]). *Myxobolus pavlovskii* (Achmerov, 1954), infecting silver carp (*Hypophthalmichthys molitrix* [Valenciennes, 1844] [Cypriniformes: Xenocyprididae]), disrupts the respiratory surface of the gill and can reportedly cause mortality in culture (Molnár, [33]). *Myxobolus okamurae* Gupta and Kaur, 2018 forms intra-lamellar plasmodia in the gills of *Labeo bata* (Hamilton, 1822) and has been observed associated with necrosis of the gill epithelium (Gupta & Kaur, [34]). *Henneguya ictaluri* Pote, Hanzon, and Shivaji, 2000, the causative agent of proliferative gill

disease in cultured channel catfish (*Ictalurus punctatus* [Rafinesque, 1818] [Siluriformes: Ictaluridae]) in the southeast United States, interrupts the supporting cartilage of the gill filaments and can induce significant mortality events in catfish culture (Pote et al. [35]). We observed no hemorrhagic lesion indicative of myxospore dispersal from the gill lamellae. The lesions observed herein do not support that infections are pathogenic among Watauga River smallmouth bass.

Acknowledgements: We thank Thomas Johnson, Dylan Owensby, Kenneth Lingerfelt, and Raymond Starmack (North Carolina Wildlife Resources Commission, Marion, North Carolina) for aid in collecting smallmouth bass; and Micah Warren, Triet Truong, Justin Krol, and Stephen Curran (Auburn University) for assistance in fish necropsy.

References

[1] D.K. Cone, R.M. Overstreet, Species of *Myxobolus* (Myxozoa) from the bulbus arteriosus of centrarchid fishes in North America, with a description of two new species, J. Parasitol. 84 (1998) 371–374. https://doi.org/10.2307/3284499.

[2] J.A. Herrick, Two new species of *Myxobolus* from fishes of Lake Erie, Trans. Am. Micro. Soc. 55 (1936) 194–198. https://doi.org/10.2307/3222611.

[3] F.F. Fish, Notes on *Myxobolus inornatus,* n. sp., a myxosporidian, parasitic in the black bass (*Huro floridana*) Le Sueur, Trans. Am. Fish. Soc. 68 (1939) 173–177. https://doi.org/10.1577/1548-8659(1938)68[173:NOMINS]2.0.CO;2

[4] H.L. Walsh, L.R. Iwanowicz, G.W. Glenney, D.D. Iwanowicz, V.S. Blazer, Description of two new gill myxozoans from smallmouth (*Micropterus dolomieu*) and largemouth (*Micropterus salmoides*) bass, J. Parasitol. 98 (2012) 415–422. https://doi.org/10.1645/GE-2918.1.

[5] R.L. Price, J.W. Mellen, *Myxobolus microcystus* sp. n. (Protozoa: Myxosporida) from the gills of *Micropterus salmoides* (Lacépède 1802) in southern Illinois, J. Parasitol. 66 (1980) 1019–1021. https://doi.org/10.2307/3280408.

[6] D.A. Etnier, W.C. Starnes, The Fishes of Tennessee, University of Tennessee Press, Knoxville, 1993.

[7] H.T. Boschung, R.L. Mayden, Fishes of Alabama, Smithsonian Books, Washington, 2004.

[8] S.J. Cooke, D.P. Phillips, Centrarchid Fishes: Diversity, Biology and Conservation, Blackwell Publishing, United Kingdom, 2009.

[9] Fricke, R., Eschmeyer, W. N., Van Der Laan, R. (eds), Eschmeryer's catalog of fishes: Genera, species, references. Accessed on July 20, 2021, from http://researcharchive.calacademy.org/research/ichthyology/catalog/fishcatmain.asp.

[10] J. Lom, J.R. Arthur, A guideline for the preparation of species descriptions in Myxosporea, J. Fish. Dis. 12 (1989) 151–156. https://doi.org/10.1111/j.1365-2761.1989.tb00287.x.

[11] J. Lom, On a new taxonomic character of Myxosporidia, as demonstrated in descriptions of two new species of *Myxobolus*, Folia Parasitol. 16 (1969) 97–103.

[12] L.G. Luna, Manual of histologic staining methods of the armed forces institute of pathology, McGraw–Hill, New York, 1968.

[13] S.P. Ksepka, J.M. Rash, N. Whelan, S.A. Bullard, A new species of *Myxobolus* (Myxozoa: Bivalvulida) infecting the medulla oblongata and nerve cord of brook trout *Salvelinus fontinalis* in southern Appalachia (New River, NC, USA), Parasitol. Res. 118 (2019) 3241–3252. https://doi.org/10.1007/s00436-019-06472-x.

[14] S.P. Ksepka, N. Whelan, C.M. Whipps, S.A. Bullard, (2020b). A new species of *Thelohanellus* Kudo, 1933 (Myxozoa: Bivalvulida) infecting the skeletal muscle of blacktail shiner, *Cyprinella venusta* Girard, 1856 (Cypriniformes: Cyprinidae) in the Chattahoochee River Basin, Georgia, J. Parasitol. 106 (2020) 350–359. https://doi.org/10.1645/19-162.

[15] Y. Liu, A. Lovy, Z. Gu, I. Fiala, Phylogeny of Myxobolidae (Myxozoa) and the evolution of myxospore appendages in the *Myxobolus* clade. Int. J. Parasitol. 49 (2019) 523–530. https://doi.org/10.1016/j.ijpara.2019.02.009.

[16] K. Katoh, D.M. Standley, MAFFT multiple sequence alignment software version 7: improvements in performance and usability, Mol. Biol. Evol. 30 (2013) 772–780. https://doi.org/10.1093/molbev/mst010.

[17] D. Darriba, G.L. Taboada, R. Doallo, D. Posada, jModelTest 2: more models, new heuristics, and parallel computing, Nat. Methods. 9 (2012) 772. https://doi.org/10.1038/nmeth.2109.

[18] A. Rambaut, A.J. Drummond, D. Xie, G. Baele, M.A. Suchard, Posterior summarization in Bayesian phylogenetics using Tracer 1.7, Syst. Biol. 67 (2018) 901–904. https://doi.org/10.1093/sysbio/syy032.

[19] A. Rambaut, M.A. Suchard, D. Xie, A.J. Drummond, FigTree v1.4.3. Available from http://tree.bio.ed.ac.uk/software/figtree.

[20] K. Molnar, Site preference of fish myxosporeans in the gills, Dis. Aquat. Org. 48 (2002) 197–207. doi:10.3354/dao048197.

[21] H.L. Walsh, V.S. Blazer, Development of a multiplex fluorescence in situ hybridization assay to identify coinfections in young-of-the-year smallmouth bass, J. Aquat. Anim. Health (2021) 1–8. https://doi.org/10.1002/aah.10144.

[22] M. Barton, C.E. Bond, Bond's Biology of Fishes, Thomson Brooks, Belmont, California, 2007.

[23] M.H. Kotob, S. Menanteau-Ledouble, G. Kumar, M. Abdelzaher, M. El-Matbouli, The impact of co-infections on fish: a review, Vet. Res. 47 (2017) 1–12. https://doi.org/10.1186/s13567-016-0383-4.

[24] G.W. Esch, T.C. Hazen, R.V. Dimcock, J.W. Gibbons, Thermal effluent and the epizootiology of the ciliate *Epistylis* and the bacterium *Aeromonas* in association with centrarchid fish, Trans. Am. Micro. Soc. 95 (1976) 687–693. https://doi.org/10.2307/3225393.

[25] S.P. Ksepka, S.A. Bullard, Morphology, phylogenetics and pathology of "red sore disease" (coinfection by *Epistylis* cf. *wuhanensis* and *Aeromonas hydrophila*) on sportfishes from reservoirs in the South-Eastern United States, J. Fish. Dis. (2021) 541–551. https://doi.org/10.1111/jfd.13344.v.

[26] L.A. Carvalho, S.K. Whyte, L.M. Braden, S.L. Purcell, A.J. Manning, A. Muckle, M.D. Fast, Impact of co-infection with *Lepeophtheirus salmonis* and *Moritella viscosa* on the inflammatory and immune responses of Atlantic salmon (*Salmo salar*), J. Fish. Dis. 43 (2020) 459–473. https://doi.org/10.1111/jfd.13144.

[27] M.T. Cutuli, A. Gibello, A. Rodriguez-Bertos, M.M. Blanco, M. Villarroel, A. Giraldo, J. Guarro, Skin and subcutaneous mycoses in tilapia (*Oreochromis niloticus*) caused by *Fusarium oxysporum* in coinfection with *Aeromonas hydrophila*, Med. Mycol. Cas. Rep. 9 (2015) 7–11. https://doi.org/10.1016/j.mmcr.2015.06.002.

[28] H.M.R. Abdel-Latif, A.F. Khafaga, Natural co-infection of cultured Nile tilapia *Oreochromis niloticus* with *Aeromonas hydrophila* and *Gyrodactylus chichlidarum* experiencing high mortality during summer, Aqua. Res. 51 (2020) 1880–1892. https://doi.org/10.1111/are.14538.

[29] M.A. Mahmoud, M.M. Attia, M. Abdelsalam, D.A. Abdel-Moneam, M.A.Z. Ewiss, *Ergasilus extensus* and bacterial co-infection in flathead grey mullet, *Mugil cephalus* (Linnaeus, 1758, are associated with pathological changes and immunological gene expression alterations, Aqua. Res. 00 (2021) 1–9. https://doi.org/10.1111/are.15476.

[30] J.A. Bader, K.E. Nusbaum, C.A. Shoemaker, Comparative challenge model of *Flavobacterium columnare* using abraded and unabraded channel catfish, *Ictalurus punctatus* (Rafinesque), J. Fish. Dis. 26 (2003) 461–467. https://doi.org/10.1046/j.1365-2761.2003.00479.x.

[31] D. Zhang, D. Xu, C. Shoemaker, Experimental induction of motile *Aeromonas* septicemia in channel catfish (*Ictalurus punctatus*) by waterborne challenge with virulent *Aeromonas hydrophila,* Aqua. Rep. 3 (2016) 18–23. https://doi.org/10.1016/j.aqrep.2015.11.003.

[32] H. Kaur, A. Katoch, S.A. Dar, R. Singh, *Myxobolus nanokiensis* sp. nov. (Myxozoa: Bivalvulidae), a new pathogenic myxosporean parasite caqusing haemorrhagic gill disease in cultured Indian major carp fish, *Labeo rohita* (Hamilton 1822) in Punjab, India, J. Parasit. Dis. 39 (2015) 405–413. https://doi.org/10.1007/s12639-013-0351-0.

[33] K. Molnár, *Myxobolus pavlovskii* (Achmerov, 1954) (Myxosporidia) infection in the silver carp and bighead, Acta Vet. Acad. Sci. Hung. 27 (1979) 207–216.

[34] A. Gupta, H. Kaur, *Myxobolus okamurae* sp. nov. (Myxosporea: Myxozoa) causing severe gill myxoboliosis in the cyprinid *Lateo bata* in cold water wetland, Punjab (India), Micro. Pathog. 115 (2018) 86–92. https://doi.org/10.1016/j.micpath.2017.12.041.

[35] L.M. Pote, L.A. Hanson, R. Shivaji, Small subunit ribosomal RNA sequences link the cause of proliferative gill disease in channel catfish to *Henneguya* n. sp. (Myxozoa: Myxosporea), J. Aquat. Anim. Health 12 (2000) 230–240. https://doi.org/10.1577/1548-8667(2000)012%3C0230:SSRRSL%3E2.0.CO;2.

[36] G.L. Hoffman, R.E. Putz, C.E. Dunbar, Studies on *Myxosoma cartilaginis* n. sp. (Protozoa: Myxosporidia) of centrarchid fish and a synopsis of the Myxosoma of North American freshwater fishes, J. Protozool. 12 (1965) 319–332. https://doi.org/10.2307/3280408.

[37] D.K. Cone, R.W. Horner, G.L. Hoffman, Description of *Myxobolus corneus* (Myxosporea): a new species from the eye of bluegill from Illinois, J. Aquat. Anim. Health. 2 (1990) 132–134. https://doi.org/10.1577/1548-8667(1990)002%3C0132:DOCANS%3E2.3.CO;2.

[38] D.K. Cone, R.C. Anderson, Myxosporidian parasites of pumpkinseed (*Lepomis gibbosus* L) from Ontario, J. Parasitol. 83 (1977) 122–124. https://doi.org/10.2307/3279565.

[39] R. Kudo, Histozoic myxosporidia found in fresh-water fishes of Illinois, U.S.A., Arch. Protistenkd. 65 (1929) 364–378.

[40] G.R. Otto, T.L. Jahn, Internal myxosporidian infections of some fishes of the Okoboji region. Proc. Iowa Acad. Sci. 50 (1943) 323–335.

[41] L. Li, S.S. Desser, The protozoan parasites of fish from two lakes in Algonquin Park, Ontario, Can. J. Zool. 63 (1985) 1846–1858. https://doi.org/10.1139/z85-275.

[42] T.G. Rosser, W.A. Baumgartner, M.A. Barger, M.J. Griffin, *Myxobolus Lepomis* n. sp. (Cnidaria: Myxobolidae), a gill myxozoan infecting *Lepomis marginatus* Holbrook and *Lepomis miniatus* Jordan (Perciformes: Centrarchidae), in the Big Thicket National Preserve, Texas, USA, Syst. Parastitol. 94 (2017) 535–545. https://doi.org/10.1007/s11230-017-9719-3.

[43] R. Kudo, Studies on Myxosporidia. A synopsis of genera and species of Myxosporidia, Ill. Biol. Monogr. 5 (1919) 1–265. https://doi.org/10.5962/bhl.title.16800.

[44] R.L. Price, J.W. Mellen, *Myxobolus microcystus* sp. n. (Protozoa: Myxosporidia) from the gills of *Micropterus salmoides* (Lacepede 1802) in southern Illinois, J. Parasitol. 66 (1980) 1019–1021. https://doi.org/10.2307/3280408.

[45] V.J. Rice, T.L. Jahn, Myxosporidian parasites from the gills of some fishes of the Okoboji region, Proc. Iowa Acad. Sci. 50 (1943) 313–321.

[46] P.S. Lalitha Kumari, Studies on parasitic protozoa (Myxosporidia) of fresh water fishes of Andhra Pradesh, India, Riv. Parassitol. 30 (1969) 161–164.

[47] D.P. Haldar, K.K. Samal, D. Mukhopadhyaya, Studies on the protozoan parasites of fishes in Orissa: eight species of *Myxobolus* Bütschli (Myxozoa: Bivalvulida). J. Bengal Nat. Hist. Soc. 16 (1998) 3–24.

[48] R.K. Azevedo, D.H. Vieira, G.H. Vieira, R.J. Silva, V.D. Abdallah, Phylogeny, ultrastructure and histopathology of *Myxobolus lomi* n. sp., a parasite of *Prochilodus lineatus* (Valenciennes, 1836) (Characiformes: Prochilodontidae) from the Peixes River, São Paulo State, Brazil, Parasitol. Int. 63 (2014) 303–307. https://doi.org/10.1016/j.parint.2013.11.008.

[49] A.I. Miroshnichenko, *Myxobolus tauricus* sp. n., a new myxosporidian (Cnidosporidea: Myxosporidea) of the Crimean barbel, Parazitol. 13 (1979) 436–437.

[50] A. Lövy, M. Smirnov, V. Brekhman, T. Ofek, T. Lotan, Morphological and molecular characterization of a novel myxosporean parasite *Myxobolus bejeranoi* n. sp. (Cnidaria, Myxosporea) from hybrid tilapia in Israel, Parasitol. Res. 117 (2018) 491–499. https://doi.org/10.1007/s00436-017-5725-2.

[51] R. Kudo, Studies on some protozoan parasites of fishes of Illinois, Ill. Biol. Monogr. 13 (1934) 7–44. https://doi.org/10.5962/bhl.title.50234.

[52] A.K. Akhmerov, Myxosporidia of fishes of the Amur River Basin, Rybnoe Khozyaistvo Vnutrikh Vodoemov Latviiskoi SSR. 5 (1960) 239–308.

[53] H. Yokohama, K. Ogawa, H Wakabayashi, *Myxobolus cultus* n. sp. (Myxosporea, Myxobolidae) in the goldfish *Carassius auratus* transformed from the actinosporean stage in the oligochaete *Branchiura sowerbyi*, J. Parasitol. 81 (1995) 446–451. https://doi.org/10.2307/3283830.

[54] H.B. Fantham, A. Porter, L.R. Richardson, Some new myxosporidia found in certain freshwater fishes in Quebec Province, Canada, Parasitol. 31 (1939) 1–77. doi:10.1017/S0031182000012634.

[55] J.C. Eiras, C.F. Cruz, A. Saraiva, E.A. Adriano, Synopsis of the species of *Myxobolus* (Cnidaria, Myxozoa, Myxosporea) described between 2014 and 2020, Folia Parasitol. 68 (2021) 012. DOI: 10.14411/fp.2021.012.

[56] J.C. Eiras, K. Molnár, Y.S. Lu, Synopsis of the species of *Myxobolus* Bütschli, 1882 (Myxozoa: Myxosporea: Myxobolidae), Syst. Parasitol. 61 (2005) 1–46. doi: 10.1007/s11230-004-6343-9.

Figure legends

Fig. 1 Smallmouth bass, *Micropterus dolomieu* Lacepède, 1802 (Centrarchiformes: Centrarchidae) infected with plasmodia of *Myxobolus* spp. (Bivalvulida: Myxobolidae) from the Watauga River, French Broad River Basin, North Carolina. A: Gill lamellae infected with *Myxobolus intralamina* Ksepka & Bullard n. sp. (arrows). B: Scales infected with *Myxobolus infrabractea* Ksepka & Bullard n. sp. (arrows).

Fig. 2 Myxospores of *Myxobolus infrabractea* Ksepka & Bullard n. sp. (Bivalvulida: Myxobolidae) and *Myxobolus intralamina* Ksepka & Bullard n. sp. collected from smallmouth bass, *Micropterus dolomieu* Lacepède, 1802 (Centrarchiformes: Centrarchidae) from Watauga River, French Broad River Basin, North Carolina; photographed with differential interference contrast optical components. A: *Myxobolus intralamina* n. sp. B: *Myxobolus infrabractea* n. sp.

Fig. 3 Myxospores of *Myxobolus intralamina* Ksepka & Bullard n. sp. (Bivalvulida: Myxobolidae) collected from smallmouth bass, *Micropterus dolomieu* Lacepède, 1802 (Centrarchiformes: Centrarchidae) from Watauga River, French Broad River Basin, North Carolina. A–C: frontal view. D: sutural view. Abbreviation: s – suture; pc – polar capsule; pt– polar tubule; n – nuclei; iv – iodinophilic vacuole.

Fig. 4 Myxospores of *Myxobolus infrabractea* Ksepka & Bullard n. sp. (Bivalvulida: Myxobolidae) collected from smallmouth bass, *Micropterus dolomieu* Lacepède, 1802 (Centrarchiformes: Centrarchidae) from Watauga River, French Broad River Basin, North Carolina. A–C: frontal view. D: sutural view. Abbreviation: s – suture; pc – polar capsule; pt – polar tubule; n – nuclei; iv – iodinophilic vacuole.

Fig. 5 Histological sections (hematoxylin and eosin) of smallmouth bass, *Micropterus dolomieu* Lacepède, 1802 (Centrarchiformes: Centrarchidae) scales infected by *Myxobolus infrabractea* Ksepka & Bullard n. sp. (Bivalvulida: Myxobolidae) and gill lamellae infected by *Myxobolus intralamina* Ksepka & Bullard n. sp. A: Infected gill lamellae showing fusion of gill lamellae (*) B: Infected scale showing plasmodium on interior surface of scale (P) and raised end of scale perforating epidermis (arrow).

Fig. 6 Phylogenetic relationships of species of Myxobolidae infecting centrarchids and genetically similar species to *Myxobolus intralamina* Ksepka & Bullard n. sp. (Bivalvulida: Myxobolidae) and *Myxobolus infrabractea* Ksepka & Bullard n. sp. reconstructed with the SSU rDNA using Bayesian inference. Scale bar is in substitutions per site. Nodes labelled with posterior probability. New species in bold.

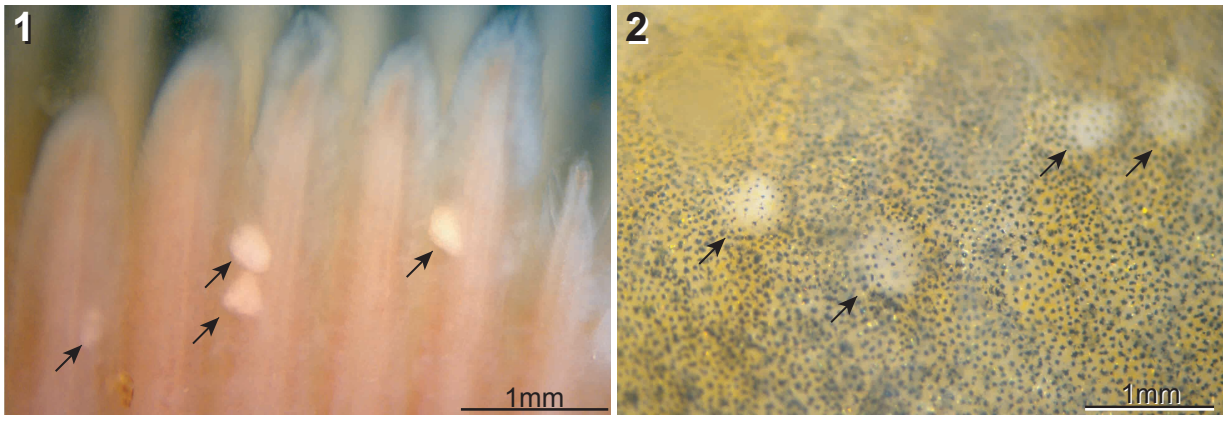
1
1mm
2
1mm

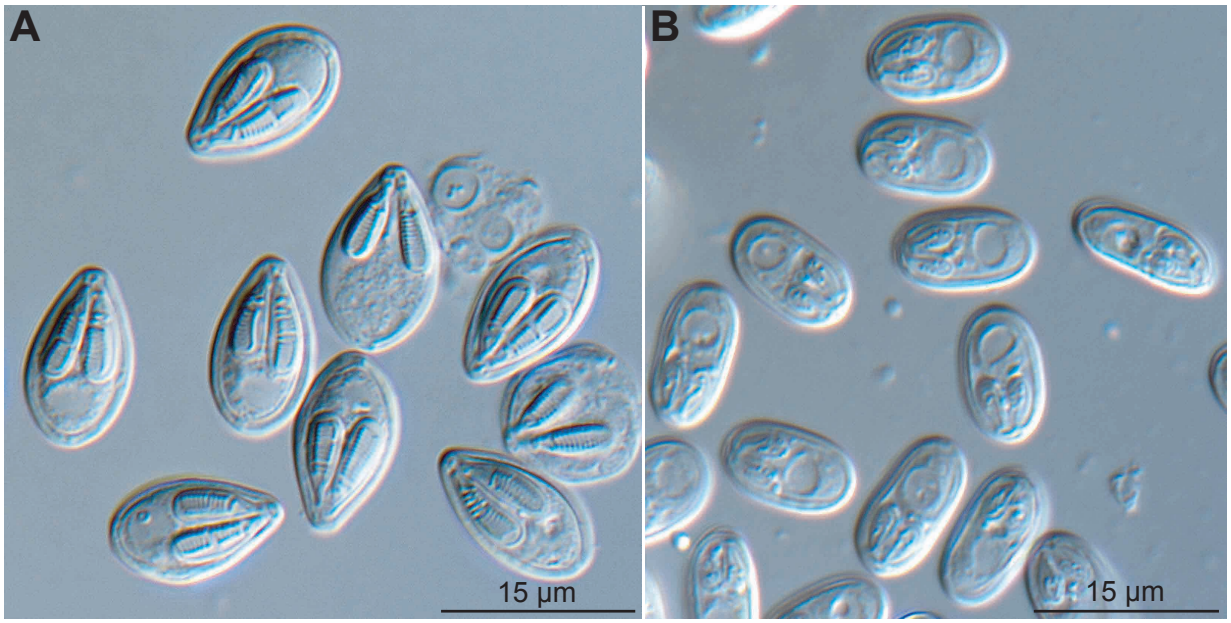
A
15 µm
B
15 µm

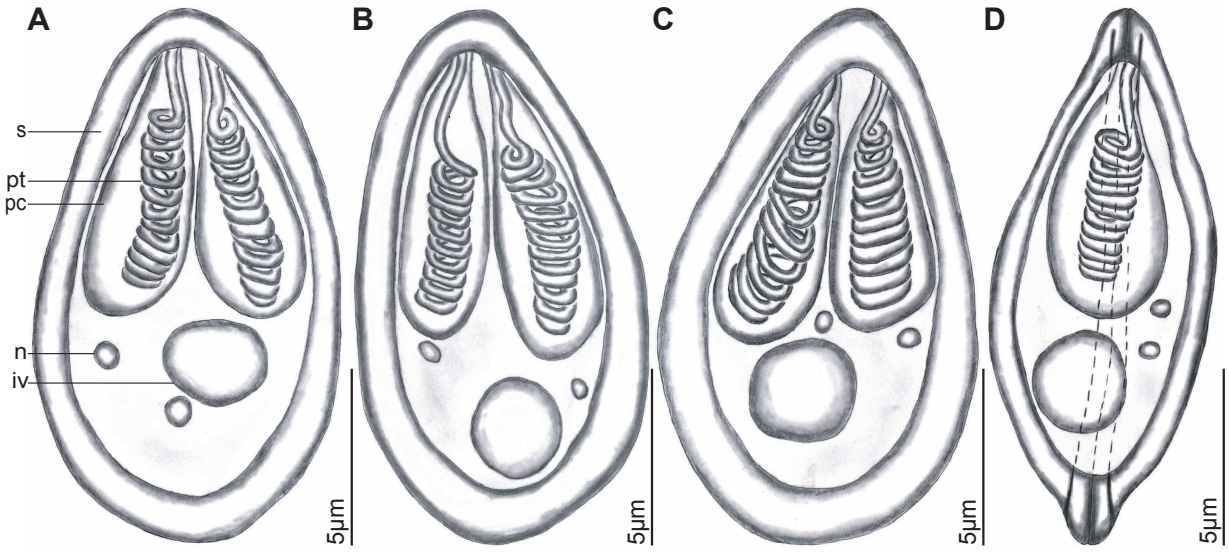
A
B
C
D
s
pt
pc
n
iv
5µm
5µm
5µm
5µm

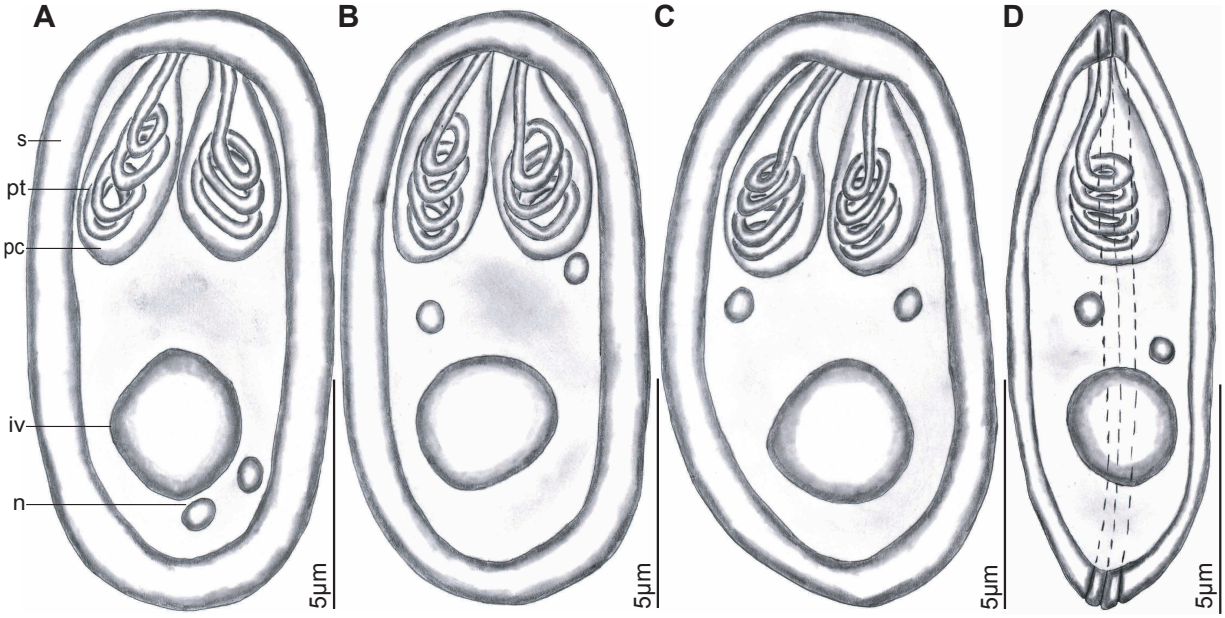
A
B
C
D
s
pt
pc
iv
n
5µm
5µm
5µm
5µm

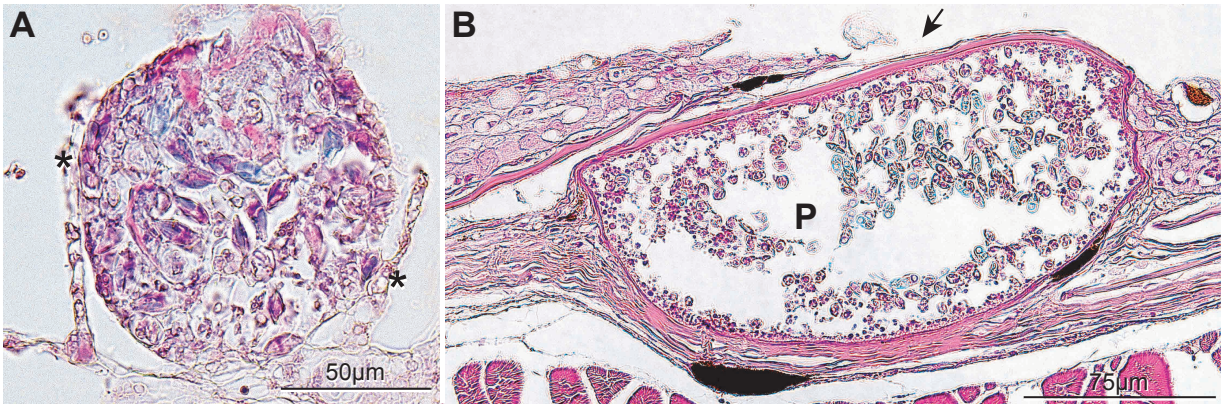
A
B
*
*
P
50µm
75µm

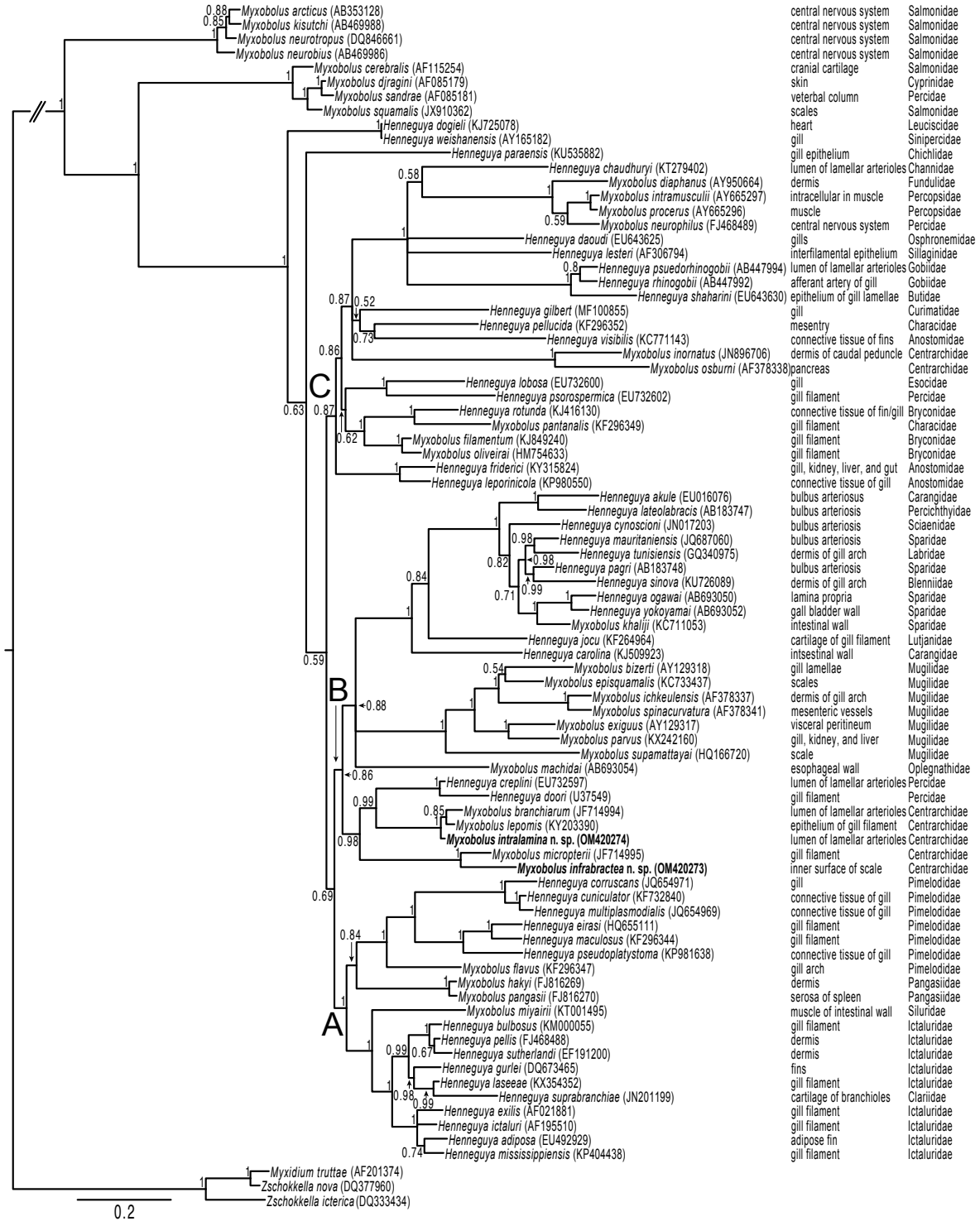
Myxobolus arcticus (AB353128) central nervous system Salmonidae
Myxobolus kisutchi (AB469988) central nervous system Salmonidae
Myxobolus neurotropus (DQ846661) central nervous system Salmonidae
Myxobolus neurobius (AB469986) central nervous system Salmonidae
Myxobolus cerebralis (AF115254) cranial cartilage Salmonidae
Myxobolus djragini (AF085179) skin Cyprinidae
Myxobolus sandrae (AF085181) veterbal column Percidae
Myxobolus squamalis (JX910362) scales Salmonidae
Henneguya dogieli (KJ725078) heart Leuciscidae
Henneguya weishanensis (AY165182) gill Sinipercidae
Henneguya paraensis (KU535882) gill epithelium Chichlidae
Henneguya chaudhuryi (KT279402) lumen of lamellar arterioles Channidae
Myxobolus diaphanus (AY950664) dermis Fundulidae
Myxobolus intramusculii (AY665297) intracellular in muscle Percopsidae
Myxobolus procerus (AY665296) muscle Percopsidae
Myxobolus neurophilus (FJ468489) central nervous system Percidae
Henneguya daoudi (EU643625) gills Osphronemidae
Henneguya lesteri (AF306794) interfilamental epithelium Sillaginidae
Henneguya psuedorhinogobii (AB447994) lumen of lamellar arterioles Gobiidae
Henneguya rhinogobii (AB447992) afferant artery of gill Gobiidae
Henneguya shaharini (EU643630) epithelium of gill lamellae Butidae
Henneguya gilbert (MF100855) gill Curimatidae
Henneguya pellucida (KF296352) mesentry Characidae
Henneguya visibilis (KC771143) connective tissue of fins Anostomidae
Myxobolus inornatus (JN896706) dermis of caudal peduncle Centrarchidae
Myxobolus osburni (AF378338) pancreas Centrarchidae
Henneguya lobosa (EU732600) gill Esocidae
Henneguya psorospermica (EU732602) gill filament Percidae
Henneguya rotunda (KJ416130) connective tissue of fin/gill Bryconidae
Myxobolus pantanalis (KF296349) gill filament Characidae
Myxobolus filamentum (KJ849240) gill filament Bryconidae
Myxobolus oliveirai (HM754633) gill filament Bryconidae
Henneguya friderici (KY315824) gill, kidney, liver, and gut Anostomidae
Henneguya leporinicola (KP980550) connective tissue of gill Anostomidae
Henneguya akule (EU016076) bulbus arteriosus Carangidae
Henneguya lateolabracis (AB183747) bulbus arteriosis Percichthyidae
Henneguya cynoscioni (JN017203) bulbus arteriosis Sciaenidae
Henneguya mauritaniensis (JQ687060) bulbus arteriosis Sparidae
Henneguya tunisiensis (GQ340975) dermis of gill arch Labridae
Henneguya pagri (AB183748) bulbus arteriosis Sparidae
Henneguya sinova (KU726089) dermis of gill arch Blenniidae
Henneguya ogawai (AB693050) lamina propria Sparidae
Henneguya yokoyamai (AB693052) gall bladder wall Sparidae
Myxobolus khaliji (KC711053) intestinal wall Sparidae
Henneguya jocu (KF264964) cartilage of gill filament Lutjanidae
Henneguya carolina (KJ509923) intsestinal wall Carangidae
Myxobolus bizerti (AY129318) gill lamellae Mugilidae
Myxobolus episquamalis (KC733437) scales Mugilidae
Myxobolus ichkeulensis (AF378337) dermis of gill arch Mugilidae
Myxobolus spinacurvatura (AF378341) mesenteric vessels Mugilidae
Myxobolus exiguus (AY129317) visceral peritineum Mugilidae
Myxobolus parvus (KX242160) gill, kidney, and liver Mugilidae
Myxobolus supamattayai (HQ166720) scale Mugilidae
Myxobolus machidai (AB693054) esophageal wall Oplegnathidae
Henneguya creplini (EU732597) lumen of lamellar arterioles Percidae
Henneguya doori (U37549) gill filament Percidae
Myxobolus branchiarum (JF714994) lumen of lamellar arterioles Centrarchidae
Myxobolus lepomis (KY203390) epithelium of gill filament Centrarchidae
Myxobolus intralamina n. sp. (OM420274) lumen of lamellar arterioles Centrarchidae
Myxobolus micropterii (JF714995) gill filament Centrarchidae
Myxobolus infrabractea n. sp. (OM420273) inner surface of scale Centrarchidae
Henneguya corruscans (JQ654971) gill Pimelodidae
Henneguya cuniculator (KF732840) connective tissue of gill Pimelodidae
Henneguya multiplasmodialis (JQ654969) connective tissue of gill Pimelodidae
Henneguya eirasi (HQ655111) gill filament Pimelodidae
Henneguya maculosus (KF296344) gill filament Pimelodidae
Henneguya pseudoplatystoma (KP981638) connective tissue of gill Pimelodidae
Myxobolus flavus (KF296347) gill arch Pimelodidae
Myxobolus hakyi (FJ816269) dermis Pangasiidae
Myxobolus pangasii (FJ816270) serosa of spleen Pangasiidae
Myxobolus miyairii (KT001495) muscle of intestinal wall Siluridae
Henneguya bulbosus (KM000055) gill filament Ictaluridae
Henneguya pellis (FJ468488) dermis Ictaluridae
Henneguya sutherlandi (EF191200) dermis Ictaluridae
Henneguya gurlei (DQ673465) fins Ictaluridae
Henneguya laseeae (KX354352) gill filament Ictaluridae
Henneguya suprabranchiae (JN201199) cartilage of branchioles Clariidae
Henneguya exilis (AF021881) gill filament Ictaluridae
Henneguya ictaluri (AF195510) gill filament Ictaluridae
Henneguya adiposa (EU492929) adipose fin Ictaluridae
Henneguya mississippiensis (KP404438) gill filament Ictaluridae
Myxidium truttae (AF201374)
Zschokkella nova (DQ377960)
Zschokkella icterica (DQ333434)
A
B
C
0.2

Table 1. Comparison of *Myxobolus* spp. that infect species of Centrarchidae. Mean measurements with range provided in µm. *MXL,* myxospore length; *MXW,* myxospore width; *MXT,* myxospore thickness; *PCL*, polar capsule length; *PCW,* polar capsule width; *PTC,* polar tubule coils; *ME,* mucous envelope (present or absent); *IV*, iodinophilic vacuole in sporoplasm (present or absent); *SM*, sutural markings (present or absent); *IP*, intercapsular process (present or absent).

Species	Host	MXL	MXW	MXT	PCL	PCW	PTC	ME	IV	SM	IP	Site*	Locality	Reference
M. branchiarum Walsh, Iwanowicz, Glenney, Iwanowicz and Blazer, 2012	*Micropterus dolomieu* Lacepede	12.8; 8.1–15.1	6.7; 4.0–9.0	5.7; 4.8–7.1	–	–	8–9	–	–	A	A	1	West Virginia, USA	Walsh et al. [4]
M. cartilaginis Hoffman, Putz and Dunbar, 1965	*Lepomis macrochirus* Rafinesque	10.8; 10.0–12.0	9.5; 9.0–11.0	6.1; 6.0–7.0	5.3; 5.0–6.0	3.1; 3.0–3.5	5–7	–	A	P	A	2	West Virginia, USA	Hoffman et al. [32]
M. corneus Cone, Horner and Hoffman, 1990	*Lepomis macrochirus* Rafinesque	9.4; 8.0–10.5	8.0; 6.5–9.0	–	5.3; 4.0–5.5	2.4; 2.5–3.0	7–8	A	A	P	P	3	Illinois, USA	Cone et al. [33]
M. dechtiari Cone and Anderson, 1977	*Lepomis gibbosus* (Linnaeus)	11.5; 10.0–14.0	8.0; 7.0–9.0	7.5; 7.0–8.0	5.0; 4.0–6.0	2.5; 2.0–3.0	7–8	A	P	P	A	1	Ontario, Canada	Cone and Anderson [34]
***M. infrabractea* n. sp. Ksepka and Bullard**	***Micropterus dolomieu* Lacepede**	**11.8; 11.0–13.0**	**6.7; 6.0–7.0**	**4.6; 4.0–5.0**	**4.0; 3.0–5.0**	**2.1; 2.0–3.0**	**3–4**	**A**	**P**	**A**	**A**	**7**	**North Carolina, USA**	**Present study**
***M. infrabractea* n. sp. Ksepka and Bullard (ethanol preserved)**	***Micropterus dolomieu* Lacepede**	**11.6; 11.0–13.0**	**6.6; 6.0–7.0**	**4.2; 4.0–5.0**	**3.6; 3.0–5.0**	**2.2; 2.0–3.0**	**3–4**	**A**	**P**	**A**	**A**	**7**	**North Carolina, USA**	**Present study**
M. inornatus Fish, 1938	*Micropterus dolomieu* Lacepede	11.3; 8.6–17.4	8.6; 7.1–13.7	6.6; 5.7–7.8	5.6; 4.2–9.5	2.6; 1.7–4.6	6–8	–	P	P	A	4	Pennsylvania, USA	Walsh et al. [4]
M. intestinalis Kudo, 1929	*Pomoxis nigromaculatus* (Leseur)	12.0–13.0	10.0–12.5	8	7.5–8.5	3.5–4.0	10–12	–	P	P	P	5	Illinois, USA	Kudo [35]
***M. intralamina* n. sp. Ksepka and Bullard**	***Micropterus dolomieu* Lacepede**	**14.4; 14.0–15.0**	**8.4; 8.0–9.0**	**6.3; 6.0–7.0**	**8.3; 7.0–9.0 7.5; 6.0–8.0**	**2.9; 2.0–3.0, 2.8; 2.0–3.0**	**11–13, 10–13**	**A**	**P**	**P**	**A**	**1**	**North Carolina, USA**	**Present study**
***M. intralamina* n. sp. Ksepka and Bullard (ethanol preserved)**	***Micropterus dolomieu* Lacepede**	**14.0; 13.0–15.0**	**8.1; 7.0–9.0**	**6.2; 6.0–7.0**	**7.9; 7.0–9.0 6.9; 6.0–8.0**	**2.8; 2.0–3.0 2.5; 2.0–3.0**	**11–13 10–13**	**A**	**P**	**P**	**A**	**1**	**North Carolina, USA**	**Present study**
M. iowensis Otto and Jahn, 1943	*Pomoxis nigromaculatus* (Leseur)	12.2–12.9	10.6–11.4	7.6	7.6	3.0–3.8	8–9	–	P	P	A	1	Iowa, USA	Otto and Jahn [36]
M. jollimorei Cone and Overstreet, 1998	*Lepomis macrochirus* Rafinesque	11.0; 10.5–11.5	13.8; 12.0–14.5	7.5; 6.5–8.0	6.0; 5.5–6.0	3.8; 3.5–4.5	6–9	A	A	P	A	6	Mississippi, USA	Cone and Overstreet [1]

M. kostiri Herrick, 1936	*Micropterus dolomieu* Lacepede	9.7; 8.8–11.2	7.4; 6.4–8.0	5.4; 4.9–5.8	4.4; 3.3–4.9 4.7; 4.1–4.9	2.5; 1.6–2.8 2.5; 2.4–3.3	13	–	P	A	A	7	Ohio, USA	Herrick [2]
M. lepomicus Li and Desser 1985	*Lepomis gibbosus* (Linnaeus)	14.5; 12.5–16.5	9.5; 9.0–9.6	7.0–7.5	5.5; 5.0–6.5	3.5; 3.0–4.0	5–7	–	–	–	P	8, 9	Canada	Li and Desser [37]
M. lepomis Rosser, Baumgartner, Barger and Griffin, 2017	*Lepomis marginatus* (Holbrook)	19.0; 16.8–21.3	7.9; 7.0–8.8	5.8; 5.3–6.1	9.0; 8.3–9.8	2.5; 2.2–2.7	10–12	A	A	A	A	1	Texas, USA	Rosser et al. [38]
M. magnaspherus Cone and Anderson, 1977	*Lepomis gibbosus* (Linnaeus)	18.0; 16.0–22.0	20.0; 18.0–22.0	12.0; 11.0–13.0	10.0; 9.0–12.0	6.0; 5.0–7.0	10–12	A	P	P	A	10	Ontario, Canada	Cone and Anderson [34]
M. manueli Cone and Overstreet, 1998	*Pomoxis nigromaculatus* (Leseur)	10.8; 10.0–11.0	9.1; 8.0–10.0	7.0; 6.5–7.0	5.3; 4.5–6.0	2.9; 2.5–3.0	6–7	A	A	A	A	6	Ohio, USA	Cone and Overstreet [1]
M. mesentericus Kudo, 1919	*Lepomis cyanellus Rafinesque*	10.0–11.5	8.5–9.5	6.5	4.7	1.5–2.0	–	–	P	P	A	11	Illinois, USA	Kudo [39]
M. microcystus Price and Mellen, 1980	*Micropterus salmoides* (Lacepede)	12.5; 11.0–14.0	7.5; 7.0–10.0	5.5; 5.0-–7.0	6.5; 5.0–7.0	2.5; 2.0–4.0	6–7	A	P	A	P	1	Illinois, USA	Price and Mellen [40]
M. micropterii Walsh, Iwanowics, Glenney, Iwamowicz and Blazer, 2012	*Micropterus salmoides* (Lacepede)	11.0–13.0	10.0–12.0	7.0–8.0	4.0–5.0	2.0–3.0		–	P	A	A	8	West Virginia, USA	Walsh et al [4]
M. mississipiensis Cone and Overstreet, 1998	*Lepomis macrochirus* Rafinesque	17.7; 16.4–18.7	5.2; 3.9–6.2	5.4; 5.0–5.3	7.2; 5.5–7.8	6.3; 5.5–7.0	9–10	A	A	A	A	1	Mississippi, USA	Cone and Overstreet [1]
M. okobojiensis Otto and Jahn 1943	*Pomoxis nigromaculatus* (Leseur)	11.7	10.2–11.7	–	5.8	–	8	–	P	P	A	5	Iowa, USA	Otto and Jahn [36]
M. osburni Herrick, 1936	*Micropterus dolomieu* Lacepede	10.2; 9.6–11.2	11.8; 9.6–12.8	6.8; 6.4–8.0	4.8–5.6	–	6–7	–	P	P	A	11	Ohio, USA	Herrick [2]
M. paralintoni Li and Desser, 1985	*Lepomis gibbosus* (Linnaeus)	12.3; 11.7–13.5	10.4; 9.0–10.6	–	5.4; 4.5–6.5	3.1; 2.7–3.8	6–9	–	P	P	A	6	Maryland, USA	Li and Desser [37]
M. sparoides Otto and Jahn, 1943	*Pomoxis nigromaculatus* (Leseur)	11.7–12.4	8.8–9.3	8.5	4.4–5.4	–	9–10	–	P	A	A	5	Iowa, USA	Otto and Jahn [36]
M. symmetricus Rice and Jahn, 1943	*Pomoxis nigromaculatus* (Leseur)	10.0	9.3	–	3.1	2.3	12–14	–	P	A	P	8	Iowa, USA	Rice and Jahn [41]
M. uvuliferis Cone and Anderson, 1977	*Lepomis gibbosus* (Linnaeus)	9.0; 7.0–12.0	11.5; 10.0–13.0	6.5; 6.0–7.0	4.5; 3.0–5.0	2.5; 2.0–3.0	5–7	A	P	P	A	12	Ontario, Canada	Cone and Anderson [34]

*Site: 1, gill lamellae; 2, cranial cartilage; 3, eye; 4, muscle; 5, intestine; 6, scales; 7, dermis; 8, gill filaments; 9, gall bladder; 10, Kidney; 11, mesentery; 12, tissue encapsulating *Uvulifer* spp. infections.

Table 2. Comparison of *Myxobolus* spp. that infect non-centrarchids and that are morphologically similar to *Myxobolus intralamina* n. sp. Mean measurements with range provided in µm. *MXL,* myxospore length; *MXW,* myxospore width; *MXT,* myxospore thickness; *PCL*, polar capsule length; *PCW,* polar capsule width; *PTC,* polar tubule coils; *ME,* mucous envelope (present or absent); *IV*, iodinophilic vacuole in sporoplasm (present or absent); *SM*, sutural markings (present or absent); *IP*, intercapsular process (present or absent).

Species	Host	MXL	MXW	MXT	PCL	PCW	PTC	ME	IV	SM	IP	Site*	Locality	Reference
M. andhrae Lalitha Kumari, 1969	*Channa punctata* (Block)	13.5; 12.1–15.7	6.4; 5.7–8.6	–	9.0; 8.6–10.0	1.7; 1.4–2.1	9	–	A	P	A	1	India	Lalitha Kumari [46]
M. indiae Lalitha Kumari, 1969	*Systomus sarana* (Hamilton)	13.7; 12.4–15.0	7.3; 6.4–8.6	–	5.9; 5.7–7.1	2.1; 1.4–2.5	8–10	–	A	P	A	2	India	Lalitha Kumari [46]
***M. intralamina* n. sp. Ksepka and Bullard**	***Micropterus dolomieu* Lacepede**	**14.4; 14.0–15.0**	**8.4; 8.0–9.0**	**6.3; 6.0–7.0**	**8.3; 7.0–9.0 7.5; 6.0–8.0**	**2.9; 2.0–3.0 2.8; 2.0–3.0**	**10–13**	**A**	**P**	**P**	**A**	**3**	**North Carolina, USA**	**Present study**
M. orissae Haldar, Samal and Mukhopadhyaya, 1996	*Cirrhinus cirrhosus* (Bloch)	15.7; 13.0–19.0	6.8; 4.9–8.1	–	8.8; 7.3–11.8	1.7; 2.4–3.2	–	–	–	A	P	2	India	Haldar et al. [47]
M. prochilodus (Azevedo, Vieira, Vieira, Silva and Abdallah, 2014)	*Prochilodus lineatus* (Valenciennes)	14.2; 11.8–15.8	11.1; 8.7–12.5	–	6.4; 5.2–7.9 6.0; 4.7–7.4	3.1; 2.3–4.0 2.9; 2.2–4.2	8–11	A	P	A	P	4	Brazil	Azevedo et al. [48]
M. tauricus Miroshnichenko, 1979	*Barbus tauricus* (Kessler)	11.5–14.5	9.0–11.0	–	6.0–8.5	2.7–3.5	–	–	A	A	P	2, 5, 6	Ukraine	Miroshnichenko [49]

*Site: 1, intestine; 2, gill; 3, gill lamellae; 4, gill filament; 5, fin; 6, muscle.

Table 3. Comparison of *Myxobolus* spp. that infect non-centrarchids and are morphologically similar to *Myxobolus infrabractea* n. sp. Mean measurements with range provided in µm. *MXL,* myxospore length; *MXW,* myxospore width; *MXT,* myxospore thickness; *PCL*, polar capsule length; *PCW,* polar capsule width; *PTC,* polar tubule coils; *ME,* mucous envelope (present or absent); *IV*, iodinophilic vacuole in sporoplasm (present or absent); *SM*, sutural markings (present or absent); *IP*, intercapsular process (present or absent).

Species	Host	MXL	MXW	MXT	PCL	PCW	PTC	ME	IV	SM	IP	Site*	Locality	Reference
M. bejeranoi Lovy, Smirnov, Brekhman, Ofek and Lotan, 2018	*Oreochromis aureus* × *Oreochromis niloticus*	10.8; 9.6–11.8	6.8; 5.7–8.6	–	5.2; 4.1–6.4	2.2; 1.5–2.6	3–5	–	A	A	A	1	Israel	Lovy et al. [50]
M. bellus Kudo, 1934	*Carpiodes carpio* (Rafinesque)	10.0–11.0	6.5–7.0	4.0–5.0	4.0–5.0	1.5–2.5	9–11	–	P	P	A	2	Illinois, USA	Kudo [51]

*M. bramaeformis A*khmerov, 1960	*Hypophthalmichthys molitrix* (Valenciennes)	11.0–12.0	7.0–7.5	–	4.5–5.0	2.8–3.0		–	P	A	P 3	Amur Basin	Akhmerov [52]
M. cultus Yokohama, Ogawa and Wakabayashi, 1995	*Carassius auratus* (Linnaeus)	10.2; 9.3–11.3	6.0; 5.2–7.2	4.3; 3.6–4.6	4.0; 3.1–4.9	1.9; 1.5–2.1	3–5	–	P	A	P 4	Tokyo, Japan	Yokoyama et al. [53]
M. dentium Fantham, Porter and Richardson, 1939	*Esox masquinongy* Mitchell	11.8–14.5	5.5–7.3	–	4.5–7.3	1.3–3.2	5–7	–	P	A	A 5	Missouri, USA	Fantham et al. [54]
***M. infrabractea* n. sp. Ksepka and Bullard**	***Micropterus dolomieu* Lacepede**	**11.8; 11.0–13.0**	**6.7; 6.0–7.0**	**4.6; 4.0–5.0**	**4.0; 3.0–5.0**	**2.1; 2.0–3.0**	**3–4**	**A**	**P**	**A**	**A 6**	**North Carolina, USA**	**Present study**
M. magai Deli, Folefack and Fomena, 2017	*Labeo batesii* Boulenger	10.6; 9.0–12.0	6.3; 5.5–7.0	–	2.8; 2.4–3.4	2.3; 2.0–3.0	4–5	–	A	A	A 7	Cameroon	Eiras et al. [55]
M. ophiocephaili Ma, 1998	*Channa striata (*Bloch)	12.0; 11.4–13.6	6.4; 6.0–6.8	4.7; 4.4–4.8	5.2; 4.8–5.0	1.7; 1.6–2.0	5	–	–	–	A 8, 9	China	Eiras et al. [56]
M. strelkovi Kostarev and Kulemina, 1971	*Phoxinus phoxinus* (Linnaeus)	8.0–12.2	6.0–11.0	4.0–7.0	3.3–5.4	2.0–4.1		–	–	–	P 7, 10	Russia	Eiras et al. [56]

*Site: 1, muscle; 2, dermis; 3, kidney; 4, cartilage; 5, palate; 6, scales; 7, gill lamellae; 8, skin; 9, fins; 10, liver.

CHAPTER 4: A NEW SPECIES OF *HENNEGUYA* THÉLOHAN, 1892 (CNIDARIA: BIVALVULIDA: MYXOBOLIDAE) INFECTING THE SUBMUCOSA OF THE INTESTINE AND PYLORIC CAECA OF RED DRUM, *SCIAENOPS OCELLATUS* (LINNAEUS) (PERCIFORMES: SCIAENIDAE) FROM COASTAL ALABAMA

***Published in Journal of Parasitology (Available 13 June 2023)**

Authors: Steven P. Ksepka and Stephen A. Bullard

ABSTRACT

A new species of *Henneguya* Thélohan, 1892 (Bivalvulida: Myxobolidae) is described from the submucosa of the intestine and pyloric caeca of red drum (*Sciaenops ocellatus* [Linnaeus, 1766] [Perciformes: Sciaenidae]) from the Gulf of Mexico off Gulf Shores, Alabama, United States. *Henneguya albomaculata* n. sp. differs from all congeners by the combination of myxospore dimensions, polar tubule coil count, the presence of an iodinophilic vacuole in the sporoplasm, and small subunit ribosomal DNA (*SSU* rDNA) sequence. A phylogenetic analysis of the *SSU* rDNA recovered *H. albomaculata* sister to *Henneguya cynosioni* Dykova, de Buron, Roumillat, and Fiala, 2011 in a clade composed of 11 species of *Henneguya* and 1 species of *Myxobolus* Bütschli, 1882 (Bivalvulida: Myxobolidae) that collectively infect fishes in marine or estuarine systems. Histological sections of infected intestine and pyloric caeca revealed plasmodia of *H. albomaculata* n. sp. developing in the loose connective tissue of the submucosa. The new species comprises the second species of *Henneguya* reported from red drum.

INTRODUCTION

Henneguya Thélohan, 1892 (Bivalvulida: Myxobolidae), the second most species-rich myxozoan genus, comprises >200 species infecting predominately freshwater intermediate hosts;

however, 59 species infect estuarine and marine fishes (Eiras, 2002; Eiras and Adriano, 2012; Wagner, 2016). There is little taxonomic information regarding species of *Henneguya* infecting drums (Sciaenidae) worldwide. The family Sciaenidae consists of 298 species that are principally marine, 28 species have secondarily invaded freshwater; including several species of recreational importance to the Southeast United States (Nelson, 2006; Fricke et al., 2022). Only 4 of the 298 accepted species of Sciaenidae reported as hosting a species of *Henneguya* (see Ganapati, 1941; Iversen and Yokel, 1963; Joy, 1972; Dykova et al., 2011). Only 4 species of *Henneguya* reportedly infect sciaenids: *Henneguya otolithi* Ganapati, 1972, *Henneguya texana* Joy, 1972, *Henneguya cynoscioni* Dykova, de Buron, Roumillat, and Fiala, 2011, and *Henneguya ocellata* Iverson and Yokel, 1963. *Henneguya otolithi* infects the heart of tigertooth croaker (*Otolithus ruber* [Bloch and Schneider, 1801] [Perciformes: Sciaenidae]) in India (Ganapati, 1941). *Henneguya texana* infects the gill filaments of black drum (*Pogonias cromis* [Linnaeus, 1766] [Perciformes: Sciaenindae]) in Clear Lake, Texas (Joy, 1972). *Henneguya cynoscioni* infects the heart of spotted seatrout (*Cynoscion nebulosus* [Cuvier, 1830] [Perciformes: Sciaenidae]) from estuaries in South Carolina (Dykova et al., 2011). *Henneguya ocellata* infects the epithelium of the pyloric caeca and intestine of red drum (*Sciaenops ocellatus* [Linnaeus, 1766] [Perciformes: Sciaenidae]) from Everglades National Park, Florida (Iverson and Yokel, 1963).

The United States National Marine Fisheries Commission reported 3 sciaenids in the top recreational marine species by number caught in 2020, i.e., spotted seatrout and Atlantic croaker (*Micropogonias undulatus* [Linnaeus, 1766] [Perciformes: Sciaenidae]) were the top 2 species by total catch with ~54 million and ~53 million individuals caught, respectively, and spot croaker (*Leiostomus xanthurus* Lacepede, 1802 [Perciformes: Sciaenidae]) as the top species by number harvested with ~20 million individuals harvested (National Marine Fisheries Service, 2022). Red

drum is among the most highly valued littoral sportfish in the US. It is prohibited from commercial harvest in all Gulf States except Mississippi (Bennetts et al., 2019). Recreational fisheries for this species have been estimated to be worth $498,000,000 and $350,000,000 per year in Louisiana and Texas respectively (Vega et al., 2011; Smith et al., 2022). Due to their recreational value and that they have been routinely cultured in the Gulf of Mexico, parasites and potential pathogens of red drum are of interest to resource managers because of their potential to impact wild stocks and cause disease in culture.

During necropsy of red drum related to a fish kill event in Gulf Shores, Alabama, numerous plasmodia containing myxospores consistent with *Henneguya* were observed in the submucosa of the intestine and pyloric caeca (Figs. 1-5). Herein, we use morphology, histology, and phylogenetics to describe this new species of *Henneguya*. The new species is the fifth of *Henneguya* reported from a sciaenid, the second from the intestine of red drum.

MATERIALS AND METHODS

Two moribund red drum related to a fish kill event were collected from Gulf Shores, Alabama, by the Alabama Marine Resources Division on 29 March 2022, bagged individually, placed on ice, and shipped overnight to the Southeast Cooperative Fish Parasite and Disease Laboratory at Auburn University for examination.

The morphological diagnosis was based on 50 myxospores (10 stained with Lugol's iodine; 10 stained with India ink) (Lom and Arthur, 1989). Measurements were taken from formalin-fixed myxospores at ×1,000 magnification using differential interference contrast (DIC) optical components. Lugol's iodine and India ink were used to stain the iodinophilic vacuole and mucous envelope respectively (Lom and Arthur, 1989). All measurements are reported in micrometers unless otherwise specified. To illustrate myxospores, plasmodia were ruptured and

vortexed to suspend myxospores before a drop of the suspension was cover-slipped, inverted, placed onto a thin layer of 1% agar (Lom, 1969), and illustrated using a ×100 oil immersion objective on an Olympus BX51(Olympus, Tokyo, Japan) compound scope equipped with a ×1.6 magnifier, differential interference contrast (DIC) components, and drawing tube. After fixation, one 1 cm^2 segment of infected intestine and pyloric caeca were rinsed in distilled water for 2 hr, dehydrated in an ethanol series, embedded in paraffin, sectioned at 4 µm, and stained with Gill's 3 hematoxylin and eosin per Luna (1992). Twenty-five slides were cut from each block yielding >300 sections on 50 slides.

DNA was extracted from two microscopically confirmed isolates of myxospores, one sourced from the intestine and the other from the pyloric caeca, each isolate contained myxospores from a single plasmodium using the DNeasy Blood and Tissue kit (Qiagen, Hilden, Germany). Extraction followed the manufacturer's protocol, with the exception that the proteinase K incubation step was extended overnight and 100 µl of AE buffer was used for the elution step to increase DNA concentration. Following extraction, concentration was measured using a NanoDrop-1000 spectrophotometer (Thermo Scientific, Nanodrop Technologies, Wilmington, Delaware), diluted to 20 ng/µl, and stored at -20 C. A fragment of the small subunit ribosomal DNA (SSU rDNA) was amplified using primers M153–F (5'–CATTGGATAACCGTGGGAAATCT–3') and M2192–R (5'–TAGTAGCGACGGGCGGTGT–3') (Ksepka et al., 2019, 2020b). PCR amplification used the following thermocycler parameters: initial denaturation step of 95 C, for 4 min, followed by 35 cycles of 95 C for 30 sec, 58 C for 30 sec, and 72 C for 1 min, with a final extension step of 72 C for 5 min. PCR products were visualized on a 1% agarose gel, purified using the QIAquick PCR Purification Kit (Qiagen) following manufacturers protocol, and sequenced by Genewiz (South Plainfield, New Jersey).

Sequencing primers M473–F (5'–GCTTGAGAAWCGGCTACCAC–3') and M1480–R (5'–GTGGTGCCCTTCCGTCAATTCC–3') were used to improve sequencing coverage (Ksepka et al., 2019, 2020b). Chromatograms were assembled based on sequence overlap, proofread by eye, and had low-quality read ends trimmed in Geneious version 2021.1.1 (Katoh and Standley, 2013) resulting in sequences of 1,713 base pairs.

Additional taxon selection for phylogenetic analysis was based on BLAST search of NCBI GenBank and a recent phylogenetic analysis of Myxobolidae in Ksepka et al. (2022) and included 75 species of Myxobolidae from clade A–C, 4 species of Myxobolidae infecting the central nervous system of salmonids, all available sequences of *Henneguya* spp. infecting sciaenids and 3 species of Myxidiidae as an outgroup (Liu et al., 2019). Sequences were aligned using MAFFT with an E–INS–i alignment strategy and a maxiterate value of 1,000 in Geneious version 2021.1.1 (Katoh and Standley, 2013). The alignment was trimmed to the length of the sequences presented herein (2,029 base pairs) to minimize missing data at the 5' and 3' end of the alignment. JModelTest2 version 2.1.10 was used to select best-fit models of nucleotide substitution based on Bayesian information criteria (Darriba et al., 2012). Bayesian inference was performed in MrBayes version 3.2.5 (Ronquist and Huelsenbeck, 2003) using substitution model averaging (nst = mixed) and a gamma distribution to model rate heterogeneity. Defaults were used for all other parameters. Three runs with four Metropolis-coupled chains were run for 5,000,000 generations. Stationarity was checked using Tracer 1.7 (Rambaut et al., 2018) and a burn-in of 25% of generations was determined. Evidence of convergence was further checked with the "sump" command in MrBayes. All parameters had a potential scale reduction factor of 1.00. A majority rule consensus tree of the post burn-in posterior distribution was generated with

the “sumt” command in MrBayes. The phylogenetic tree was visualized in FigTree v1.4.3 (Rambaut et al., 2014) and rendered for publication with Adobe Illustrator (Adobe Systems).

DESCRIPTION

***Henneguya albomaculata* n. sp.**

(Figs. 1–13)

Diagnosis of myxospores (based on 50 formalin-fixed myxospores using differential interference contrast microscopy [10 stained with Lugol’s iodine; 10 stained with India ink]; USNM coll. Nos. 1522383–1522385): Myxospore comprising 2 smooth symmetrical valves juxtaposed at sutural rim, 2 polar capsules, 2 caudal processes, and sporoplasm; total myxospore length 22.0–39.0 (mean ± SD = 26.7 ± 3.2; n =50), myxospore body subcircular, 9.0–11.0 (9.5 ± 0.5; 50) long (Figs. 6–8), 8.0–10.0 (8.9 ± 0.5; 40) wide (Figs. 6–8), 7.0–8.0 (7.4 ± 0.5; 10) thick (Fig. 9); sutural rim with prominent seam (Figs. 6–8), 1.0–2.0 (1.5 ± 0.5; 40) thick (lateral margin in frontal view) (Figs. 6–8), without flanking lateral ridges (sutural), lacking sutural markings; polar capsules equal (Figs. 6–8), clavate (Figs. 6–8), 4.0–5.0 (4.4 ± 0.5; 80) long (Figs. 6–8), 2.0–3.0 (2.4 ± 0.4; 80) wide (Figs. 6–8), with 3–5 polar tubule coils; caudal processes 2, projecting from the posterior of the myxospore valve and tapering, 11.0–30.0 (16.5 ± 4.0; 50) long; sporoplasm with iodinophilic vacuole 3–4 (3.3 ± 0.4; 10) in diameter (Figs. 6–8), having 2 nuclei (Figs. 6–8).

Taxonomic summary

Type host: Sciaenops ocellatus (Linnaeus, 1766) (Percirformes: Sciaenidae), red drum.

Type locality: Gulf of Mexico (30°13′28.4″N, 87°41′12.5″W) off Gulf Shores, Alabama.

Specimens deposited: Myxospores of fixed in 10% NBF (1 vial; syntype; USNM 1522383), and within paraffin sections (2 slides; syntypes; USNM 1522384– 1522385); GenBank No. (SSU rDNA): OQ269720.

Site in host: Intercellular, infecting the submucosa of the intestine and pyloric caeca.

Prevalence: Myxospores were detected in 2 of 2 (prevalence=100%) red drum.

ZooBank registration: urn:lsid:zoobank.org:act:4BCCA231-8E22-4C14-8D36-18AFFE51B466.

Etymology: The Latin specific name "*albomaculata*" is from "albus" (white) and "maculata" (spotted) referring to the gross appearance of infected intestine and pyloric caeca.

Remarks

The myxospore of *H. albomaculata* differs from that of its 4 congeners infecting sciaenids (*H. texana, H. otolithi, H. cynoscioni, H. ocellata)* by myxospore dimensions. The myxospore of the new species differs from those of *H. otolithi* and *H. texana* by being wider (8.0–10.0 vs. 6.0–8.5 and 6.0–7.0 respectively), thicker (7.0–8.0 vs. 4.0–5.0), and by having longer polar capsules (4.0–5.0 x 2.0–3.0 vs. 3.0–4.0 x 2.0–2.5 and 3.6–4.4 x 1.9–2.2 respectively). The myxospore of the new species differs from that of *H. cynoscioni* by being thicker (7.0–8.0 vs. 5.88) and having larger polar capsules (4.0–5.0 x 2.0–3.0 vs. 3.3 x 2). The myxospore of the new species differs from that of *H. ocellata* by being longer (22.0–38.0 vs. 17.2–21.1), thicker (7.0–8.0 vs. 5.9–6.6), and tissue infected (submucosa vs epithelium of intestine and pyloric caeca) (Table I).

A total of 7 species of *Henneguya* that infect non–sciaenid intermediate hosts have overlapping myxospore dimensions with the new species (Table I). The myxospores of the new species differ from those of *Henneguya bayerii* Pronin and Pronin 2002 by total myxospore length (22.0–38.0 vs. 44.0–56.8) and polar capsule length (4.0–5.0 vs. 3.2–3.9); those of

Henneguya brachydeuteri Fall, Fomena, Kostingue, Diebakate, Faye, and Toguebaye, 2000 by total myxospore length (22.0–38.0 vs. 41.0–56.0) and caudal process length (11.0278.0 vs. 26.0–29.0); those of *Henneguya mbourensis* Fall, Fomena, Kostingue, Diebakate, Faye, and Toguebaye, 2000 by caudal process length (16.6; 11.0–27.0 vs. 20.7; 20.0–22.5); those of *Henneguya ouakamensis* Fall, Fomena, Kostingue, Diebakate, Faye, and Toguebaye, 2000 by total myxospore length (22.0–38.0 vs. 16.0–24.0), myxospore width (8.0–10.0 vs. 5.0–9.0), and polar capsule length (4.0–5.0 vs. 3.0–4.0); and those *Henneguya sarotherodoni* Fall, Fomena, Kostingue, Diebakate, Faye, and Toguebaye, 2000 by total myxospore length (22.0–38.0 vs. 39.0–42.0), myxospore width (8.0–10.0 vs. 6.0–8.0); those of *Henneguya shackletoni* Brickle, Kalavatti, and MacKenzie, 2006 by polar tubule number (3–5 vs. 6–7); and those of *Henneguya tegidiensis* Nicholas and Jones, 1959 by total myxospore length (22.0–39.0 vs.30.0–68.0) and myxospore thickness (7.0–8.0 vs. 6.0–7.0) (Table I).

Histopathology

Plasmodia of *H. albomaculata* were intercellular in the loose connective tissue of the submucosa of the intestine and pyloric caeca (Figs. 10–13). Myxospore development in the plasmodium was asynchronous; mature myxospores occupied the interior of the plasmodium, whereas developing myxospores occupied the periphery of the plasmodium (Figs. 10, 12). The severity of the accompanying inflammatory response varied by the site of infection (Figs. 11, 13). In both sites, the granulomatous inflammatory response was characterized by numerous lymphocytes within proliferating loose connective tissue adjacent to the plasmodium; however, a myriad of eosinophilic granulocytes was present in the proliferating loose connective tissue of the pyloric caeca (Figs. 11, 13). Around 3 of 4 plasmodia infecting the intestine, a gap filled with an extracellular fluid and loose myxospores between the wall of the plasmodium and the loose

connective tissue of the submucosa was present (Figs. 10–11). These 3 plasmodia were incomplete, having perforations where the contents of the plasmodia were spilling into the space between the plasmodium and the submucosa. The overlying epithelium in sections of both tissues showed necrosis and waterlogging, evident by the vacuolated appearance and low staining intensity of the tissue; which could represent postmortem autolysis of cells, as these fish were collected from a mortality event and we cannot be sure how long fish had been deceased before collection (Figs. 10, 12). A lack of evidence of bacteria in the lesion suggests that putrefaction is not responsible for the lesion observed.

Phylogenetic analysis

The amplified *SSU* rDNA fragments of *H. albomaculata* from intestine and pyloric caeca comprised 2,029 nucleotides after alignment, were identical, and were similar to a sequence from *H. cynoscioni* (JN017203) in NCBI GenBank, which was included in the phylogenetic analysis, and differed from it by 123 (7.2%) nucleotides. We recovered 2 clades (nodal support >0.88): A) an unresolved clade containing 18 species of *Henneguya* and 12 species of *Myxobolus* Bütschli, 1882 (Bivalvulida: Myxobolidae) and B) containing 26 species of *Henneguya* and 14 species of *Myxobolus* (Fig. 14). Consistent with recent phylogenetic analyses of myxobolids, *Henneguya* and *Myxobolus* were recovered as para/polyphyletic (Liu et al., 2019; Ksepka et al., 2022). The new species was recovered sister to *H. cynoscioni*, the only other sciaenid infecting species with available sequence data, in a clade of myxobolids infecting connective tissues of fish in marine or estuarine environments (Fig. 14). With the exception of *Myxobolus machidai* Li, Sato, Kamata, Ohnishi, and Sugita-Konishi 2012, infecting the esophagus of spotted knifejaw (*Oplegnathus punctatus* [Temminck and Schlegel 1844] [Perciformes: Oplegnathidae]) in Japan, all species infecting fish from marine or estuarine environments were recovered in clade A (Fig.

14). Species in the analysis infect predominately connective tissues; however, no pattern was observed in the type of connective tissue or organ infected (Fig. 14).

DISCUSSION

Few fish species have been systematically detailed with histology, and published work characterizing the organ systems of fishes with histology are few. As a result, for most fishes, the pathologist cannot be sure what normal is nor have anything with which to compare their findings. A lack of baseline data on the histological features of the digestive tract of different fish lineages makes assessing host response to parasitic infections difficult. Fishes show diverse patterns of arrangement of their gastrointestinal tract (GI) with varying amounts of gut-associated lymphoid tissue, which plays an important role in their immune response (Ferguson, 2006; Roberts, 2012). As a result, immune cells are resident, to varying degrees, in the tissue of the GI tract; however, we only have baseline data for a select few fish lineages important in culture or as model organisms (Ferguson, 2006). The submucosa of the GI tract of salmonids is flanked by a layer of eosinophilic granulocytes (Amin et al., 1992). The spiral valve of lungfishes contains extensive lymphatic tissue containing numerous granulocytes and lymphocytes (Rafn and Wingstrand, 1981; Icardo et al., 2014). Channel catfish (*Ictalurus punctatus* [Rafinesque, 1818] [Siluriformes: Ictaluridae]) have few eosinophilic granulocytes in the GI tract; however, have resident lymphocytes in the mucosa (Grizzle and Rogers, 1976). This variability complicates determining if the presence of these immune cells observed in histological sections of parasitic infections in the GI tract of fishes represent resident immune cells or a host response to the infection. This lack of baseline data makes determining if immune cells observed adjacent to plasmodia represent an immune response to the infection or resident

cells. An atlas of the histological features of the GI tract of fishes that details the variation among fish lineages would prove an invaluable resource for assessment of host response in the GI tract.

We generally know little about how myxozoans get out of the fish host and come to infect the definitive host; however, histological observations of the plasmodium-mucosal interface could suggest that an infected fish can shed viable myxospores, i.e., transmission to the definitive host can occur without the fish host being eaten or dying. While it is generally accepted that myxospores can outlive their fish host to be shed by postmortem putrefaction of the host or predators defecating viable myxospore into the environment, we know little about if and how myxospores are shed from living fish hosts (Bjork and Bartholomew, 2009; Koel et al., 2010; Alexander at al., 2015). Stilwell et al., (2019), observed myxospores of *Henneguya adiposa* (Minchew 1977), infecting the adipose fin of channel catfish, loose in tissue adjacent to ruptured plasmodia that, in some cases, reached the epithelium of the adipose fin, suggesting that myxospores could be passively dispersed from the host without host death. Ksepka et al. (2020a), observed lesions consistent with late-stage *Myxobolus cerebralis* (Hofer 1903), the causative agent of salmonid whirling disease, infections that lacked myxospores in whirling disease symptomatic trout, suggesting that trout may have the ability to clear *M. cerebralis* infections without host death. The loose myxospores around plasmodia observed herein in the intestine may represent a dispersal strategy, which does not rely on host death, as loose myxospores could become phagocytized by the host and released into the lumen of the intestine to be dispersed into the environment. However, as the fish were collected from a mortality event, we cannot be certain it does not simply represent the postmortem deterioration of the plasmodium. Experimental life cycle studies, which pay special care to myxospore dispersal

from the fish host, could illuminate potential novel dispersal mechanisms for myxozoans, expanding our understanding of how myxospores are dispersed into the environment.

ACKNOWLEDGMENTS

We thank Max Westendorf (Alabama Marine Resources Division) for collecting the red drums. This work was funded by the Southeastern Cooperative Fish Parasite and Disease Project, Federal Aid in Sport Fish Restoration (administered by the Alabama Department of Conservation and Natural Resources, Marine Resources Division), Alabama Agricultural Experiment Station, and Auburn University College of Agriculture.

LITERATURE CITED

Alexander, J. D., B. L. Kerans, M. El-Matbouli, S. L. Hallett, and L. Stevens. 2015. Annelid-myxosporean interactions. *In* Myxozoan Evolution, Ecology and Development, B. Okamura, A. Gruhl, and J. L. Bartholomew (eds.). Springer International Publishing, Cham, Switzerland, p. 295–313.

Amin, A. B., L. Mortensen, and T. Poppe. 1992. Histology Atlas, Normal Structure of Salmonids: A Colour Atlas – English, German, French and Spanish Legends. Grafisk produksjon, Bodø, Norway, 222 p.

Bennetts, C. F., R. T. Leaf, and N. J. Brown-Peterson. 2019. Sex-specific growth and reproductive dynamics of red drum in the northern Gulf of Mexico. Marine and Coastal Fisheries: Dynamics, Management, and Ecosystem Science 11: 213–230.

Bjork, S. J., and J. L. Bartholomew. 2009. The effect of water velocity on the *Ceratomyxa shasta* infectious cycle. Journal of Fish Diseases 32: 131–142.

Brickle, P., C. Kalavati, and K. MacKenzie. 2006. *Henneguya shackletoni* sp. nov. (Myxosporea, Bivalvulida, Myxobolidae) from the Falklands mullet, *Eleginops maclovinus* (Cuvier) (Teleostei, Eleginopidae) in the Falklands Islands. Acta Parasitologica 51: 36–39.

Darriba, D., G. L. Taboada, R. Doallo, and D. Posada. 2012. jModelTest 2: more models, new heuristics, and parallel computing. Nature Methods 9: 772. doi:10.1038/nmeth.2109.

Dykova, I., I. de Buron, W. A. Roumillat, and I. Fiala. 2011. *Henneguya cynoscioni* sp. n. (Myxosporea: Bivalvulida) an agent of severe cardiac lesions in the spotted sea trout, *Cynoscion nebulosus* (Teleostei: Sciaenidae). Folia Parasitologica 58: 169–177.

Eiras, J. C. 2002. Synopsis of species of *Henneguya* Thèlohan, 1892 (Myxozoa: Myxosporea: Myxobolidae). Systematic Parasitology 52: 43–54.

Eiras, J. C., and E. A. Adrian. 2012. A checklist of new species of *Henneguya* Thèlohan, 1892 (Myxozoa: Myxosporea: Myxobolidae) described between 2002 and 2012. Systematic Parasitology 83: 95–104.

Fall, M., A. Fomena, B. Kostoingue, C. Diebakate, N. Faye, and B. S. Toguebaye. 2000. Myxosporidies (Myxozoa: Myxosporea) parasites des poissons Cichlidae du Cameroun, du Senegal et du Tchad avec la description de deux Nouvelles especes. Annales des Sciences Naturelles-Zoologie et Biologie Animale 22: 81–92.

Ferguson, H. W. 2006. Systemic pathology of fish: a text and atlas of normal tissues in teleosts and their responses to disease, 2nd edn., H. W. Ferguson (ed.). Scotian Press, London, England, 367 p.

Fricke, R., W. N. Eschmeyer, and R. van der Laan. 2022. Eschmeyer's catalog of fishes: Genera, species, references. Available at:

http://researcharchive.calacademy.org/research/icthyology/catalog/fishcatmain.asp. Accessed 10 August 2022.

Ganapati, P. N. 1941. On a new myxosporidian *Henneguya otolithi* n. sp. a tissue parasite from the bulbus arteriosus of two species of fish of the genus *Otolithus*. Proceedings of the Indian Academy of Science 13: 135–150.

Grizzle, J. M., and W. A. Rogers. 1976. The Anatomy and Histology of the Channel Catfish. Auburn Printing, Auburn, Alabama, 94 p.

Icardo, J. M., W. P. Wong, E. Colvee, A. M. Loong, A. G. Zapata, and Y. K. Ip. 2014. Lympho-granulocytic tissue associated with the wall of the spiral valve in African lungfish *Protopterus annectens*. Cell and Tissue Research 355: 397–407.

Iverson, E. S., and B. Yokel. 1963. A myxosporidian (Sporozoan) parasite in red drum, *Sciaenops ocellatus*. Bulletin of Marine Science of the Gulf and Caribbean 13: 449–453.

Joy, J. E. 1972. A new species of *Henneguya* (Myxosporidia: Myxobolidae) from the black drum *Pogonias cromis* in Clear Lake, Texas. Journal of Protozoology 19: 126–128.

Katoh, K., and D. M. Standley. 2013. MAFFT multiple sequence alignment software version 7: improvements in performance and usability. Molecular Biology and Evolution 30: 772–780.

Koel, T. M., B. L. Kerans, S. C. Barras, K. C. Hanson, and J. S. Woods. 2010. Avian piscivores as vectors for *Myxobolus cerebralis* in the Greater Yellowstone ecosystem. Transactions of the American Fisheries Society 139: 976–988.

Kpatcha, T. K., N. Faye, C. Diebakate, M. Fall, and B. S. Toguebaye. 1997. Nouvelles espèces d'Henneguya Thélohan, 1895 (Myxozoa, Myxosporea) parasites des poissons marins du Sénégal: Étude en microscopie photonique et électronique. Annales des Sciences Naturelles, Zoologie, 13e Série, 18, 81–91.

Ksepka, S. P., J. M. Rash, and S. A. Bullard. 2022. Two new species of *Myxobolus* (Myxozoa: Myxobolidae) infecting the gill and scales of the smallmouth bass, *Micropterus dolomieu* (Centrarchiformes: Centrarchidae) in the French Broad River Basin, North Carolina. Parasitology International 91. doi: 10.1016/j.parint.2022.102615.

Ksepka, S. P., J. M. Rash, B. L. Simcox, D. A. Besler, H. R. Dutton, M. B. Warren, and S. A. Bullard. 2020a. An updated geographic distribution of *Myxobolus cerebralis* (Hofer, 1903) (Bivalvulida: Myxobolidae) and the first diagnosed case of whirling disease in wild-caught trout in the south-eastern United States. Journal of Fish Diseases 43: 813–820.

Ksepka, S. P., J. M. Rash, N. V. Whelan, and S. A. Bullard. 2019. A new species of *Myxobolus* (Myxozoa: Bivalvulida) infecting the medulla oblongata and nerve cord of brook trout *Salvelinus fontinalis* in southern Appalachia (New River, NC, USA). Parasitology Research 118: 3241–3252.

Ksepka, S. P., N. V. Whelan, C. M. Whipps, and S. A. Bullard. 2020b. A new species of T*helohanellus* Kudo, 1933 (Myxozoa: Bivalvulida) infecting the skeletal muscle of blacktail shiner, *Cyprinella venusta* Girard, 1856 (Cypriniformes: Cyprinidae) in the Chattahoochee River Basin, Georgia. Journal of Parasitology 106: 350–359.

Liu, Y., A. Lovy, Z. Gu, and I. Fiala. 2019. Phylogeny of Myxobolidae (Myxozoa) and the evolution of myxospore appendages in the *Myxobolus* clade. International Journal for Parasitology 49: 523–530.

Lom, J. 1969. On a new taxonomic character in Myxosporidia, as demonstrated in descriptions of two new species of *Myxobolus*. Folia Parasitologica 16: 97−103.

Lom, J., and J. R. Arthur. 1989. A guideline for the preparation of species descriptions in myxosporea. Journal of Fish Diseases 12: 151–156.

Luna, L. G. 1992. Histopathologic Methods and Color Atlas of Special Stains and Tissue Artifacts. Johnson Printers, Downers Grove, Illinois, 767 p.

National Marine Fisheries Service. 2022. Fisheries of the United States, 2020. U.S. Department of Commerce, NOAA Current Fishery Statistics No. 2020. Available at: https://www.fisheries.noaa.gov/national/sustainable-fisheries/fisheries-united-states. Accessed 10 August 2022.

Nelson, J. S. 2006. Fishes of the World, 4th edn. John Wiley & Sons, Hoboken, New Jersey, 601 p.

Nicholas, W. L., and J. W. Jones. 1959. *Henneguya tegidiensis* sp. nov. (Myxosporidia) from the freshwater fish *Coregonus clupeoides pennantii* (the gwyniad). Parasitology 49: 1–5.

Pronina, S. V., and N. M. Pronin. 2002. New species of myxosporidians (Myxosporea: Cnidosporea) from the oilfishes (*Comephorus* spp.) of Baikal Lake. Parazitologiia 36: 327–330.

Rafn, S., and K. G. Wingstrand. 1981. Structure of intestine, pancreas, and spleen of the Australian lungfish *Neoceratodus forsteri* (Krefft). Zoologica Scripta 10: 223–239.

Rambaut, A., A. J. Drummond, D. Xie, G. Baele, and M. A. Suchard. 2018. Posterior summarization in Bayesian phylogenetics using Tracer 1.7. Systematic Biology 67: 901–904.

Rambaut, A., M. A. Suchard, D. Xie, and A. J. Drummond. 2014. FigTree v1.4.3. Available at: http://tree.bio.ed.ac.uk/software/figtree. Accessed August 10, 2022.

Roberts, R. J.(ed.). 2012. Fish Pathology, 4th edition. Wiley-Blackwell Publishing, West Sussex, England, 581 p.

Ronquist, F., and J. P. Huelsenbeck. 2003. MrBayes 3: Bayesian phylogenetic inference under mixed models. Bioinformatics 19:1572–1574.

Smith, D. R., S. R. Midway, R. H. Caffey, and J. M. Penn. 2022. Economic values of potential regulation changes for the southern flounder fishery in Louisiana. Marine and Coastal Fisheries: Dynamics, Management, and Ecosystem Science 14: e10195. doi:10.1002/mcf2.10195.

Stilwell, J. M., A. C. Camus, J. H. Leary, H. H. Mohammed, and M. J. Griffin. 2019. Molecular confirmation of *Henneguya adiposa* (Cnidaria: Myxozoa) and associated histologic changes in the adipose fins of channel catfish, *Ictalurus punctatus* (Teleost). Parasitology Research 118: 1639–1645.

Vega, R. R., W. H. Neill, J. R. Gold, and M. S. Ray. 2011. Enhancement of Texas sciaenids (red drum and spotted seatrout). NOAA Technical Memorandum NMFS-F/SPO-113: 85–92.

Wagner, E. J. 2016. A Guide to the Identification of Tailed Myxobolidae of the World: *Dicauda*, *Hennegoides*, *Henneguya*, *Laterocaudata*, *Neohenneguya*, *Phlogospora*, *Tetauromena*, *Trigonosporus* and *Unicauda*. Fish Creek Records, Logan, Utah, 166 p.

Figures 1–5. (**1**) Red drum (*Sciaenops ocellatus* [Linnaeus, 1766] [Perciformes: Sciaenidae]) intestine infected with plasmodia (arrows) of *Henneguya albomaculata* n. sp. Ksepka and Bullard (Bivalvulida: Myxobolidae) from the Gulf of Mexico, Alabama; photographed using a Olympus tough TG–6 camera. (**2–5**) Myxospores of *H. albomaculata* n. sp. Ksepka and Bullard (Bivalvulida: Myxobolidae) from the Gulf of Mexico, Alabama; photographed with differential interference contrast optical components.

Figures 6–9. Schematic drawings of myxospores of *Henneguya albomaculata* n. sp. Ksepka and Bullard (Bivalvulida: Myxobolidae) from the Gulf of Mexico, Alabama. (**6–8**) Frontal view. (**9**) Sutural view. Suture (s), polar tubules (pt), polar capsule (pc), nucleus (n), iodinophilic vacuole (iv), and caudal process (cp).

Figures 10–13. Histological sections (hematoxylin and eosin) of red drum (*Sciaenops ocellatus* [Linnaeus, 1766] [Perciformes: Sciaenidae]) intestine and pyloric caeca infected by *Henneguya albomaculata* Ksepka and Bullard n. sp. (Bivalvulida: Myxobolidae). (**10**) Infected intestine showing plasmodium of myxospores (P) in the loose connective tissue of the submucosa and space between the plasmodium and submucosa filled with extracellular fluid (*). (**11**) Infected intestine showing myxospores being released through gap in plasmodium (*), lymphocytic inflammatory infiltrates (arrows), and developing myxospores on periphery of plasmodium (arrowheads). (**12**) Infected pyloric caeca showing plasmodium in the loose connective tissue of the submucosa (P). (**13**) Infected pyloric caeca showing lymphocytic inflammatory infiltrates (arrows) and eosinophilic granulocytes in the inflammatory response (arrowheads).

Figure 14. Phylogenetic relationships of species of Myxobolidae infecting sciaenids and genetically similar species to *Henneguya albomaculata* Ksepka and Bullard n. sp. (Bivalvulida: Myxobolidae) reconstructed with the *SSU* rDNA gene using Bayesian

inference. Scale bar is in substitutions per site. New species in bold. Species infecting fishes in marine or estuarine ecosystems boxed in gray.

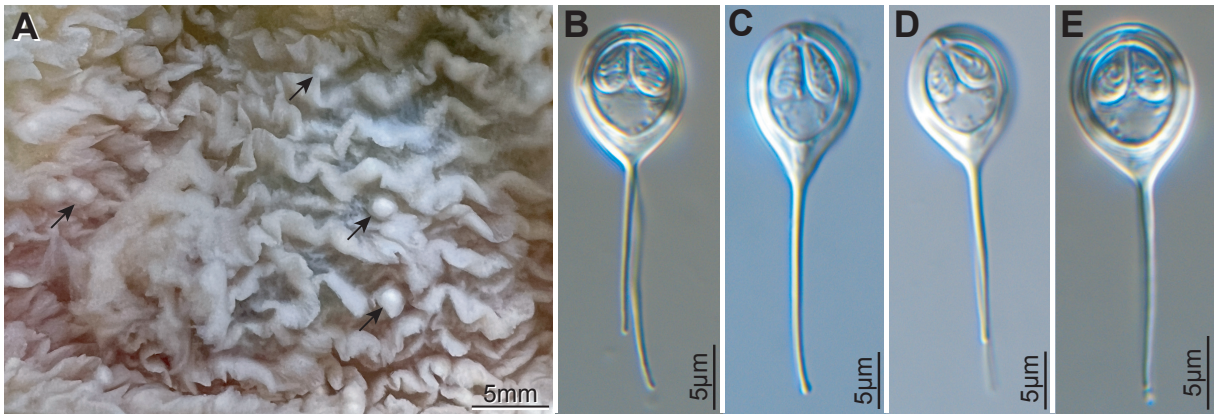
A
B
C
D
E
5mm
5µm
5µm
5µm
5µm

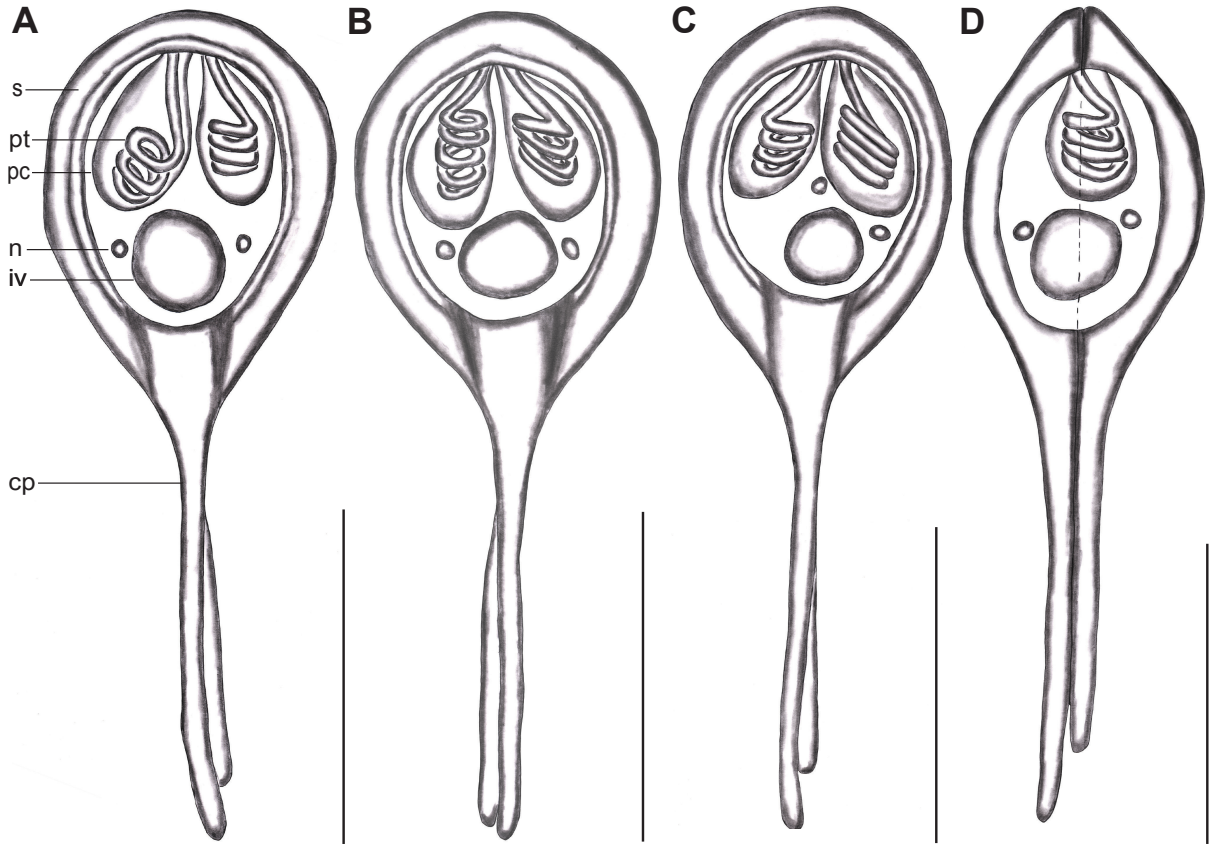
A
B
C
D
s
pt
pc
n
iv
cp

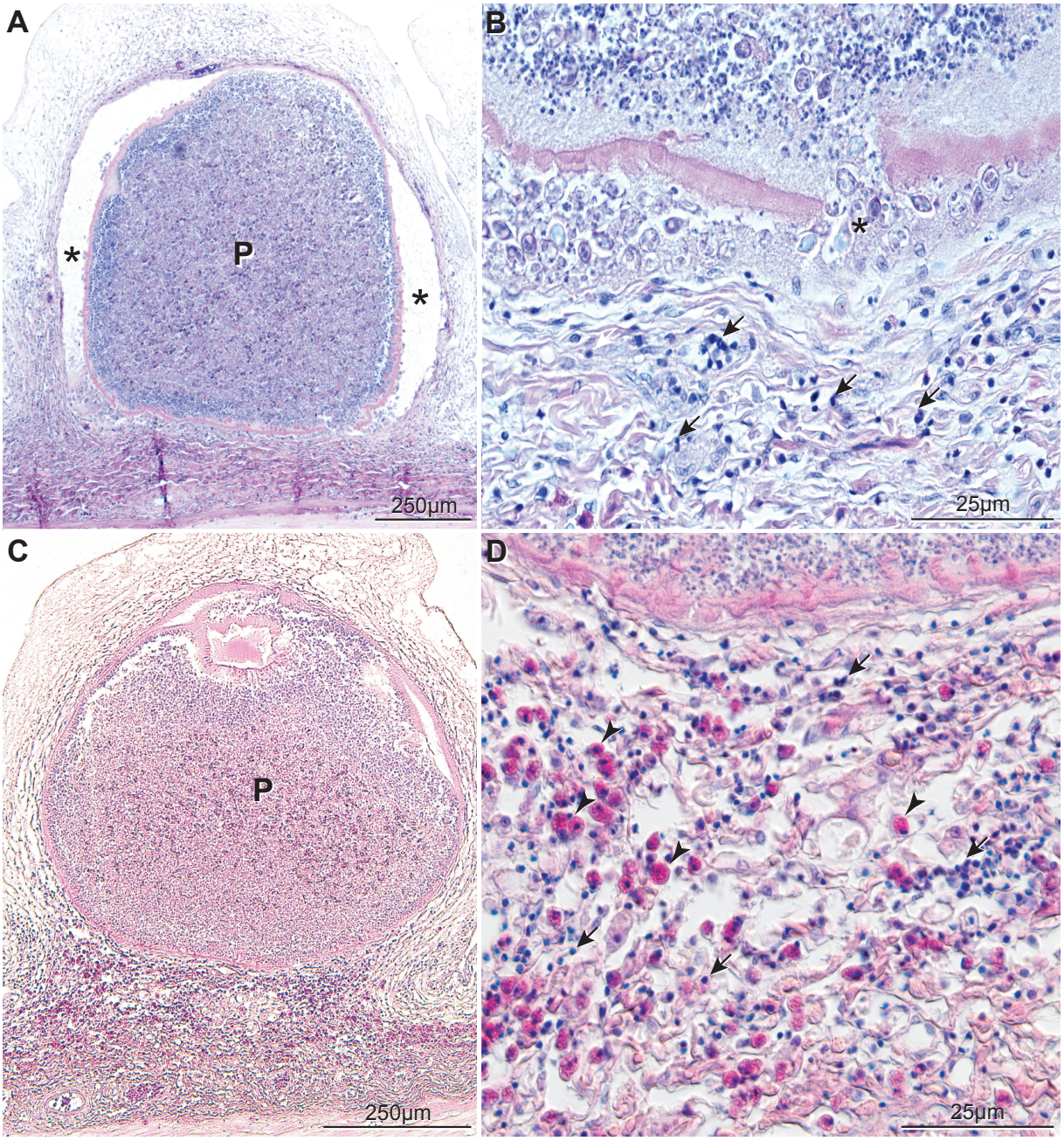
A
P
*
*
250µm
B
*
25µm
C
P
250µm
D
25µm

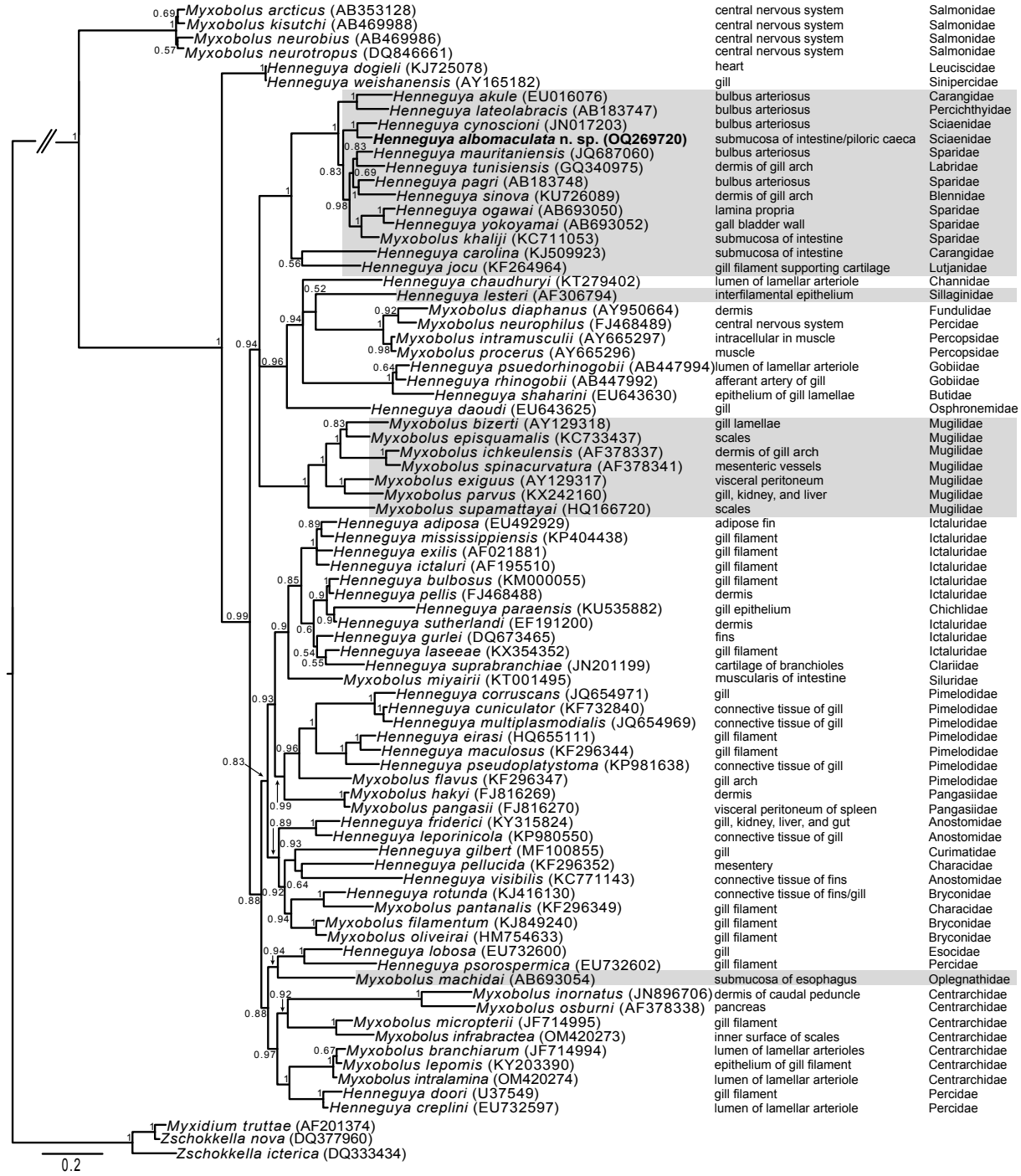
Myxobolus arcticus (AB353128) central nervous system Salmonidae
Myxobolus kisutchi (AB469988) central nervous system Salmonidae
Myxobolus neurobius (AB469986) central nervous system Salmonidae
Myxobolus neurotropus (DQ846661) central nervous system Salmonidae
Henneguya dogieli (KJ725078) heart Leuciscidae
Henneguya weishanensis (AY165182) gill Siniperciae
Henneguya akule (EU016076) bulbus arteriosus Carangidae
Henneguya lateolabracis (AB183747) bulbus arteriosus Percichthyidae
Henneguya cynoscioni (JN017203) bulbus arteriosus Sciaenidae
***Henneguya albomaculata* n. sp. (OQ269720)** submucosa of intestine/piloric caeca Sciaenidae
Henneguya mauritaniensis (JQ687060) bulbus arteriosus Sparidae
Henneguya tunisiensis (GQ340975) dermis of gill arch Labridae
Henneguya pagri (AB183748) bulbus arteriosus Sparidae
Henneguya sinova (KU726089) dermis of gill arch Blennidae
Henneguya ogawai (AB693050) lamina propria Sparidae
Henneguya yokoyamai (AB693052) gall bladder wall Sparidae
Myxobolus khaliji (KC711053) submucosa of intestine Sparidae
Henneguya carolina (KJ509923) submucosa of intestine Carangidae
Henneguya jocu (KF264964) gill filament supporting cartilage Lutjanidae
Henneguya chaudhuryi (KT279402) lumen of lamellar arteriole Channidae
Henneguya lesteri (AF306794) interfilamental epithelium Sillaginidae
Myxobolus diaphanus (AY950664) dermis Fundulidae
Myxobolus neurophilus (FJ468489) central nervous system Percidae
Myxobolus intramusculii (AY665296) intracellular in muscle Percopsidae
Myxobolus procerus (AY665296) muscle Percopsidae
Henneguya psuedorhinogobii (AB447994) lumen of lamellar arteriole Gobiidae
Henneguya rhinogobii (AB447992) afferant artery of gill Gobiidae
Henneguya shaharini (EU643630) epithelium of gill lamellae Butidae
Henneguya daoudi (EU643625) gill Osphronemidae
Myxobolus bizerti (AY129318) gill lamellae Mugilidae
Myxobolus episquamalis (KC733437) scales Mugilidae
Myxobolus ichkeulensis (AF378337) dermis of gill arch Mugilidae
Myxobolus spinacurvatura (AF378341) mesenteric vessels Mugilidae
Myxobolus exiguus (AY129317) visceral peritoneum Mugilidae
Myxobolus parvus (KX242160) gill, kidney, and liver Mugilidae
Myxobolus supamattayai (HQ166720) scales Mugilidae
Henneguya adiposa (EU492929) adipose fin Ictaluridae
Henneguya mississippiensis (KP404438) gill filament Ictaluridae
Henneguya exilis (AF021881) gill filament Ictaluridae
Henneguya ictaluri (AF195510) gill filament Ictaluridae
Henneguya bulbosus (KM000055) gill filament Ictaluridae
Henneguya pellis (FJ468488) dermis Ictaluridae
Henneguya paraensis (KU535882) gill epithelium Chichlidae
Henneguya sutherlandi (EF191200) dermis Ictaluridae
Henneguya gurlei (DQ673465) fins Ictaluridae
Henneguya laseeae (KX354352) gill filament Ictaluridae
Henneguya suprabranchiae (JN201199) cartilage of branchioles Clariidae
Myxobolus miyairii (KT001495) muscularis of intestine Siluridae
Henneguya corruscans (JQ654971) gill Pimelodidae
Henneguya cuniculator (KF732840) connective tissue of gill Pimelodidae
Henneguya multiplasmodialis (JQ654969) connective tissue of gill Pimelodidae
Henneguya eirasi (HQ655111) gill filament Pimelodidae
Henneguya maculosus (KF296344) gill filament Pimelodidae
Henneguya pseudoplatystoma (KP981638) connective tissue of gill Pimelodidae
Myxobolus flavus (KF296347) gill arch Pimelodidae
Myxobolus hakyi (FJ816269) dermis Pangasiidae
Myxobolus pangasii (FJ816270) visceral peritoneum of spleen Pangasiidae
Henneguya friderici (KY315824) gill, kidney, liver, and gut Anostomidae
Henneguya leporinicola (KP980550) connective tissue of gill Anostomidae
Henneguya gilbert (MF100855) gill Curimatidae
Henneguya pellucida (KF296352) mesentery Characidae
Henneguya visibilis (KC771143) connective tissue of fins Anostomidae
Henneguya rotunda (KJ416130) connective tissue of fins/gill Bryconidae
Myxobolus pantanalis (KF296349) gill filament Characidae
Myxobolus filamentum (KJ849240) gill filament Bryconidae
Myxobolus oliveirai (HM754633) gill filament Bryconidae
Henneguya lobosa (EU732600) gill Esocidae
Henneguya psorospermica (EU732602) gill filament Percidae
Myxobolus machidai (AB693054) submucosa of esophagus Oplegnathidae
Myxobolus inornatus (JN896706) dermis of caudal peduncle Centrarchidae
Myxobolus osburni (AF378338) pancreas Centrarchidae
Myxobolus micropterii (JF714995) gill filament Centrarchidae
Myxobolus infrabractea (OM420273) inner surface of scales Centrarchidae
Myxobolus branchiarum (JF714994) lumen of lamellar arterioles Centrarchidae
Myxobolus lepomis (KY203390) epithelium of gill filament Centrarchidae
Myxobolus intralamina (OM420274) lumen of lamellar arteriole Centrarchidae
Henneguya doori (U37549) gill filament Percidae
Henneguya creplini (EU732597) lumen of lamellar arteriole Percidae
Myxidium truttae (AF201374)
Zschokkella nova (DQ377960)
Zschokkella icterica (DQ333434)
0.2

Table I. Comparison of *Henneguya* spp. that infect species of Sciaenidiae or are morphologically similar to *Henneguya albomaculata* n. sp. Mean measurements with ranges provided in micrometers. Abbreviations: *TML*, total myxospore length; *MBL*, myxospore body length; *CPL*, caudal process length; *MXW*, myxospore width; *MXT*, myxospore thickness; *PCL*, polar capsule length; *PCW*, polar capsule width; *PTC*, polar tubule coil number; *IV*, iodinophilic vacuole in sporoplasm (present or absent); *SM*, sutural markings (present or absent).

Henneguya spp.	Host	TML	MBL	CPL	MXW	MXT	PCL	PCW	PTC	IV	SM	Site*	Locality	Reference
***H. albomaculata* n. sp. Ksepka & Bullard**	***Sciaenops ocellatus* (Linnaeus)**	**26.7; 22.0–38.0**	**9.5; 9.0–11.0**	**16.6; 11.0–27.0**	**8.9; 8.0–10.0**	**7.4; 7.0–8.0**	**4.4; 4.0–5.0**	**2.4; 2.0–3.0**	**3–5**	**P**	**A**	**1, 2**	**GOM**	**Present study**
H. bayerii Pronina & Pronin 2002	*Comephorus baicalensis* (Pallas)	44.0–56.8	11.1; 10.0–11.8	34.0–45.0	8.7; 7.9–9.5	7.9–8.4	3.2–3.9	1.5–3.2	6	A	P	3	Russia	Pronina and Pronin, 2002
H. brachydeuteri Kpathca, Faye, Diebakate, Fall, & Tobguebaye 1997	*Brachydeuterus auritus* (Valenciennes)	37.2; 36.0–41.0	11.5; 10.0–12.0	26.9; 26.0–29.0	8.4; 7.0–9.0		4.3; 4.0–5.0	2.6; 2.0–3.0	-	A	A	4	Senegal	Eiras et al. 2002
H. cynoscioni Dykova, de Buron, Roumillat & Fiala, 2011	*Cynoscion nebulosus* (Cuvier)	38.6; 34.3–44.1	10.4; 9.8–11.7	28.1; 23.5–33.3	8.82	5.88	3.3	2	3–4	-	-	4	South Carolina, USA	Dykova et al. 2011
H. mbourensis Kpatcha, Faye, Diebakate, Fall, & Toguebaye 1997	*Dentex canariensis* Steindachner	29.6; 28.0–33.0	10.3; 10.0–11.0	20.7; 20.0–22.5	8.0; 6.5–9.0		4.8; 3.5–5.0	2.4; 2.0–3.2	-	A	A	3	Senegal	Eiras et al. 2002
H. ocellata Iverson & Yokel, 1963	*Sciaenops ocellatus* (Linnaeus)	19.2; 17.2–21.2	8.8; 7.9–9.6		8.3; 7.3–8.9	6.3; 5.9–6.6	4.1; 3.6–4.3	2.6; 2.0–2.6	-	A	-	1	GOM	Iverson and Yokel, 1963
H. otolithi Ganapti 1941	*Otolithus ruber* (Block & Schneider)	35.0–47.0	10.0–12.0	35.0–40.0	6.0–8.5	4.0–5.0	3.0–4.0	2.0–2.5	4–6	P	A	4	India	Ganapti 1941
H. ouakamensis Kpatcha, Faye, Diebakate, Fall, & Tobguebaye 1997	*Mugil cephalus* Linnaeus	20.9; 16.0–24.0	10.9; 9.0–13.0	9.9; 6.0–14.0	7.0; 5.0–9.0		3.8; 3.0–4.0	2.4; 2.0–3.0	-	A	A	4,5	Senegal	Eiras et al. 2002
H. sarotherodoni Fall, Fomena, Kostingue, Diebakate, Faye, & Toguebaye 2000	*Sarotherodon galilaeus* (Linnaeus)	40.8; 39.0–42.0	11.7; 11.0–12.0	29.2; 28.0–30.0	6.9; 6.0–8.0		3.9; 3.0–5.0	2.3; 2.0–3.0	-	A	A	6	Chad	Fall et al. 2000
H. shackletoni Brickle, Kalavati, & MacKenzie 2006	*Eleginops maclovinus* (Cuvier)	49.0; 34.5–65.5	11.8; 9.6–14.4	37.3; 24.8–51.2	8.5; 7.2–11.2	7.0; 5.4–8.6	3.7; 3.2–4.8	3.1; 2.6–3.6	6–7	P	A	7	Falklands Islands	Brickle et al. 2006
H. tegidiensis Nicholas & Jones, 1959	*Coregonus clupeoides* Lacepede	30.0–68.0	9.8; 8.0–12.0	30.2; 11.0–46.0	7.8; 8.0–12.0	6.7; 6.0–7.0	4.0–5.0	2.0–3.0	5	P	A	8	North Wales	Nicholas and Jones 1959
H. texana Joy 1972	*Pogonias cromis* (Linnaeus)	43.0–68.0	8.1; 7.0–9.0	48.7; 36.0–59.0	6.7; 6.0–7.0	4.6; 4.0–5.0	4.0; 3.6–4.4	2.0; 1.9–2.2	3	A	A	5	Texas, USA	Joy 1972

* Site: 1, submucosa of intestine; 2, submucosa of pyloric caeca; 3, kidney; 4, heart; 5, gill; 6, intestine; 7, mesentery; 8, skin.

CHAPTER 5: FIRST REPORT OF *MYXOBOLUS NEUROFONTINALIS* (BIVALVULIDA: MYXOBOLIDAE) INFECTING ANADROMOUS BROOK TROUT, *SALVELINUS FONTINALIS* (SALMONIFORMES: SALMONIDAE) FROM PRINCE EDWARD ISLAND, CANADA

***Accepted with revisions at Journal of Aquatic Animal Health (31 July 2023)**

Authors: Steven P. Ksepka, David Groman, Laura Bourque, and Stephen A. Bullard

ABSTRACT

During routine histological examination of tissues from mortality events of anadromous Brook Trout *Salvelinus fontinalis* (Mitchell, 1802) (Salmoniformes: Salmonidae) from Prince Edward Island (PEI), Canada, myxospores consistent with *Myxobolus* Butschli, 1882 (Bivalvulida: Myxobolidae) were observed infecting the central nervous system. Using morphology, small subunit ribosomal DNA (SSU rDNA) data, and histology these myxospores were identified as *Myxobolus neurofontinalis* Ksepka and Bullard, (2019), which was previously described from the central nervous system of Brook Trout from the New River Basin, North Carolina, USA. Myxospore measurements from the PEI samples matched those reported in the description of *M. neurofontinalis* from North Carolina. A 1057 base pair fragment of the SSU rDNA from myxospores collected from Brook Trout in PEI was identical to an isolate of *M. neurofontinalis* (MN191598) collected previously from the type locality, New River Basin, North Carolina. Histological sections confirmed infections were intercellular in the central nervous system. Minimal host response was observed, with only sparse mononuclear inflammatory infiltrates present at the periphery of and within dispersed myxospores, suggesting infections are not

pathogenic to Brook Trout. This constitutes the first time *M. neurofontinalis* has been documented outside of the New River Basin in North Carolina.

[A]Introduction

A total of 8 species of *Myxobolus* infect the central nervous system of salmonids: *Myxobolus farionis* Gonzalez-Lanza and Alvarez-Pellitro, 1984 (Bivalvulida: Myxobolidae); *Myxobolus neurobius* Schuberg and Schroder, 1905, *Myxobolus kisutchi* Yasutake and Wood, 1957; *Myxobolus neurotropus* Hogge, Campbell, and Johnson, 2008; *Myxobolus murakamii* Urawa, Iida, Freeman, Yanagida, Karlsbakk, and Yokoyama, 2009; *Myxobolus arcticus* Pugachev and Khokhlov, 1979; *Myxobolus fryeri* Ferguson, Atkinson, Whipps, and Kent, 2008; and *Myxobolus neurofontinalis* Ksepka and Bullard, 2019. *Myxobolus farionis* infects Brown Trout *Salmo trutta* Linnaeus, 1758 (Salmoniformes: Salmonidae) in the Duero Basin, Spain (Gonzalez-Lanza and Alvarez-Pellitro 1984). *Myxobolus kisutchi* infects Coho Salmon *Oncorhynchus kisutch* (Walbaum, 1792) (Salmoniformes: Salmonidae) in Washington (Hogge et al. 2008a). *Myxobolus neurobius* infects Brown Trout in Norway (Urawa et al. 2009). *Myxobolus neurotropus* infects Rainbow Trout *Oncorhynchus mykiss* (Walbaum, 1792) in Idaho (Hogge et al. 2008b). *Myxobolus murakamii* infects Masu Salmon *Oncorhynchus masou* (Brevoort, 1856) in Hokkaido, Japan (Urawa et al. 2009). *Myxobolus arcticus* infects *Oncorhynchus* Suckley, 1861 species in the Kamchatka Peninsula, Russia (Pugachev and Khokhlov 1979). *Myxobolus fryeri* infects Coho Salmon in Oregon (Ferguson et al. 2008). *Myxobolus neurofontinalis* infects Brook Trout in the New River Basin, North Carolina (Ksepka et al. 2019).

Salmonid central nervous system infecting species are not typically pathogenic or immunogenic. Only *M. murakamii*, the causative agent of salmonid sleeping disease, which

impairs swimming, reported as pathogenic in cultured Masu Salmon in Japan (Urawa et al. 2009). Given the morphological similarity of *Myxobolus* spp. and significant impacts false positives for pathogenic species of *Myxobolus* can have on culture facilities and government agencies, documenting the range of non-pathogenic salmonid central nervous system infecting *Myxobolus* species will reduce the potential for false positives for *Myxobolus cerebralis* Hofer, 1903.

We herein use myxospore morphology, small subunit ribosomal DNA (SSU rDNA), and histology to report infections by *M. neurofontinalis* from Brook Trout collected as periodic mortalities from Prince Edward Island (PEI) watersheds for histologic screening for neurotropic myxozoan infections (Table 1). This is the first report of *M. neurofontinalis* outside of the New River Basin, North Carolina.

[A]Methods

From July 10, 2014 to June 24, 2021, 27 wild Brook Trout mortalities were submitted by either private citizens or provincial conservation officers from 12 localities in PEI, Canada and were necropsied at the Atlantic Veterinary College (Table 1). Following necropsy, tissues were fixed in 10% neutral buffered formalin (n.b.f) for histology and morphology and preserved in 95% ethanol for DNA extraction. After fixation, the brain was trimmed to fit into tissue processing cassettes, dehydrated in an ethanol series, embedded in paraffin, sectioned, stained with hematoxylin and eosin, and examined histologically for potential pathological conditions. Samples, containing tissues from individual fish, confirmed by histology to be infected by myxozoans were shipped to Auburn University for further processing. Myxospores were isolated

by macerating infected tissue in a small stender dish filled with sterilized deionized water and pipetting released myxospores into formalin for morphology or lysis buffer for DNA extraction.

Measurements were generated from 50 n.b.f-fixed myxospores sourced from 3 infected fish at ×1000 magnification. Micrographs were taken from n.b.f.-fixed myxospores from all infected fish myxospore measurements were sourced from at ×1000 magnification. Lugol's iodine and India ink were used to stain the iodiniphilic vacuole and mucous envelope, respectively, per Lom and Arthur (1989). All measurements are reported in micrometers unless otherwise specified. To photograph myxospores, myxospores were suspended by vortexing before a drop of the suspension was cover-slipped, inverted, placed onto a thin layer of 1% agar (Lom and Arthur, 1989), and photographed using a 100× oil immersion objective on an Olympus BX51 compound scope equipped with differential interference contrast (DIC) components.

DNA was extracted from one microscopically confirmed isolate of myxospores from one ethanol preserved portion of infected tissue, using the DNeasy Blood & Tissue kit (Qiagen) following the manufacturer's protocol, with the exceptions that the proteinase K incubation step was extended overnight and 100 µl of AE buffer were used for the elution step to increase DNA concentration. Following extraction, concentration was measured using a NanoDrop-1000 spectrophotometer (Thermo Scientific, Nanodrop Technologies) and stored at -20ºC. A fragment of a variable region of the small subunit ribosomal DNA (SSU rDNA) was amplified using primers M153–F (5'–CATTGGATAACCGTGGGAAATCT–3') and M1480–R (5'–GTGGTGCCCTTCCGTCAATTCC –3') (Ksepka et al. 2019). PCR amplification followed Ksepka et al. (2019). PCR products were visualized on a 1% agarose gel, purified using the

QIAquick PCR Purification Kit (Qiagen) following manufacturers protocol, with the exception that sterile water was substituted for AE buffer for eluting DNA, and sequenced in both directions using primers from PCR amplification by Genewiz (South Plainfield, New Jersey). Chromatograms were assembled based on sequence overlap, proofread by eye, and had low-quality read ends trimmed in Geneious version 2021.1.1 (http://www.geneious.com). The resulting sequence was compared to those in GenBank by nucleotide BLAST search.

[A]Results

[B]Screening results

Myxobolus neurofontinalis was detected in Brook Trout from 7 of 12 collection events (Table 1). Myxospores were observed in histological sections of nerve tissue in 1 of 1 (100%) Brook Trout from West River (2016 collection), Morell River (2017 collection), and Whitlock's Pond; 2 of 2 (100%) Brook trout from West River (2020 collection); 3 of 3 (100%) Brook trout from Morell River (2014 collection); 6 of 6 (100%) of Brook Trout from Trout River; and 1 of 2 (50%) of Brook Trout from MacLure's Pond (Table 1).

[B]Myxospore morphology

Dimensions of n.b.f-fixed myxospores sourced from the central nervous system of Brook Trout from PEI were indistinguishable from those of n.b.f- fixed myxospores of *M. neurofontinalis*, which suggests samples collected herein are conspecific with *M. neurofontinalis* (see Ksepka et al., 2019). Our myxospores were 13.0–15.0 (mean ± SD = 14.2 ± 0.6; N = 50) long, 9.0–11.0 (10.4 ± 0.7; 40) wide, and 8.0–10.0 (8.5 ± 0.7; 10) thick (Figure 1). Polar capsules were 7.0–9.0 (8.2 ± 0.7; 80) long and 3.0–4.0 (3.1 ± 0.4; 80) wide, with 7–10 polar tubule coils (Figure 1). Like the specimens of *M. neurofontinalis* from North Carolina (Ksepka et al., 2019),

an intercapsular process, iodinophilic vacuole in the sporoplasm, mucous envelope on the rounded posterior margin of the myxospore, and sutural markings are likewise present in the collected samples (Figure 1).

[B]Sequence comparison

The 1057 base pair SSU rDNA (*18S*) sequence fragment generated herein for *M. neurofontinalis* (GenBank accession number: OR452314) was identical to the sequence of *M. neurofontinalis* (MN191598) from its type locality, which supports the morphological assertion that samples collected herein are conspecific with *M. neurofontinalis* (Ksepka et al. 2019). Hence, we consider the samples collected herein conspecific with *M. neurofontinalis*, as they are morphologically and molecularly indistinguishable from isolates of *M. neurofontinalis* infecting Brook Trout in North Carolina.

[B]Histological comparison

Myxospores of *M. neurofontinalis* were observed in the central nervous system of 15 of 27 (55%) Brook Trout sampled. Histological observations were consistent with those of Ksepka et al. (2019). Myxospores were observed in intercellular foci, with no defined plasmodium, and loosely dispersed within the neuropil (Figure 2A–B). A mild inflammatory response was observed on the periphery of dispersed myxospores, characterized by the presence of sparce mononuclear inflammatory infiltrates within and on the periphery of the cluster of myxospores (Figure 2B). No host response was observed in association with developing presporogonic stages (Figure 2C).

[A]Discussion

Myxobolids infecting catadromous and anadromous fishes have obligately freshwater definitive hosts (Eszterbauer et al. 2015). Of the 28 myxobolid life cycles known, 4 infect fishes that can be anadromous or catadromous, all of which have freshwater definitive hosts: *M. arcticus*, *M. cerebralis*, *Myxobolus portaucalensis* Saraiva and Molnar, 1990, and *Henneguya nuesslini* Schuberg and Schroder, 1905 (Bivalvulida: Myxobolidae) (Eszterbauer et al. 2015). *Myxobolus arcticus*, infecting the central nervous system of *Oncorhynchus* spp. in the Pacific Basin, matures in *Styolodrilus heringianus* Claparède, 1862 (Clitella: Lumbriculidae) and *Lumbriculus variegatus* (Muller, 1774) (Clitella: Lumbriculidae) (Kent et al. 1993; Urawa, 1994; Urawa et al. 2011). The bone- and cartilage-infecting *M. cerebralis* has been introduced extensively outside of its theoretical native range and infects a number of anadromous salmonids and matures in "*Tubifex tubifex*" *sensu lato* (Clitella: Lumbriculidae) (Markiw & Wolf 1983; El-Matbouli et al. 1992; Hedrick & El- Matbouli 2002; Ksepka et al. 2021). *Henneguya nuesslini*, infecting the connective tissue of Brown Trout, matures in *T. tubifex* (Kallert et al. 2005). *Myxobolus portaucalensis*, infecting the connective tissue of the catadromous European Eel *Anguilla anguilla* (Linnaeus, 1758) (Anguilliformes: Anguillidae), matures in "*T. tubifex*" (see El-Mansy et al. 1998). This, in combination with Brook Trout from the type locality (North Carolina) for *M. neurofontinalis* being landlocked, suggests that the brook trout sampled from PEI were infected in freshwater (Ksepka et al. 2019). No record of a marine invertebrate definitive host for a myxobolid exists.

[A]Acknowledgements

We thank personnel from the Atlantic Node of the Canadian Wildlife Health Cooperative (CWHC) and staff of Diagnostic Services at the Atlantic Veterinary College at the University of Prince Edward Island, Canada for assistance in fish necropsy and histological processing of samples. This study was supported by the Southeastern Cooperative Fish Parasite and Disease Project, the US Fish and Wildlife Service (Department of Interior), National Sea Grant (National Oceanic and Atmospheric Administration), United States Department of Agriculture (National Institute of Food and Agriculture), Federal Aid in Sport Fish Restoration (Alabama Department of Conservation and Natural Resources, Inland and Marine Resources Divisions), the Alabama Agricultural Experiment Station (Auburn University, College of Agriculture), and the Atlantic Node of the CWHC in Prince Edward Island.

[A]References

El-Mansy, A., K. Molnar, and C. Szekely. 1998. Development of *Myxobolus portucalensis* Saraiva (Molnar, 1990) (Myxosporea: Myxobolidae) in the oligochaete *Tubifex tubifex* (Muller). Systematic Parasitology 41: 95–103.

El-Matbouli M., T. Fischer-Scherl, and R. W. Hoffmann. 1992. Present knowledge on the life cycle, taxonomy, pathology and therapy of some Myxosporea spp. important for freshwater fish. Annual Review of Fish Diseases 2: 367–402.

Eszterbauer, E., S. Atkinson, A. Diamant, D. Morris, M. El-Matbouli, and H. Hartikainen. 2015. Myxosporean life cycles: Practical approaches and insights. *In* Myxozoan Evolution, Ecology and Development, B. Okamura, A. Gruhl, and J. L. Bartholomew (eds.). Springer International Publishing, Switzerland, pp. 175–198.

Ferguson, J. A., S. D. Atkinson, C. M. Whipps, and M. L. Kent. 2008. Molecular and morphological analysis of myxobolus spp. of salmonid fishes with the description of a new *Myxobolus*s species. Journal of Parasitology 94:1322–1334.

Gonzalez-Lanza, C., and M. P. Alvarez-Pellitero. 1984. *Myxobolus farionis* n. sp. and *M. ibericus* of *Salmo trutta* from the Duero basin (NW Spain). Description and population dynamics. Angewandte Parasitologie 25:181–189.

Hedrick R. P., and M. El-Matbouli. 2002. Recent advances with taxonomy, life cycle, and development of *Myxobolus cerebralis* in the fish and oligochaete hosts. American Fisheries Society Symposium 29: 45–53.

Hogge, C. I., M. R. Campbell, and K. A. Johnson. 2008a. Redescription and molecular characterization of *Myxobolus kisutchi* Yasutake & Wood, 1957. Journal of Fish Diseases 31:707–712.

Hogge, C. I., M. R. Campbell, and K. A. Johnson. 2008b. A new species of Myxozoan (Myxosporea) from the brain and spinal cord of rainbow trout (*Oncorhynchus mykiss*) from Idaho. Journal of Parasitology 94:218–222.

Kallert, D. M., E. Eszterbauer, M. El-Matbouli, C. Erseus, and W. Haas. 2005. The life cycle of *Henneguya nuesslini* Schuberg and Schroder, 1905 (Myxozoa) involves a triactinomyxon-type actinospore. Journal of Fish Diseases 28: 71–79.

Kent, M. L., D. J. Whitaker, and L. Margolis. 1993. Transmission of *Myxobolus arcticus* Pugachev and Khokhlov, 1979, a myxosporean parasite of Pacific salmon, via triactinomyxon from the aquatic oligochaete *Stylodrilus heringianus* (Lumbriculidae). Canadian Journal of Zoology 71: 1207–1211.

Ksepka, S. P., J. M. Rash, N. Whelan, and S. A. Bullard. 2019. A new species of Myxobolus (Myxozoa: Bivalvulida) infecting the medulla oblongata and nerve cord of brook trout *Salvelinus fontinalis* in southern Appalachia (New River, NC, USA). Parasitology Research 118:3241–3252.

Ksepka, S. P., J. M. Rash, W. Cai, and S. A. Bullard. 2021. Detection of *Myxobolus cerebralis* (Bivalvulida: Myxobolidae) in two non-Tubifex-tubifex oligochaetes in the southeastern USA. Diseases of Aquatic Organisms 143: 51–56.

Lom, J., and J. R. Arthur. 1989. A guideline for the preparation of species descriptions in Myxosporea. Journal of Fish Diseases 12: 151–156.

Markiw, M. E., anf K. Wolf. 1983. *Myxosoma cerebralis* (Myxozoa: Myxosporea) etiologic agent of salmonid whirling disease requires tubificid worm (Annelida: Oligochaeta) in its life cycle. Journal of Protozoology 30: 561–564.

Pugachev, O. N., and P. P. Khokhlov. 1979. Myxosporea of the genus *Myxobolus*–parasites of the salmonids head and spinal brain. *In* Systematic and ecology of fish from continental water bodies of the Far East Region. Vladivostok, pp 137–139 (In Russian).

Urawa, S. 1994. Life cycle of *Myxobolus arcticus*, a myxosporean parasite of salmonid fishes. International Symposium of Aquatic Animal Health, Programs and Abstarcts, 4–8 September 1994, p. W-10.3.

Urawa, S., Y. Iida, M. A. Freeman, T. Yanagida, E. Karlsbakk, and H. Yokoyama. 2009. Morphology and molecular comparisons of *Myxobolus* spp. in the nerve tissues of salmonids

with the description of *Myxobolus murakamii* n. sp., the causative agent of myxosporean sleeping disease. Fish Pathology 44:72–80.

Urawa, S., M. A. Freeman, S. C. Johnson, S. R. M. Jones, and H. Yokoyama. 2011. Geographical variation in spore morphology, gene sequences, and host specificity of *Myxobolus arcticus* (Myxozoa) infecting salmonid nerve tissue. Diseases of Aquatic Organisms 96: 229–237.

FIGURE 1. (A–H) Myxospores of *Myxobolus neurofontinalis* (Myxobolidae) collected from the central nervous system of Brook Trout, *Salvelinus fontinalis* (Salmonidae) from Prince Edward Island, Canada; photographed with differential interference contrast optical components. Intercapsular process (ip), iodinophilous vacuole (iv), sutural markings (sm), and mucous envelope (me). Scale bars = 5µm.

FIGURE 2. Histological sections (hematoxylin and eosin) of Brook Trout, *Salvelinus fontinalis* (Salmonidae) nerve tissue infected by *Myxobolus neurofontinalis* (Myxobolidae). **(A)** Foci of myxospores. **(B)** Dispersed myxospores showing sparse mononuclear inflammatory infiltrates (arrows). **(C)** Presporogonic stage (P).

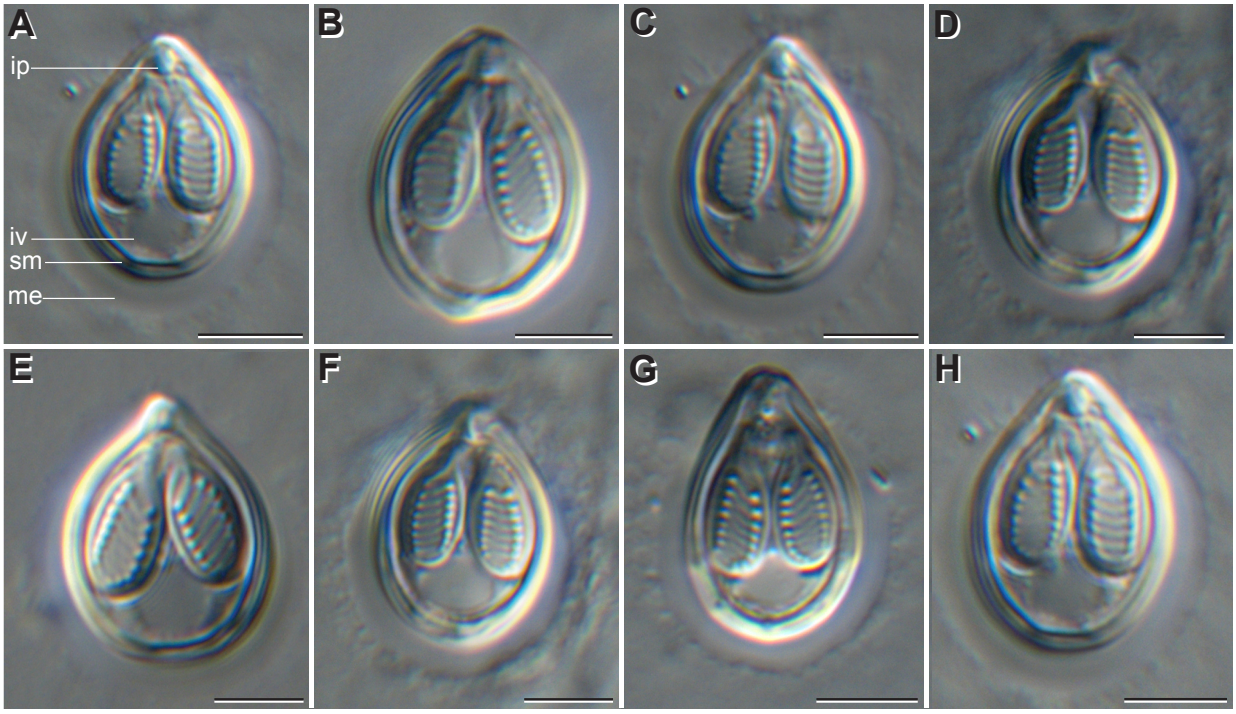
A
ip
iv
sm
me
B
C
D
E
F
G
H

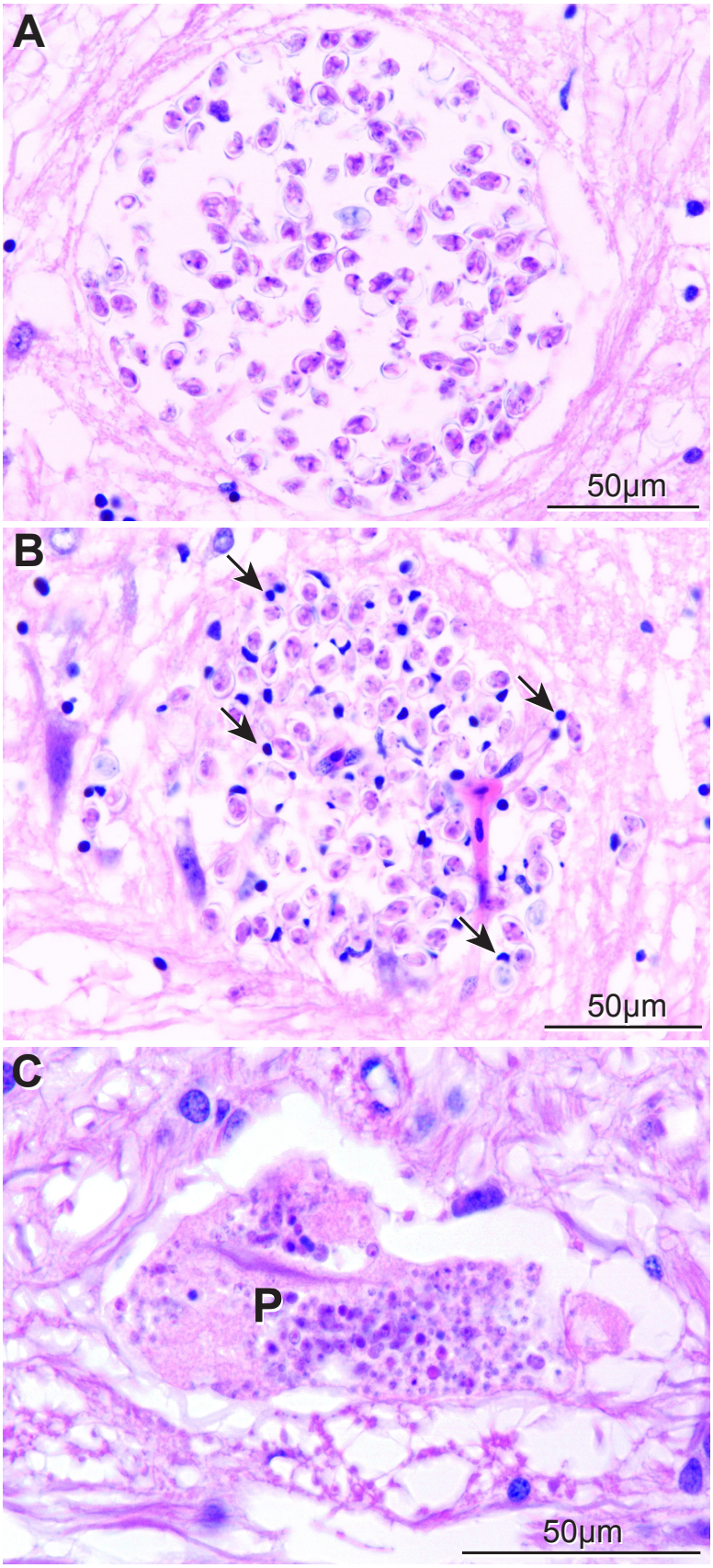
A
50μm
B
50μm
C
P
50μm

Table 1. Results of histology screening for *Myxobolus neurofontinalis* Ksepka and Bullard, 2019 (Bivalvulida: Myxobolidae) infections in Brook Trout (*Salvelinus fontinalis* [Mitchell, 1814][Salmoniformes: Salmonidae]) from Prince Edward Island Canada. For histology results, N: number of fish sampled; H+: number of fish infections were detected in.

Date	Locality	Coordinates	Histology results	
			N	H+
18 Jul 2014	Morell River	–	3	3
26 Jul 2016	Clyde River	46°14'35.0"N, 63°15'59.0"W	2	0
24 Nov 2016	West River	46°14'47.0"N, 63°21'30.3"W	1	1
8 Sep 2017	Morell River	46°24'55.8"N, 62°41'58.2"W	1	1
20 Oct 2017	Hyde Creek	46°14'13.6"N, 63°12'46.6"W	3	0
7 Nov 2017	Dunk River	46°21'13.3"N, 63°33'19.7"W	1	0
14 Nov 2017	MacLure's Pond	46°00'41.9"N, 62°38'20.0"W	2	1
14 Aug 2018	Whitlock’s Pond	46°21'00.8"N, 62°31'40.6"W	1	1
5 Jun 2020	Cousin's Pond tributary	46°31'37.2"N, 63°34'25.3"W	4	0
10 Nov 2020	West River	46°13'00.5"N, 63°21'25.6"W	2	2
15 Nov 2020	Trout River	46°41'36.6"N, 64°08'53.9"W	6	6
24 Jun 2021	Pond, Dougan Rd.	46°21'15.1"N, 63°00'59.8"W	1	0

CHAPTER 6: A NEW SPECIES OF ELLIPSOMYXA KØIE, 2003 (BIVALVULIDA) INFECTING THE GALL BLADDER OF PANGASIUS MACRONEMA BLEEKER (SILURIFORMES: PANGASIIDAE) FROM THE MEKONG RIVER DELTA, VIETNAM

***Published in Sytematic Parasitology (28 September 2023)**

Authors: Steven P. Ksepka, Triet N. Truong, and Stephen A. Bullard

Abstract During a parasitological survey of freshwater fishes in the Mekong River Delta, Vietnam, disporic plasmodia containing myxospores morphologically consistent with *Ellipsomyxa* Køie, 2003 (Bivalvulida) were observed infecting the gall bladder of *Pangasius macronema* Bleeker (Siluriformes: Pangasiidae). Herein, we use morphology and small subunit ribosomal DNA (*SSU* rDNA, *18S*) sequence data to describe *Ellipsomyxa intravesica* Ksepka & Bullard **n. sp.** and relate it to other myxidiids. The new species resembles *Ellipsomyxa adlardi* Whipps & Font, 2013, which infects the naked goby, *Gobiosoma bosc* (Lacepede, 1800) (Gobiiformes: Gobiidae) in Lake Pontchartrain, Louisiana, but differs from it by having a longer myxospore (mean = 13.3; range = 12.0–15.0 vs. 12.4; 11.3–14.4) and shorter polar capsules (3.7; 3.0–4.0 vs. 4.3; 3.9–4.9). The *18S* phylogenetic analysis recovered the sequence of the new species sister to those ascribed to *Ellipsomyxa ariusi* Chandran, Zacharia, Sathianandan & Sanil, 2020 and *Ellipsomyxa* sp. (MK561979); both of which infect the gall bladder of the threadfin sea catfish, *Arius arius* (Hamilton) (Siluriformes: Ariidiae) from the southwest coast of India. Consistent with previous phylogenetic analyses of *Ellipsomyxa* spp., *Ellipsomyxa* was recovered as monophyletic. The new species is the first species of *Ellipsomyxa* reported from a freshwater fish in Asia and the first myxozoan reported from *P. macronema*.

Introduction

Ellipsomyxa Køie, 2003 (Bivalvulida) comprises 18 species infecting the gall bladder of 15 marine fishes and 3 freshwater fishes (Table 1). Three of 18 species of *Ellipsomyxa* infect catfishes (Siluriformes): *Ellipsomyxa amazonensis* Zatti, Atkinson, Maia, Correa, Bartholomew & Adriano, 2018, *Ellipsomyxa arariensis* Silva, Matos, Lima, Furtado, Hamoy & Matos, 2018, and *Ellipsomyxa ariusi* Chandran, Zacharia, Sathianandan & Sanil, 2020 (Table 1). No species of *Ellipsomyxa* has been reported to infect a shark catfish (Pangasiidae).

The shark catfishes comprise 30 species that are endemic to riverine and estuarine localities in southern Asia (Roberts & Vidthayanon 1991; Fricke et al. 2022). Several pangasiids comprise important commercial and artisanal fisheries (Roberts & Vidthayanon 1991; Baird et al. 2001; Wang & Hsieh, 2016). Sutchi catfish, *Pangasianodon hypophthalmus* (Sauvage) (Siluriformes: Pangasiidae), basa catfish, *Pangasius bocourti* Sauvage, pangas catfish, *Pangasius pangasius* (Hamilton), *Pangasius djambal* Bleeker, and spot pangasius, *Pangasius larnaudii* Bocourt are extensively cultured in southeast Asia, with sutchi catfish and basa catfish being lumped together as "pangasius" and marketed by a variety of names internationally (Roberts & Vidthayanon, 1991; Wang & Hsieh, 2016; FAO, 2022). Vietnam produced 1.6 million tons of pangasius in 2020, representing 40% of the world's production and having an export value of ~$1.6 billion (FAO, 2022). The culture of pangasius is increasing in China, Bangladesh, and Indonesia; which collectively accounts for ~50% of global production. However, these are produced largely for domestic markets, leaving Vietnam as the main exporter (FAO, 2022). *Pangasius macronema* Bleeker, 1850, which is a relatively small species, has historically been abundant in the Mekong

Delta and comprises an important local fishery during low-water season, during spawning. Habitat loss and overfishing have hastened increased culture of this species (Baird et al., 2001). Considering the importance of these catfishes to aquaculture detailing the taxonomy of evidently benign myxozoans, such as gall bladder infecting species, is valuable, as it prevents wasting resources to treat infections that are of no threat to cultured stocks.

During a parasitological survey of freshwater fishes in Vietnam in September 2018, myxospores that were morphologically consistent with *Ellipsomyxa* were observed infecting the gall bladder of *P. macronema*, a potamodramous catfish of the Mekong River (Figs. 1–4). Herein, we use morphology to describe the new species and a phylogenetic analysis of the *18S* to test its phylogenetic position The new species is the fourth of *Ellipsomyxa* reported from a catfish and the first from a freshwater fish in Asia.

Materials and Methods

Catfish were opportunistically sampled from Cao Lãnh Fish Market, Cao Lãnh City, Đồng Tháp Province, Vietnam (Mekong River). A subsample of bile was collected from the gall bladder with a syringe, wet-mounted, and examined with an Olympus BX51 (Olympus, Tokyo, Japan) compound microscope equipped with differential interference contrast (DIC) optical components. Infected gall bladders were bisected such that half was fixed in 10% neutral buffered formalin (n. b. f.) for morphology and the other half was preserved in 95% ethanol for DNA extraction.

The morphological diagnosis was based on 50 myxospores sourced from 3 infected gall bladders. Measurements were taken from formalin-fixed myxospores at ×1000 magnification using DIC. Lugol's iodine and India ink were used to determine the presence or absence of an iodiniphilic vacuole and mucous envelope respectively (Lom & Arthur, 1989). All measurements are reported in micrometers unless otherwise specified. To illustrate myxospores, bile from formalin-fixed infected gall bladders was placed on a coverslip, inverted, placed onto a thin layer of 1% agar (Lom, 1969), and illustrated using a ×100 oil immersion objective and drawing tube.

DNA was extracted from myxospores rinsed from three ethanol preserved gall bladder using the DNeasy Blood and Tissue kit (Qiagen, Hilden, Germany). Extraction followed the manufacturers protocol, with the exceptions that the proteinase K incubation step was extended overnight and 100 µl of AE buffer were used for the elution step to increase DNA concentration. Following extraction, concentration was measured using a NanoDrop-1000 spectrophotometer (Thermo Scientific, Nanodrop Technologies, Wilmington, Delaware), diluted to 20 ng/µl, and stored at -20 C. A fragment of the small subunit ribosomal DNA (*SSU* rDNA) was amplified using primers M153–F (5'–CATTGGATAACCGTGGGAAATCT–3') and M2192–R (5'–TAGTAGCGACGGGCGGTGT–3') (Ksepka et al., 2019, 2020). PCR amplification used the following thermocycler parameters: initial denaturation step of 95ºC, for four min, followed by 35 cycles of 95 C for 30 sec, 58 C for 30 sec and 72 C for 1 min, with a final extension step of 72 C for 5 min (Ksepka et al., 2019, 2020). PCR products were visualized on a 1% agarose gel, purified using the QIAquick PCR Purification Kit (Qiagen, Hilden, Germany) following manufacturers protocol, and sequenced by Genewiz (South Plainfield, New Jersey). Sequencing primers M473–F (5'–GCTTGAGAAWCGGCTACCAC–3') and M1480–R (5'–GTGGTGCCCTTCCGTCAATTCC–3') were used to improve sequencing coverage (Ksepka et

al., 2019, 2020). Chromatograms were assembled based on sequence overlap, proofread by eye, and had low-quality read ends trimmed in Geneious version 2021.1.1 (Katoh & Standley, 2013) resulting in sequences of 1409 base pairs.

Additional taxon selection for phylogenetic analysis was based on BLAST search of NCBI GenBank and included all available sequences from *Ellipsomyxa* spp. in GenBank, 8 species of *Myxidium* Butschli, 1882 (Bivalvulida: Myxidiidae), one species of *Zschokkella* Auerbach, 1910 (Bivalvulida: Myxidiidae), 3 species of *Coccomyxa* (Leger & Hesse, 1907) (Bivalvulida: Myxidiidae), 6 species of *Auerbachia* (Meglitsch, 1968) (Bivalvulida: Myxidiidae), 2 species of *Sigmomyxa* (Thelohan, 1892) (Bivalvulida: Myxidiidae), one species of *Sinulinea* (Davis, 1916) (Bivalvulida: Myxidiidae), and 2 species of *Kudoa* (Hahn, 1917) (Multivalvulida: Kudoiidae) as an outgroup. Sequences were aligned using MAFFT with an E–INS–i alignment strategy and a maxiterate value of 1,000 in Geneious version 2021.1.1 (Katoh & Standley, 2013). The alignment was trimmed to the length of the sequences presented herein (1580 base pairs) to minimize missing data at the 5’ and 3’ end of the alignment. JModelTest2 version 2.1.10 was used to select best-fit models of nucleotide substitution based on Bayesian information criteria (Darriba et al., 2012). Bayesian inference was performed in MrBayes version 3.2.5 using substitution model averaging (nst=mixed) and a gamma distribution to model rate heterogeneity (Ronquist & Huelsenbeck 2003). Defaults were used for all other parameters. Three runs with four Metropolis-coupled chains were run for 5,000,000 generations. Stationarity was checked using Tracer 1.7 (Rambaut et al., 2018) and a burn-in of 25% of generations was determined. Evidence of convergence was further checked with the “sump” command in MrBayes. All parameters had a potential scale reduction factor of 1.00. A majority rule consensus tree of the post burn-in posterior distribution was generated with the “sumt” command in MrBayes. The

phylogenetic tree was visualized in FigTree v1.4.3 (Rambaut et al., 2014) and rendered for publication with Adobe Illustrator (Adobe Systems).

Ellipsomyxa **Køie, 2003**

Type species: *Ellipsomyxa gobii* Køie, 2003, by monotypy

Ellipsomyxa intravesica **Ksepka & Bullard n. sp. (Figs. 1–8)**

Type host: Pangasius macronema (Bleeker) (Siluriformes: Pangasiidae).

Type locality**:** Lower Mekong River 10°25'52.4"N, 105°37'07.9"E (Cao Lanh Fish Market, Đồng Tháp Province, Vietnam).

Type material: Myxospores fixed in 10% NBF (1 vial; syntype; USNM XXXXXXX); GenBank No. (SSU rDNA: OR457656–OR457658).

Site in host: Gall bladder.

Prevalence: A total of 15 of 39 (38%) *P. macronema* were infected with the new species.

Zoobank registration: To comply with the regulations set out in Article 8.5 of the emended 2012 version of the International Code for Zoological Nomenclature (ICZN 2012), details of the new species have been submitted to ZooBank. The Life Science Identifier (LSID) for *Ellipsomyxa intravesica* **n. sp.** is 75A834F4-E7A9-AF7C-FF82D7008D1A.

Etymology: The Latin specific name "*intravesica*" is from "intra" (within) and "vesicae" (bladder) referring to the site of infection.

Description

Diagnosis of myxospores (based on 50 n.b.f-fixed myxospores using differential interference contrast microscopy; USNM coll. Nos. XXXXXX): Ellipsoid myxospores comprising 2 smooth valves juxtaposed at curved sutural rim with raised pore at polar capsule attachment, 2 polar capsules, and sporoplasm; myxospore, 12.0–15.0 (13.3 ± 0.9; 47) long (Figs. 5–8), 8.0–9.0 (8.4 ± 0.5; 42) wide (Figs. 5–7), 8.0–9.0 (8.5 ± 0.5; 11) thick (Fig. 8), space between polar capsules 2.0–5.0 (3.3 ± 0.8; 41) (Figs. 5–8); polar capsules equal in length and width (Figs. 5–8), slightly pyriform (Figs. 5–7), 3.0–4.0 (3.7 ± 0.5; 78) long (Figs. 5–7), 3.0–4.0 (3.6 ± 0.5; 78) wide (Figs. 5–7), with 5–7 (5.5 ± 0.5; 78) polar tubule coils (Figs. 5–7).

Discussion

The myxospore of *E. intravesica* differs from those of its 18 congeners (*Ellipsomyxa adlardi* Whipps & Font, 2013, *Ellipsomyxa apogoni* Heiniger & Adlard, 2014, *E. amazonensis*, *E. arariensis*, *E. ariusi*, *Ellipsomyxa arothroni* Heiniger & Adlard, 2014, *Ellipsomyxa boleophthalmi* Vandana, Poojaray, Tripathi, Pavan-Kumar, Pratapa, Sanil & Rajendran, 2021, *Ellipsomyxa fusiformis* [Davis, 1917], *Ellipsomyxa gobii* Køie, 2003, *Ellipsomyxa gobiodes* Azevedo, Videira, Casal, Matos, Oliveira, Al-Quraishy & Matos, 2013, *Ellipsomyxa kalthoumi*

Thabet, Tlig-Zouari, Al Omar & Mansour, 2016, *Ellipsomyxa manilensis* Heiniger & Adlard, 2014, *Ellipsomyxa mugilis* [Sitja-Bobadilla & Alcarez-Pellitero, 1993], *Ellipsomyxa nigropunctatis* Heiniger & Adlard, 2014, *Ellipsomyxa paraensis* Zatti, Maia & Adriano, 2020*, Ellipsomyxa plagioscioni* Zatti, Maia & Adriano, 2020, *Ellipsomyxa syngnathi* Køie & Karlsbakk, 2009, *Ellipsomyxa tucujuensis* Ferreira, Silva, Carvalho, Bittencourt, Hamoy, Matos & Videira, 2021) by myxospore dimensions and polar tubule coil number. Polar tubule coil number differentiates the myxospore of the new species (5–7) from those of *E. apogoni* (2–4), *E. amazonensis* (2–3), *E. boleophthalmi* (3–4), *E. kalthoumi* (9), *E. manilensis* (3–4), and *E. paraensis* (2–3). The myxospore of the new species differs from those of *E. adlardi* and *E. nigropunctatis* by having shorter polar capsules (3.0–4.0 vs 3.9–4.9 and 3.5–5.7, respectively); from that of *E. araiensis* by having a wider myxospore (8.0–9.0 vs 6.7–8.0) and wider polar capsules (3.0–4.0 vs 2.5–3.2); from those of *E. arothroni* and *E. fusiformis* by having a shorter (12.0–15.0 vs 12.3–17.7 and 16, respectively) and more narrow myxospore (8.0–9.0 vs 9.9–13.6 and 9, respectively); from those of *E. ariusi*, *E. gobii*, *E. plagioscioni*, *E. syngnathi*, and *E. tucujuensis* by having a longer myxospore (12.0–15.0 vs 9.0–12.0, 10.8–12.0, 10.2–12.8, 9.0–10.8, and 10.1, respectively); and from those of *E. gobiodes* and *E. mugilis* by having a thicker myxospore (8.0–9.0 vs 6.5–7.0 and 5.5–8.0, respectively) with shorter polar capsules (3.0–4.0 vs 4.3–4.8) (Table 1).

Myxospore morphology does not support the assignment of *Ellipsomyxa* to Ceratomyxidae Doflein, 1899. *Ellipsomyxa* was placed within Ceratomyxidae by having valves that are elongated perpendicular to the straight central transverse suture, a characteristic of all ceratomyxid genera (Køie, 2003; Lom and Dykova, 2006). Køie & Karlsbakk (2009) and Gunter & Adlard (2010) later amended the generic diagnosis to accommodate species with sutures that

were curved, sigmoid, or formed acute angles with the valves. These features are absent from ceratomyxids (Lom & Dykova, 2006). Whipps & Font (2013) questioned whether any species of *Ellipsomyxa* have valves extended perpendicularly from a straight transverse suture. Of the 18 species of *Ellipsomyxa*, only the type species, *E. gobii*, is illustrated as having valves elongated perpendicular to a straight transverse suture. However, micrographs in the description of *E. gobii* show a myxospore that has a suture forming an acute angle with the valves (Køie 2003). Two of the remaining 17 species, *E. kalthoumi* and *E. boleophthalmi*, are illustrated with either a straight transverse suture or with valves extending perpendicularly from the suture (Thabet et al. 2016; Vandana et al. 2020). However, *E. kalthoumi* has a suture forming an acute angle with the valves and *E boleophthalmi* has a suture that is sigmoid, opposed to a strainght transverse suture perpendicular to the valves (Thabet et al. 2016; Vandana et al. 2020). Additionally, ceratomyxids have polar capsules that are close to the sutural line in a plane perpendicular to it and discharge at the anterior pole of the myxospore, whereas *Ellipsomyxa* spp.have polar capsules at opposite ends of the myxospore and, with the exception of *E. mugilis* and *E. kalthoumi*, which were only illustrated in valvular view leaving the direction the polar capsules discharge indeterminate, discharge sub-laterally to laterally in opposite directions (Davis, 1917; Sitja-Bobadilla & Alvarez-Pellitero, 1993; Køie, 2003; Lom & Dykova 2006; Azevedo et al. 2013; Whipps & Font, 2013; Heiniger & Adlard, 2014; Thabet et al. 2016; Silva et al. 2018; Zatti et al. 2018; Chandran et al. 2020; Ferreira et al. 2021; Vandana et al. 2021;). Polar capsules at opposite ends of the myxospore that that terminate sub-laterally to laterally in opposite directions and the lack of a straight transverse suture make the diagnosis of *Ellipsomyxa* in conflict with that of Ceratomyxidae. For these reasons we regard the familial placement of *Ellipsomyxa* as *incertae cedis.*

Phylogenetic analysis

The three amplified *SSU* rDNA (*18S*) fragments of *E. intravesica* comprised 1409 nucleotides each after assembly, were identical to each other, and were most similar to *Ellipsomyxa* sp. (MH212373) from the gall bladder of banded archerfish (*Toxotes jaculatrix* [Pallas, 1976] [Perciformes: Toxotidae]) from the Setiu Wetland, Malaysia; differing by 35 nucleotides (2.7%). *Ellipsomyxa intravesica* was recovered sister sequences of *E. ariusi* and *Ellipsomyxa* sp. (MN892546), both collected from ariid catfishes in southeast Asia (Chandran et al. 2020). Consistent with phylogenetic analyses of *Ellipsomyxa,* we recovered *Ellipsomyxa* as monophyletic and sister to sequences ascribed to *E. sphaerica* (as *S. sphaerica*) and*Myxidium queenslandicus* Gunter & Adlard, 2008 (Whipps &Font, 2013; Chandran et al., 2020; Zatti et al., 2020; Vandana et al., 2021). Within the *Ellipsomyxa* clade, the analysis recovered 4 clades with a loose association to their geographic locality (Fig. 9). Of the 5 species of *Ellipsomyxa* infecting freshwater fishes in the Amazon River Basin (*E. amazonensis*, *E. arariensis*, *E. paraensis*, *E. tucujuensis*, and *E. plagioscioni*), all but *E. plagioscioni* were recovered within a well-supported clade. *Ellipsomyxa* species infecting marine fishes in Australia (*E. apogoni*, *E. arothroni*, *E. nigropunctatus*, and *E. manilensis*) were recovered monophyletic and sister to *E. kalthoumi* collected from leaping mullet, *Chelon saliens* (Risso) (Mugiliformes: Mugilidae) in the Mediterranean Sea. Species infecting marine fishes in the Atlantic Ocean (*E. adlardi*, *E. gobii*, *E. mugilis*, and *E. syngnathi*) were recovered as monophyletic and sister to *E. boleophthalmi*, infecting Dussumier's mudskipper, *Boleophthalmus dussumieri* Valenciennes, 1837 (Gobiiformes: Oxudercidae) from Vaitarna River, India. Sequences ascribed to *Ellipsomyxa*

collected from catfishes in southeast Asia (*E. intravesica*, *E. ariusi*, and *Ellipsomyxa* sp. MK561979) were recovered as monophyletic. Noteworthy is the low support (0.69) for several nodes in the *Ellipsomyxa* clade.

Acknowledgements We thank Thuy Ha Nguyen, former Rector of Dong Thap Community College, for hosting us during the collection in Vietnam; Micah B. Warren (Auburn University, Auburn, Alabama, USA), and Carlos F. Ruiz (El Paso, Texas, USA) for helping with fish collection, necropsy, and identification.

References

Azevedo, C., Videira, M., Casal, G., Matos, P., Oliveira, E., Al-Quraishy, S., & Matos, E. (2013) Fine structures of the plasmodia and myxospore of *Ellipsomyxa gobioides* n. sp. (Myxozoa) found in the gall bladder of *Gobioides broussonnetii* (Teleostei: Gobiidae) from the Lower Amazon River. *Journal of Eukaryotic Microbiology* 60(5): 490–496.

Baird, I., Hogan, Z., Phylaivanh, B., and Moyle, P. (2001) A communal fishery for the migratory catfish *Pangasius macronema* in the Mekong River. *Asian Fisheries Science* 14: 25–41.

Chandran, A., Zacharia, P. U., Sathianadan, T. V., & Sanil, N. K. (2020) *Ellipsomyxa ariusi* sp. nov. (Myxosporea: Ceratomyxidae), a new myxosporean infecting the gall bladder of threadfin sea catfish *Arius arius* in India. *Diseases of Aquatic Organisms* 142: 83–97.

Darriba, D., Taboada, G. L., Doallo, R., & Posada, D. (2012) jModelTest 2: more models, new heuristics, and parallel computing. *Nature Methods* 9: 772. doi:10.1038/nmeth.2109.

Davis, H. S. (1917) The myxosporidia of the Beaufort region, a systematic and biologic study. *Bulletin of the Bureau of Fisheries* 35: 199–243.

FAO (2022) Globefish highlights: international markets for fisheries and aquaculture products. Available at: https://www.fao.org/3/cc0222en/cc0222en.pdf. Accessed 15 January 2023.

Ferreira, R. L. S., da Silva, D. T., de Carvalho, A. A., Bittencourt, L. S., Hamoy, I., Matos, E., & Videira, M. (2021) *Ellipsomyxa tucujuensis* n. sp. (Myxozoa: Ceratomyxidae), a parasite of *Satanoperca jurupari* (Osteichthyes: Cichlidae) from the Brazilian Amazon. *Parasitology International* 83: 102332.

Fricke, R., W. N. Eschmeyer, and R. van der Laan. 2022. Eschmeyer's catalog of fishes: Genera, species, references. Avalaible at: http://researcharchive.calacademy.org/research/icthyology/catalog/fishcatmain.asp. Accessed 15 January, 2023.

Gunter, N., & Adlard, R. (2010) The demise of *Leptotheca* Thélohan, 1895 (Myxozoa: Myxosporea: Ceratomyxidae) and assignment of its species to *Ceratomyxa* Thélohan, 1892 (Myxosporea: Ceratomyxidae), *Ellipsomyxa* Køie, 2003 (Myxosporea: Ceratomyxidae), *Myxobolus* Bütschli, 1882 and *Sphaerospora* Thélohan, 1892 (Myxosporea: Sphaerosporidae). *Systematic Parasitology* 75: 81–104.

Heiniger, H., & Adlard, R. D. (2014) Relatedness of novel species of *Myxidium* Butschli, 1882, *Zschokkella* Auerbach, 1910 and *Ellipsomyxa* Køie, 2003 (Myxosporea: Bivalvulida) from the gall bladders of marine fishes (Teleostei) from Australian waters. *Systematic Parasitology* 87: 47–72.

Katoh, K., & Standley, D. M. (2013) MAFFT multiple sequence alignment software version 7: improvements in performance and usability. *Molecular Biology and Evolution* 30: 772–780.

Køie, M. (2003) *Ellipsomyxa gobii* gen. et sp. n. (Myxozoa: Ceratomyxidae) in the common goby *Pomatoschistus microps* (Teleostei: Gobiidae) from Denmark. *Folia Parasitologica* 50: 269–271.

Køie, M., and Karlsbakk , E. (2009) *Ellipsomyxa syngnathi* sp. n. (Myxozoa, Myxosporea) in the pipefish *Syngnathus typhle* and *S. rostellatus* (Teleostei, Syngnathidae) from Denmark. *Parasitology Research* 105: 1611–1616.

Ksepka, S. P., Rash, J. M., Whelan, N. V., & Bullard, S. A. (2019) A new species of *Myxobolus* (Myxozoa: Bivalvulida) infecting the medulla oblongata and nerve cord of brook trout *Salvelinus fontinalis* in southern Appalachia (New River, NC, USA). *Parasitology Research* 118: 3241–3252.

Ksepka, S. P., N. V. Whelan, C. M. Whipps, S. A. Bullard. 2020. A new species of *Thelohanellus* Kudo, 1933 (Myxozoa: Bivalvulida) infecting the skeletal muscle of blacktail shiner, *Cyprinella venusta* Girard, 1856 (Cypriniformes: Cyprinidae) in the Chattahoochee River Basin, Georgia. *Journal of Parasitology* 106: 350–359.

Lom, J. 1969. On a new taxonomic character in Myxosporidia, as demonstrated in descriptions of two new species of *Myxobolus*. *Folia Parasitologica* 16: 97–103.

Lom, J., & Arthur, J. R. (1989) A guideline for the preparation of species descriptions in myxosporea. *Journal of Fish Diseases* 12: 151–156.

Lom, J., & Dykova, I. (2006) Myxozoan genera: definition and notes on taxonomy, life-cycle terminology and pathogenic species. *Folia Parasitologica* 53: 1–36.

Rambaut, A., Drummond, A. J., Xie, D., Baele, G., & Suchard, M. A. (2018) Posterior summarization in Bayesian phylogenetics using Tracer 1.7. *Systematic Biology* 67: 901–904.

Rambaut, A., Suchard, M. A., Xie, D., & Drummond, A. J. (2014) FigTree v1.4.3. Available at: http://tree.bio.ed.ac.uk/software/figtree. Accessed August 10, 2022.

Roberts, T. R., & Vidthayanon, C. (1991) Systematic revision of the Asian catfish family Pangasiidae, with biological observations and descriptions of three new species. *Proceedings of the Academy of Natural Sciences of Philadelphia* 143: 97–143.

Ronquist, F., & Huelsenbeck, J. P. (2003) MrBayes 3: Bayesian phylogenetic inference under mixed models. *Bioinformatics* 19:1572–1574.

Silva, D. T., Matos, P. S., Lima, A. M., Furtado, A. P., Hamoy, I., & Matos, E. R. (2018) *Ellipsomyxa arariensis* n. sp. (Myxozoa: Ceratomyxidae), a new myxozoan parasite of *Pygocentrus natteri* Kner, 1858 (Teleostei: Characidae) and *Pimelodus ornatus* Kner, 1858 (Teleostei: Pimelodidae) from Marajo Island, in the Brazilian Amazon region. *Parasitology Research* 117: 3537–3545.

Sitja-Bobadilla, A., & Alvarez-Pellitero, P. (1993) *Zschokkella mugilis* n. sp. (Myxosporea: Bivalvulida) from mullets (Teleostei: Mugilidae) of Mediterranean waters: light and electron microscopic description. *Journal of Eukaryotic Microbiology* 40(6): 755–764.

Thabet, A., Tlig-Zouari, S., Al Omar, S. Y., & Mansour, L. (2016) Molecular and morphological characterization of two species of the genus *Ellipsomyxa* Køie, 2003 (Ceratomyxidae) from the gall bladder of *Liza saliens* (Risso) of Tunisian coasts of the Mediterranean. *Systematic Parasitology* 93: 601–611.

Vandana, V. R., Poojary, N., Tripathi, G., Pavan-Kumar, A., Pratapa, M. G., Sanil, N. K., & Rajendran, K. V. (2021). A novel myxozoan parasite, *Ellipsomyxa boleophthalmi* sp. nov. (Myxozoa: Ceratomyxidae) in the brakishwater fish, *Boleophthalmus dussumieri* Valenciennes, 1837 (Perciformes: Gobiidae) from India. *Parasitology Research* 120: 1269–1279.

Wang, D., & Hsieh, Y. P. (2016) The use of imported fish in local restaurants. *Food Control* 65: 136–142.

Whipps, C. M., & Font, B. F. (2013) Interactions of two myxozoan parasites from naked goby *Gobiosoma bosc*, in Lake Pontchartrain, Louisiana. *Journal of Parasitology* 99(3): 441–447.

Zatti, S. A., Atkinson, S. D., Maia, A. A. M., Correa, L. L., Bartholomew, J. L., & Adriano, E. A. (2018) Novel *Myxobolus* and *Ellipsomyxa* species (Cnidaria: Myxozoa) parasiting *Brachyoplatystoma rousseauxii* (Siluriformes: Pimelodidae) in the Amazon basin, Brazil. *Parasitology International* 67(5): 612–621.

Zatti, S. A., Maia, A. A. M., & Adriano, E. A. (2020) Growing diversity supports radiation of an *Ellipsomyxa* lineage into the Amazon freshwater: description of two novel species parasitizing fish from Tapajos and Amazon rivers. *Acta Tropica* 211: 105616.

Figs. 1–4 Disporous plasmodia containing myxospores of *Ellipsomyxa intravesica* **n. sp.** Ksepka and Bullard (Bivalvulida) from the gall bladder of *Pangasius macronema* Bleeker (Siluriformes: Pangasiidae) from the Mekong Delta, Vietnam; photographed with differential interference contrast optical components.

Figs. 5–8 Schematic drawings of myxospores of *Ellipsomyxa intravesica* **n. sp.** Ksepka & Bullard (Bivalvulida) from the gall bladder of *Pangasius macronema* Bleeker (Siluriformes: Pangasiidae) from the Mekong Delta, Vietnam. 6–8, Frontal view. 9, Sutural view. Suture (su), sporoplasm (sp), polar tubules (pt), polar capsule (pc), nucleus (n). Scale bars = 5 μm.

Fig 9 Phylogenetic relationships of myxozoans genetically similar to *Ellipsomyxa intravesica* Ksepka & Bullard **n. sp.** (Bivalvulida) reconstructed with the *SSU* rDNA gene using Bayesian inference. Scale bar is in substitutions per site. New species and new combinations in bold.

.

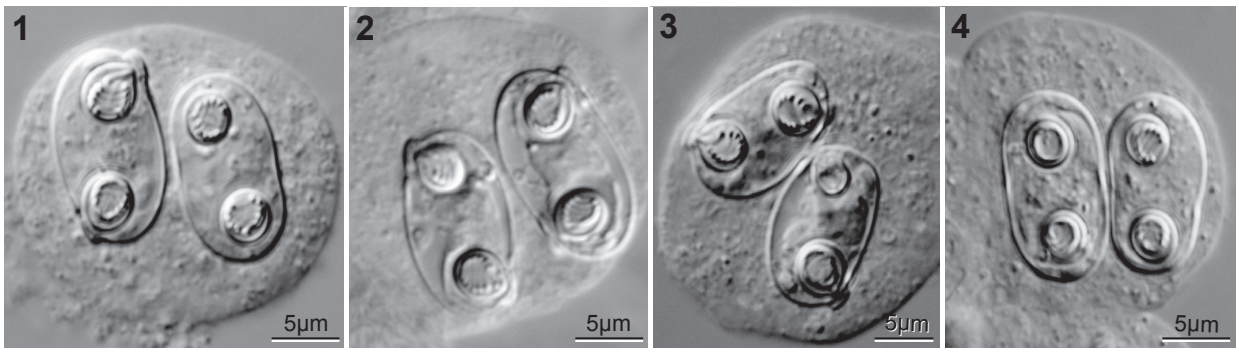
1
5µm
2
5µm
3
5µm
4
5µm

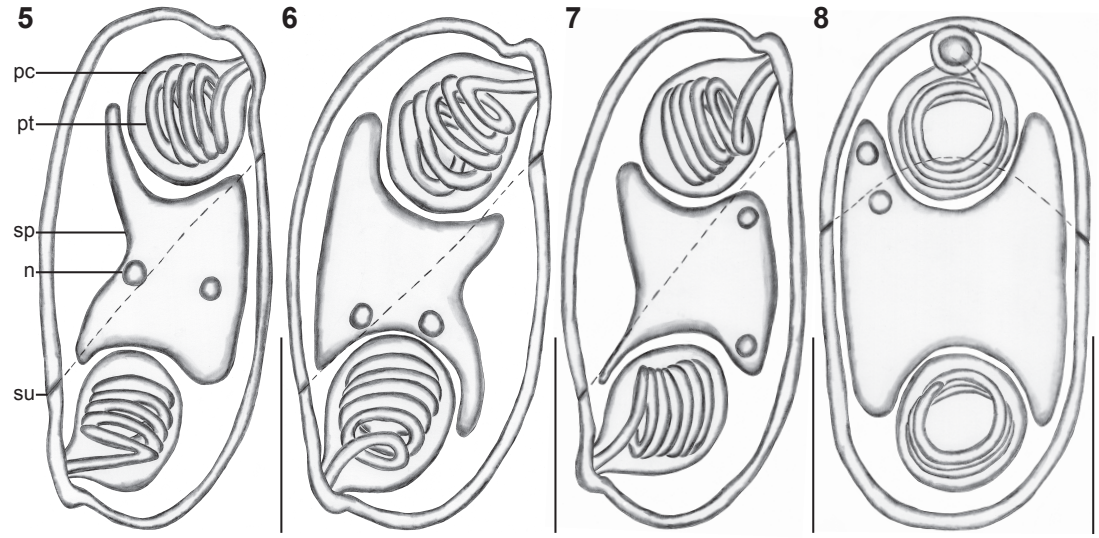
5
pc
pt
sp
n
su
6
7
8

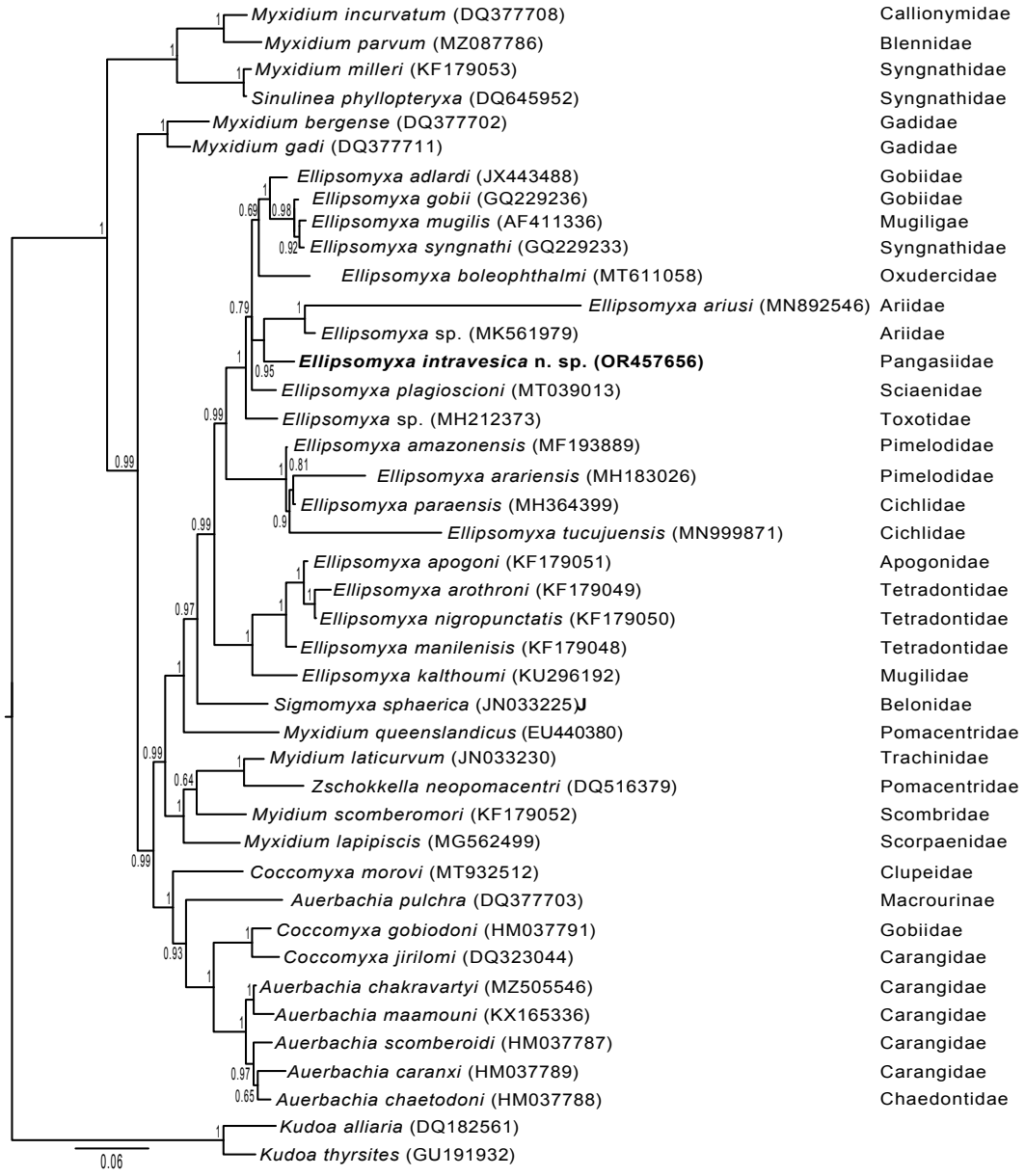
Myxidium incurvatum (DQ377708) Callionymidae
Myxidium parvum (MZ087786) Blennidae
Myxidium milleri (KF179053) Syngnathidae
Sinulinea phyllopteryxa (DQ645952) Syngnathidae
Myxidium bergense (DQ377702) Gadidae
Myxidium gadi (DQ377711) Gadidae
Ellipsomyxa adlardi (JX443488) Gobiidae
Ellipsomyxa gobii (GQ229236) Gobiidae
Ellipsomyxa mugilis (AF411336) Mugiligae
Ellipsomyxa syngnathi (GQ229233) Syngnathidae
Ellipsomyxa boleophthalmi (MT611058) Oxudercidae
Ellipsomyxa ariusi (MN892546) Ariidae
Ellipsomyxa sp. (MK561979) Ariidae
Ellipsomyxa intravesica n. sp. (OR457656) Pangasiidae
Ellipsomyxa plagioscioni (MT039013) Sciaenidae
Ellipsomyxa sp. (MH212373) Toxotidae
Ellipsomyxa amazonensis (MF193889) Pimelodidae
Ellipsomyxa arariensis (MH183026) Pimelodidae
Ellipsomyxa paraensis (MH364399) Cichlidae
Ellipsomyxa tucujuensis (MN999871) Cichlidae
Ellipsomyxa apogoni (KF179051) Apogonidae
Ellipsomyxa arothroni (KF179049) Tetradontidae
Ellipsomyxa nigropunctatis (KF179050) Tetradontidae
Ellipsomyxa manilenisis (KF179048) Tetradontidae
Ellipsomyxa kalthoumi (KU296192) Mugilidae
Sigmomyxa sphaerica (JN033225) Belonidae
Myxidium queenslandicus (EU440380) Pomacentridae
Myidium laticurvum (JN033230) Trachinidae
Zschokkella neopomacentri (DQ516379) Pomacentridae
Myidium scomberomori (KF179052) Scombridae
Myxidium lapipiscis (MG562499) Scorpaenidae
Coccomyxa morovi (MT932512) Clupeidae
Auerbachia pulchra (DQ377703) Macrourinae
Coccomyxa gobiodoni (HM037791) Gobiidae
Coccomyxa jirilomi (DQ323044) Carangidae
Auerbachia chakravartyi (MZ505546) Carangidae
Auerbachia maamouni (KX165336) Carangidae
Auerbachia scomberoidi (HM037787) Carangidae
Auerbachia caranxi (HM037789) Carangidae
Auerbachia chaetodoni (HM037788) Chaedontidae
Kudoa alliaria (DQ182561)
Kudoa thyrsites (GU191932)
0.06

Table I. Comparison of *Ellipsomyxa* spp. Mean measurements with ranges provided in micrometers. Abbreviations: *MXL*, myxospore length; *MXW*, myxospore width; *MXT*, myxospore thickness; *PCL*, polar capsule length; *PCW*, polar capsule width; *DBC*, distance between polar capsules; *PTC*, polar tubule coil number.

Ellipsomyxa spp.	Host	MXL	MXW	MXT	PCL	PCW	DBC	PTC	Locality	Reference
E. adlardi Whipps & Font, 2013	*Gobiosoma bosc* (Lacepede)	12.4; 11.3–14.4	7.7; 7.1–8.8	7.8; 7.1–9.0	4.3; 3.9–4.9	3.6; 3.3–4.1		5–6	Louisiana	Whipps & Font, 2013
E. apogoni Heiniger & Adlard, 2014	*Apogon doederleini* Jordan & Snyder	10.2 8.8–11.1	6.9; 6.0–9.1		3.7; 2.9–4.8	2.7; 2.1–3.4		2–4	Australia	Heiniger & Adlard, 2014
E. amazonensis Zatti, Atkinson, Maia, Correa, Bartholomew, & Adriano, 2018	*Brachyplatystoma rousseauxii* (Castelnau)	12.8; 12.3–13.6	7.6; 6.7–8.7		3.8; 3.8–4.0	3.1; 2.5–3.4		2–3	Brazil	Zatti et al. 2018
E. arariensis Silva, Matos, Lima, Furtado, Hamoy, & Matos, 2018	*Pimelodus ornatus*	12.6 12.0–13.4	7.3; 6.7–8.0		3.5; 3.4–4.0	2.6; 2.5–3.2		5–6	Marajo Island	Silva et al. 2018
E. ariusi Chandran, Zacharia, Sathianandan, & Sanil, 2020	*Arius arius* (Hamilton)	10.1; 9.0–12.0	6.8; 6.3–8.2	7.7; 7.1–8.7	2.8; 2.1–3.7	2.5; 1.6–3.0		4–5	India	Chandran et al. 2020
E. arothroni Heiniger & Adlard, 2014	*Arothron hispidus* (Linnaeus)	15.4; 12.3–17.7	11.7; 9.9–13.6		6.6; 5.4–7.9	4.5; 3.9–5.4		4–6	Australia	Heiniger & Adlard, 2014
E. boleophthalmi Vandana, Poojary, Tripathi, Pavan–Kumar, Pratapa, Sanil, & Rajendran, 2021	*Boleophthalmus dussumieri* Valenciennes	9.8; 9.0–10.7	7.2; 6.0–7.8		2.8; 2.7–2.8	2.8; 2.7–2.8		3–4	India	Vandana et al. 2021
E. fusiformis (Davis, 1917)	*Sphyrna zygaena* (Linnaeus)	16	9		4.5	4.5			USA	Davis, 1917
E. gobii Koie, 2003	*Pomatoschistus microps* (Kroyer)	7.0; 6.6–7.5	8.7; 8.0–9.0	11.6; 10.8–12.0	3.1; 3.0–3.2	3.1; 3.0–3.2	2.7; 2.4–3.0	6–7	Denmark	Koie, 2003
E. gobioides Azevedo, Videira, Casal, Matos, Oliveira, Al-Quraishy, & Matos, 2013	*Gobioides broussonnetii* Lacepede	6.8; 6.5–7.0	7.2; 6.9–7.5	13.1; 12.8–13.5	4.6; 4.3–4.8	2.5; 2.1–2.7	3.4; 3.1–3.8	5–6	Brazil	Azevedo et al. 2013
***E. intravesica* Ksepka & Bullard**	***Pangasius macronema* (Bleeker)**	**13.3; 12.0–15.0**	**8.4; 8.0–9.0**	**8.5; 8.0–9.0**	**3.7; 3.0–4.0**	**3.6; 3.0–4.0**	**3.3; 3.0–5.0**	**5–7**	**Vietnam**	**Present study**
E. kalthoumi Thabet, Tlig-Zouari, Al Omar, & Mansour, 2016	*Chelon saliens* (Risso)	10.5; 10.0–11.0	8.0; 7.0–9.0		2.8; 2.7–3.0	2.8; 2.7–3.0	3.2; 3.0–3.5	9	Tunisia	Thabet et al. 2016
E. manilensis Heiniger & Adlard, 2014	*Arothron manilensis* (Marion de Proce)	15.2; 13.8–17.1	11.8; 10.2–13.3		5.6; 4.6–6.6	4.5; 4.2–5.0		3–4	Australia	Heiniger & Adlard, 2014
E. mugilis (Sitja-Bobadilla & Alvarez-Pellitero, 1993)	*Chelon saliens* (Risso)	11.5; 10.0–13.5	7.3; 5.5–9.0	6.8; 5.5–8.0	2.9; 2.7–4.0	2.9; 2.7–4.0		5	Ebro River delta	Sitja-Bobadilla & Alvarez-Pellitero, 1993
E. nigropunctatis Heiniger & Adlard, 2014	*Arothron nigropunctatus* (Bloch & Schneider)	13.8; 11.9–16.3	9.9; 8.0–12.9		4.7; 3.5–5.7	3.6; 2.8–4.6		5	Australia	Heiniger & Adlard, 2014
E. paraensis Zatti, Maia, & Adriano, 2020	*Cichla monoculus* Spix & Agassiz	11.5; 10.5–12.4	7.5; 6.6–8.6		3.2; 2.1–3.9	2.6; 2.0–3.3		2–3	Brazil	Zatti et al. 2020

E. plagioscioni Zatti, Maia, & Adriano, 2020	*Plagioscion squamosissimus* (Heckel)	11.1; 10.2–12.8	6.6; 5.6–7.6		3.8; 3.2–4.4	2.8; 2.3–3.1		5–6	Brazil	Zatti et al. 2020
E. syngnathi Koie & Karlsbakk, 2009	*Syngnathus typhle* Linnaeus	6.8; 6.3–7.2	8.1; 7.2–8.6	10.0; 9.0–10.8	3.6; 3.2–4.1	2.9; 2.7–3.2	1.9; 1.8–2.4	5–6	Denmark	Koie & Karlsbakk, 2009
E. tucujuensis Ferreira, Silva, Carvalho, Bittencourt, Hamoy, Matos, & Videira, 2021	*Satanoperca jurupari* (Heckel)	10.11	7.8		3.12	2.5		5–6	Brazil	Ferreira et al. 2021

Chapter 7: Summary

In this dissertation I used morphology, histology, genetic sequencing (PCR; small subunit ribosomal DNA [18S]), and phylogenetic analysis to characterize six new species of assigned to three genera. This work contributes to myxozoan taxonomy by helping to provide a template for the necessary detail in myxospore morphology and highlighting the need for thorough histology to document a precise tissue site of infection and highlighting the need for sequence data tied to thorough morphology.

As reduced cnidarians containing few cells there are relatively few morphological characters for diagnosing myxospores, which can make differentiating morphologically similar species difficult. This is compounded by the fact that myxozoan taxonomy has been plagued by superficial descriptions. It is commonplace to find descritptions that name new species based on a few measurments accompanied by poor illustrations, the host identity, and site of infection based on the assumption that myxozoans that infect different organs and host species are novel. These descrittions make differentiating these species from known myxozoans with morphology extremely difficult. This also potentially artificially inflates the number of known myxozoans, as some species infect multiple host species or infect the same tissue type in multiple organs. Descriptions in this dissertation included detailed morphometrics and illustrations that make the species herein readily identifiable and provide a template moving forward for the necessary detail for describing myxospores.

Tissue tropism has been suggested to be an important factor in the prediciting the phylogenetic relationships of myxozoans. Despite this, the site of infection reported in descriptions is often superficial, with only an organ infected being reported. This overlooks that organs are made of unrelated tissue types and contain multiple potential habitats for myxozoans

to infect. When labelling site of infection on phylogenetic analyses we see that myxozoans infecting the same organs are distantly related, which can lead to the assumption that site of infection provides little insight on the phylogenetic placement of myxozoans. However, when we consider site of infection at the tissue level, particularly in connective tissue, which includes loose, dense, and eleastic connective tissues, adipose tissue, cartilage, bone, and blood, we start to observe patterns in site of infection in phylogenetic analyses of myxozoans. For example, ingroup taxa for phylogenetic analyses from chapters two, three, and four of this dissertation, with the exception of species where only organ infected is known, all infect connective tissues, despite infecting different organs. This work demonstrated the necessity for detailed histology on myxozoan infections to determine a precise site of infection and allow us to better understand patterns in myxozoan evolution.

These works highlight the need for thorough characterization of myxospores and tissue site of infection. Future works that include the necessary detail will allow us to better observe patterns in the of myxozoan evolution and aid in resolving extensive issues with misidentification of sequences that will allow future research to better address extensive poly/paraphyly issues with myxozoan genera.